ASSESSMENT OF EPHEMERAL GULLY EROSION USING TOPOGRAPHIC AND HYDROLOGICALLY BASED MODELS IN CENTRAL KANSAS

By

LAWRENCE SEKALUVU

B. S., Makerere University, Uganda 2013

A THESIS

Submitted in partial fulfillment of the requirements for the degree

MASTER OF SCIENCE

Department of Biological and Agricultural Engineering
College of Engineering

KANSAS STATE UNIVERSITY
Manhattan, Kansas

2015

Approved by:

Major Professor
Dr. Aleksey Sheshukov

Copyright

Abstract

The global requirements for food and agricultural products have increased enormously in recent years mainly due to increase in global population. More land is brought under human development and cultivation including marginal lands that are susceptible to degradation processes of erosion, waterlogging, and depletion of organic matter. The resulting effects include; deprivation of the roles performed by the environment, high costs of water treatment, and sedimentation of water reservoirs. This study aims at assessment of ephemeral gully (EG) erosion using topographic and hydrologically based models in two paired watersheds in Central Kansas. The effects of best management practices (BMPs) implementation on EG formation, and erosion rates within the watershed are discussed.

The topographic index (TI) models used include: slope area model *(SA),* compound topographic index model *(CTI),* wetness topographic index model *(WTI),* slope area power *(SA2),* kinematic wave model *(nLS),* and modified kinematic wave model (*nLSCSS).* EGs predicted by each model threshold were compared with observed EGs obtained through digitization and field reconnaissance. The agreement of thresholds obtained from location and length approaches were compared by means of drainage density concept. Statistical analysis was performed by error matrix for EG location analysis, and root mean square error (RMSE) and Nash–Sutcliffe efficiency (NSE) for EG length analysis. A TIN-based real-time integrated basin simulator *(tRIBS)* model, a physically-based, distributed hydrological model was coupled with an EG erosion component (Foster and Lane model) to estimate the erosion rates, and effect of installation of BMPs on reduction of EG erosion rates from agricultural fields.

The results indicated that TI models could predict EG location with a maximum total accuracy of 70%. The effectiveness of TI models at prediction of EGs is affected by watershed features such as installed structural best management practices, roads, and culverts. The CTI model outperformed all the TI models at prediction of EGs with maximum Kappa and NSE values of 0.32 and 0.55 respectively, and a minimum RMSE value of 0.087 m. Structural BMPs are effective at controlling erosion from croplands, however, the effectiveness of structural BMPs at reduction of sediment loadings from EGs vary depending on surface cover, and BMP geometry.

Keywords. *Ephemeral gully, Topography, Erosion, Hydrology, Best Management Practice*

Table of Contents

List of Figures

List of Tables

Acknowledgements

I have been delighted to be surrounded by fruitful, supportive, and encouraging group of people through my journey towards obtaining my first advance degree. It's my pleasure to send my sincere gratitude to the following people.

I would like to send my gratitude to my supervisory committee, Dr. Aleksey Sheshukov, Prof. Stacy Hutchinson, and Dr. Isaya Kisekka for all your words of guidance, and motivation. I would wish to extend to appreciations to Dr. Aleksey Sheshukov, and Prof. Stacy Hutchinson for the extra time and energy towards brainstorming ideas and helping me with the analysis that improved my research. I would also thank my fellow graduate students Vladimir Karimov, Tobias Oker, and Gia Nguyen for their endless encouragement and motivation.

My cordial gratitude goes to my parents and siblings for all their continued support and love they showed through academic career. Lastly, I would like thank the almighty for all the grace and blessing He provides through my life, without Him nothing would have been accomplished!

Dedication

I would like to consecrate this master's research to my sister, Beatrice Najjuko, and My mum Florence Nakitende. It was out of their words of encourage and motivation that I wrote all the pages of this thesis.

Abbreviations and Symbols

BMP	Best management practices
CLU	Common Land use Unit
DEM	Digital Elevation Model
ESRI	Environmental System Research Institute
FAO	Food Agricultural Organization
GIS	Geographical Information Systems
KDHE	Kansas Department of Health and Environment
NPS	Nonpoint source
UNPF	United Nation Population Fund
US EPA	United States Environmental Protection Agency
USDA NRCS	United States Department of Agriculture National Resources Conservation Service
USGS	United States Geological Survey

Chapter 1 - Introduction

The global requirements for food and other agricultural products have increased enormously in recent years mainly due to inexorable increase in global population. In 2011, the global population reached to seven billion people, and it is projected to increase to over nine billion by 2050 (UNPF, 2015). According to FAO, this increase in population growth by 2050 will require increasing food production by 70%, and in developing world, this value will need to double (FAO, 2015). It is comprehended that many governments all over the world are working hard to meet the food demands of their population. In this way, more land is brought under human development and cultivation including marginal land that is susceptible to degradation processes of erosion, waterlogging, and depletion of organic matter. Though many strategies are being set up to meet food demands, deprivation of the roles performed by the environment is at its pinnacle. Sidorchuk (1999) stated that activities involving the destruction of native forests, tilling of fallow lands change the hydrological conditions in the rainfall–runoff system thus encouraging erosion degradation processes to prevail. In countries such as United States where agriculture is chemical intensive, the effects of environmental pollution from agriculture has already been felt through processes such as high cost of water treatment, sedimentation of many water reservoirs, and increase impairment of water quality.

The cultivation of land prone to processes of erosion has degraded the quality of water resources all over the world. Water quality is dependent on a wide range of factors including physical, chemical, biological, hydrological, and societal factors (Walter et al., 2000). The amendments to Clean Water Act (1972) stressed nonpoint source (NPS) pollution as a critical cause of water quality degradation. Within the United States, more than 44% of water sources are being impaired mainly due to NPS pollution from agricultural fields (US EPA, 2015). The efforts by US EPA to address non-point source pollution are expressed in sections 208, 303(d) and 319 of the Clean Water Act including the formulation of Total Maximum Daily Loads (Boll et al., 1998).

NPS pollution is any form of pollution caused by diffusion processes of rainfall or snowmelt moving over and through the ground picking up, and carrying away natural plus human-made pollutants and depositing them into water resources (US EPA, 2010). NPS pollution encompasses transport of excess pollutants including nutrients, pesticides, fertilizers, and

pathogens into receiving waters (Walter et al., 2000). The sources of NPS pollution include pollutants from urban, forest, agricultural, and recreational lands. Agriculture is identified as a significant contributor of NPS pollution (Boll et al., 1998). Many environmental conservation agencies across the United States have particular concern about NPS pollution from farm fields as agriculture covers a major portion of the landscape in many parts of the country. The measures to control NPS pollution from agricultural fields have been incorporated in watershed management programs that maintain and improve water quality (Gérard-Marchant et al., 2005). The development of water management quality tools aimed towards reducing NPS pollution requires scientific understanding of hydrologic and transformation processes involved in pollutant transport (Agnew et al., 2006). Thus, tools that are in agreement with the current hydrological science are required to guide management decisions aimed at controlling the effects of nutrients and other agricultural chemicals on receiving water bodies.

The understanding of NPS pollutant dynamics is significant in setting up environmental protection plans for watersheds. Frankenberger et al. (1999) stated that watershed management strategy for controlling NPS pollution is to lessen pollutant loading on runoff source areas, and pollutant transport by runoff. The runoff generation process at a particular location within a watershed could be a combination of processes depending on climate, geology, topography, soil characteristics, and rainfall patterns (Leh et al., 2008). Erosion and runoff generation are such variable processes, and thus it's important to locate soil erosion areas and paths of sediment transport to alleviate soil loss problems and protect water quality within watershed (Kim and Steenhuis, 2001). Runoff from croplands is generated as a result of erosive events that carry sediments, nitrogen, and phosphorus loads downslope into existing water streams. Phosphorus and Nitrogen enriched runoff from cropland fields can led to detrimental water quality problems ranging from eutrophication of surface waters to death of aquatic animals such as fish (Andraski and Bundy, 2003; US EPA, 2010).

Soil erosion involves the detachment and transportation of soil particles by agents such as wind or water (Toy et al., 2002). Water erosion can be caused by rainfall, and surface runoff from rainfall and irrigation. The detached soil particles that result from runoff and erosion are deposited in receiving water bodies which cause sedimentation. Many water reservoirs across United States have lost their storage capacity mainly due to sedimentation from erosion. Sediment does not only carry soil particles but also carries nutrients that are found in the soil such as large amounts of nitrogen and

phosphorous. In addition, erosion decreases land productivity due to loss of top soil leading to high agricultural input costs for farmers. The locations and distances to which the eroded sediments are transported depend on the pathways of flow, and the potential for specific particles of sediment to be transported along those pathways. The mechanisms of soil erosion with its interaction with generated runoff are complex to understand, however, sheet, rill, and gully erosions are the terms used to differentiate transitions that occur during erosion process. It's understood that each of the transition stages of erosion contributes a proportion of both sediment and nutrient transport into water streams. Gully erosion adds to this problem when the overland flow accumulates silt and sediment in the water that results from eroding surfaces.

Studies indicate that ephemeral gully (EG) erosion contributes extremely to soil loss from agricultural fields as compared to other erosion types. EGs are defined as small channels eroded by concentrated flow that are filled by normal tillage only to reform again in the same location due to subsequent runoff events (Soil Science Society of America, 2015). Poesen et al. (2003) quantified that soil loss from EGs can reach as high as 94% of total soil loss from agricultural fields while (Bennett et al., 2000) stipulated that EGs typically contribute about 30% to total soil loss, but can reach as high as 100% in actively eroding areas in the United States. Within Kansas, EG erosion contributes up to 8 tons/acre/year of soil loss from agricultural fields (USDA NRCS, 1997). The quantity of soil loss attributed by both sheet and EG erosion in United States is indicated in Table 1-1.

The severity of EG erosion is often disguised by continued channel filling with soil during farm operations, which effectively diminish topsoil thickness over an area much wider than the EG itself (Gordon et al., 2008). EGs dissect agricultural fields, transferring sediment and associated agrichemicals from croplands to stream channels, thus degrading soil resources and adversely affecting water quality indices downstream. In addition, an EG is such a transitional landscape feature which possesses the characteristics of channel and hillslope erosion processes which makes it hard to be quantifiable because it requires information on landscape attributes that are not normally considered in hillslope and channel erosion assessment models (Nouwakpo and Huang, 2010). EG modeling may provide a valuable cost-effective alternative to comprehend the processes of EG erosion.

It's been problems associated with EG erosion that different agencies and departments within United States started developing management strategies aimed at reducing EG erosion from

agricultural fields. The USDA NRCS has tried delivering information to farmers about the conservation practices aimed at reducing erosion and nutrient loss from agricultural fields. Some of these practices include: grassed waterways, terraces, cover crops, and no till practices. The conservation strategies objected towards minimizing EG erosion require a proper understanding of watershed geomorphology and hydrology dynamics since EGs continue to form in the same location as long as topographic characteristics remain unchanged. The prediction of areas prone to EG formation forms a basis for the implementation of best management practices aimed at reducing soil erosion from agricultural fields.

Objectives

This study aims at assessment of EG erosion using both topographic and hydrologically based models within Little Ark watershed in Central Kansas. The specific objectives include:

i. Prediction of EG location and length using a suite of topographic index models
ii. Statistical assessment of model accuracy at predicting EG location and length.
iii. Erosion rate estimation using a combination of process-based hydrological and EG models.
iv. Assessment of selected conservation practices for reduction of EG erosion

Table 1-1: Comparison of soil losses due to sheet and rill erosion, and EG erosion in different states of United States (USDA NRCS, 1997).

Location	**Estimated sheet and rill erosion (tons/acre/year)**	**Measured EG erosion (tons/acre/year)**	**EG erosion as a percentage of sheet and rill erosion**
Alabama	15.60	9.30	59
Delaware	1.03	2.52	245
Illinois	7.10	5.2	73
Iowa	9.60	3.00	31
Kansas	21.98	8.00	36
Louisiana	17.80	6.04	34
Maine	11.21	5.15	46
Michigan	4.67	1.22	26
Mississippi	17.60	7.50	43
New Jersey	6.70	5.20	77
New York	23.77	5.05	21
North Dakota	7.54	3.55	47
Pennsylvania	2.53	1.78	71
Rhode Island	9.00	3.70	41
Vermont	4.50	6.10	136
Virginia	13.0	12.80	98
Washington	0.69	1.89	275
Wisconsin	7.87	4.19	53

Chapter 2 - Literature Review

Many studies have been conducted to understand the processes and conditions over which soil erosion occurs in a catchment. In what follows is a presentation of studies that have been presented to the erosion forms.

Soil erosion

Soil erosion refers to the detachment and transportation of soil particles by agents such as wind and water (Elliot and Laflen, 1993; Toy et al., 2002). Soil erosion by water presents the highest amount of soil loss in the world. Soil is essentially a non-renewable resource and a very dynamic system which performs many functions and delivers many services that are key to the ecosystem and human survival. It's been the role of reorganizing this purpose of soil that many studies are being conducted to comprehend the science of soil erosion across the world.

Soil erosion by water action

Soil erosion by water involve the transport and detachment of soil particles from land by water, including runoff from melted snow and ice (Rodney et al., 2013). The process of soil detachment and transport occurs primarily when the velocity of flowing water create a shear strength greater enough to overcome the cohesion forces between soil particles. Soil erosion due to water impact can be classified depending on the level of development within an area. The levels can take form of sheet, rill, EG, and classic gully erosion.

Water erosion rates are affected by rainfall energy, soil properties, slope, slope length, vegetative and residue cover, and land management practices. Kinetic energy from raindrops and runoff cause the removal of soil particles. Soil properties such as particle size distribution, texture, and composition influence the susceptibility of soil particles to be moved by the flowing water. There are possible relationships between topographic indices which consider watershed area and slope, and volumes of eroded soil from watersheds with the same climate, soil class, soil use and management. Due to their relatively small size, it is possible to assess the watershed topography and the eroded soil volumes quite accurately (De Santisteban et al., 2005).

Sheet erosion

Sheet erosion involves detachment of soil particles, and removal of a thin layer of soil from land by impact of flowing water, mainly overland flow from rainfall and runoff. Raindrops detach soil particles, and the detached sediment can reduce the infiltration rate by sealing the soil pores. The beating action of raindrops combined with surface flow causes initial riling. The eroding and transporting ability of overland flow depends on the rainfall intensity, infiltration rate, slope steepness, soil properties, and vegetative cover. Though sheet erosion is recognized form of erosion, it actions are instantaneous as it rarely occurs because small channels form almost concurrently with the initial detachment and movement of soil particles. The constant meander and change of position of these rills may obscure their presence from normal observation, hence establishing the false concept of sheet erosion.

Rill and inter-rill erosion

Rill erosion is the detachment and transport of soil by a concentrated flow of water. Rills are eroded channels that are small enough to be removed by normal tillage operations, and it's the predominant form of surface erosion under most conditions (Bruno et al., 2008; Nearing et al., 1997; Rejman and Brodowski, 2005). Rills exist shortly under field conditions, and are removed almost immediately by farmers (Rejman and Brodowski, 2005).The rill component of the erosion process is due to the channelized transport of the sediment particles both detached from the interrill areas and scoured from the rill wetted perimeter (Nearing et al., 1997). During erosive events, overland flow concentrates reaching a threshold which causes rill development resulting in high erosion rates. Rill formation is dependent on both the rilling resistance of the soil and some hydraulic characteristics of the channelized flow.

The rate of rill erosion is affected by hydraulic shear of the water flowing in the rill, the soil's rill erodibility, and critical shear, the shear below which soil detachment is insignificant (Flanagan and Nearing, 1995). There is still very limited information about the rainfall and flow characteristics that enable rill development under field conditions (Rejman and Brodowski, 2005). Bruno et al. (2008) stipulated that rill development is attributed to headcut migration and channel incision if morphological characteristics of the field are under consideration. The partition of the water erosion process on interrill and channelized components is widely recognized. In particular,

the channelized component, is due to the transport of the sediment particles both detached from the interrill areas and scoured from the channel wetted perimeter.

Ephemeral gully erosion

EGs are small channels eroded by concentrated flow, filled by normal tillage only to reform again in the same location due to subsequent runoff events (Soil Science Society of America, 2015). These incisions may form each year depending on the magnitude of the local rainfall events, but are easily erased by tillage activities. Carpra et al. (2009) EGs usually occur on cultivated land during rainstorms following seedbed preparation, planting and crop establishment periods EGs form in areas of concentrated flow that are invariably positioned on the landscape between hillslopes. It is this relationship to landscape position that distinguishes EGs from rills, which form due to overland flow and soil erosion on hillslopes (Foster, 2005). Classical gullies also form on hillslopes in areas of concentrated flow, but these features are relatively larger in size as compared to EGs. In addition, classic gullies tend to occur at the edge of fields rather than on fields, and they cannot be obliterated by common tillage operations.

EGs are identified as channels with a cross section area of one square feet with a depth of 20 cm (Capra, 2013; Poesen et al., 2003), and Poesen (1993) proposed a cross-section of 929 cm^2 to distinguish between rills and EGs. EGs usually start off as rills, but their cross-section may exceed 930 cm^2 until sedimentation occurs 20 to 50 m downslope on average (Vandekerckhove et al., 1998). The formation of EGs is affected by a combination of factors including climate, soil type, land use, lithology, vegetation cover, geomorphology, and topography (Capra, 2013; Poesen et al., 2003). The mechanism of EG evolution is strongly affected by processes causing soil stratification.

EGs may form under conditions where tilled topsoil is easily erodible, whereas the subsequent soil layer, not worked and compacted, is more resistant to erosion or even nonedible. After channel incision, the erodible layer will begin to erode the base of the channel banks and consequently the gully widens (Di Stefano and Ferro, 2011). Thus, simulation of EG processes and characteristics require a full understanding of dynamics that each factor offers to EG formation process and geometry. The summary of the characteristics and distinctions of rill, EG, and classical gully erosion were listed by Foster (1986) as illustrated in Table 2-1.

Table 2-1: Characteristics of rill erosion, EG erosion, and Classical gully erosion (Foster, 1986).

Rill erosion	**EG erosion**	**Classical gully erosion**
Rills are normally erased by tillage, and they don't reoccur in the same location	EGs are short-term features, normally covered by tillage and reoccur in the same location	Gullies are not covered by normal tillage operations
Rills are usually smaller than EGs	EGs are larger than rills but smaller than classical gullies	Gullies are larger than EGs
Rill cross sections tend to be narrow compared to depth	EG cross sections tend to be wide relative to depth; side walls are not frequently well defined, head cuts are usually invisible and are not prominent due to tillage	Gully cross sections tend to be narrow relative to depth, steep side walls, and prominent headcut
Rills occurs on smooth die slopes above drainage paths	EGs appear along shallow drainage ways upstream from incised channels	Gullies usually occur in well-defined drainage ways
Rill flow pattern develop due to small disconnected parallel channels merging to an EG, or terrace or points of deposition. Rills are generally spaced and sized	EGs usually form a dendritic flow pattern along water courses, beginning from areas of overland flow including rills, and areas of convergence. The flow patterns may be influenced by tillage, crop rows, and terraces	Gullies tend to form a dendritic flow pattern along natural water pathways, and a non-dendritic flow pattern along roads, ditches, terraces, and channel diversions.

Models for estimating sheet and rill erosion

The methods to predict upland soil erosion have been evolving to present computer based models. Field experiments have been used widely to understand processes that contribute to soil loss from upland areas. The statistical, empirical, and physical approaches have been used to develop models that are under use at simulating these processes. In what follows is a description of two modeling frame works that are widely used to estimate both sheet and rill erosion.

Universal soil loss equation (USLE)

The *USLE* is an index based, empirically derived model that estimates average annual soil loss by sheet and rill erosion on those portions of landscape profiles where erosion, but no deposition is occurring (Wischmeier and Smith, 1960). Originally developed for use on cropland though modifications were done to compute soil loss from rangelands, and urban areas. The model uses an empirical equation below, which was derived based on regression statistics of four major factors affecting erosion from large mass of field data. These factors include: climate erosivity represented by R, soil erodibility represented by K, topography represented by LS, and land use and management represented by CP.

$$A = R\ K\ L\ S\ C\ P$$

where is A computed soil loss, R is the rain fall-runoff erosivity factor, K is soil erodibility factor, L is the slope length factor, S is the slope steepness factor, C is cover management factor, and P is supporting practices factor. The description of the factors in the equation are outlined below.

R factor: Rainfall erosion index plus a factor for any significant runoff from snowmelt. It represents the input that drives the sheet and rill erosion process, and differences in values represent differences in erosion potential of the climate.

K factor: The soil-loss rate per erosion index unit for a specified soil as measured on a standard plot, which is defined as a 72.6 ft length of uniform 9% slope in continuous clean-tilled fallow, measure of the inherent credibility of a given soil under the standard condition of the unit *USLE* plot maintained in continuous fallow. The index values typically range from 0.10 to 0.4, with high-sand and high-clay content soils having the lower values, and high-silt content soils having the higher values.

LS factor: L = slope length factor, ratio of soil loss from the field slope length to soil loss from a 72.6-ft length under identical conditions, S = slope steepness factor, ratio of soil loss from

the field slope gradient to soil loss from a 9% slope under otherwise identical conditions. These indices define the role of topography in the erosion process.

C factor: The ratio of soil loss from an area with specified cover and management to soil loss from an identical area in tilled continuous fallow. It represents conditions that can be managed most easily to reduce erosion. The index values vary from near zero for a very well-protected soil to 1.5 for finely tilled, ridged surface that produces much runoff and leaves the soil highly susceptible to rill erosion.

P factor. The ratio of soil loss with a support practice like contouring, strip-cropping, or terracing to soil loss with straight-row farming up and down the slope. It represents how surface conditions affect flow paths and flow hydraulics.

USLE model represents the first-order effects of the factors that affect sheet and rill erosion. It does not estimate deposition like that at the toe of concave slopes, and it does not estimate sediment yield at downstream location (Foster et al., 2003; Wischmeier and Smith, 1978). The model does not include EG erosion, and does not also provide information on sediment characteristics, such as those needed in many water quality initiatives. The scientific limitation of the *USLE* as an empirically based equation is that it does not represent fundamental hydrologic and erosion processes explicitly (Renard et al., 1991; Tiwari et al., 2000). Considering the limitations of *USLE* model, modifications were done based on an extensive review of the model itself and its data base, and theory describing fundamental hydrologic and erosion processes leading to formulation of *RUSLE* model (revised *USLE).*

Foster et al. (2003) outlined the changes for estimating erosion by water in *RUSLE* which include:

- computerizing the algorithms to assist with the calculations,
- corrections for high R-factor areas with flat slopes to adjust for splash erosion associated with raindrops falling on ponded water,
- development of seasonally variable soil credibility term (K),
- sub factor approach for calculating the cover-management term (C), with the sub factors representing considerations of prior land use, crop canopy, surface cover, and surface roughness,
- new slope length and steepness (LS) algorithms reflecting rill to interrill erosion ratios, the capacity to calculate LS products for slopes of varying shape, and

- new conservation practice values (P) for rangelands, strip crop rotations, contour factor values, and subsurface drainage.

Revised Universal Soil loss equation version 2 (RUSLE2)

*RUSLE*2 is an advancement of the erosion prediction technology of the Revised Universal Soil Loss Equation (*RUSLE*), an erosion model for predicting longtime average annual soil loss from raindrop splash, and runoff from specific field slopes in specified cropping, management systems, and rangeland (Renard et al., 1997). The model computes sheet and rill erosion along one-dimensional hillslope profile, from the top of the hill where runoff begins to a location where runoff meets a concentrated flow channel (Vieira et al., 2015).

*RUSLE*2 currently cannot estimate concentrated flow erosion, which may be of a similar magnitude as sheet and rill erosion in fields experiencing EG erosion. It implements sediment transport methods that permit the determination of sediment deposition that occur in areas of reduced slope steepness frequently found in the concave areas. In addition, the model can't be used to estimate erosion rates within channels that end hillslope flow paths, and the locations where EGs may form (Vieira et al., 2015).

RUSLE and *RUSLE*2 are hybrid models that combine index and process-based equations though *RUSLE*2 expands on the hybrid model structure and uses a different mathematical integration (Foster et al., 2003). *RUSLE* and *RUSLE*2 have the capability to compute deposition on concave slopes, at dense vegetative strips, in terrace channels, and in sediment basins using process-based equations for transport capacity and deposition (Renard et al., 1991). *RUSLE* computes deposition as a function of soil texture.

*RUSLE*2 splits sediment into five particle classes based on soil texture. *RUSLE*2 treats each particle class separately with interaction among the classes. *RUSLE*2 computes deposition as a function of soil texture and how deposition changes sediment characteristics along the slope, which in turn affects computed deposition (Foster et al., 2003). *RUSLE*2 has the potential to compute the ratio of specific surface area of the sediment to specific surface area of the soil subject to erosion for the sediment exiting the end of the slope.

Water Erosion Prediction Project (WEPP)

WEPP is a physically based, distributed parameter model that has been used widely to simulate the physical processes related to runoff, soil erosion, percolation, and infiltration at

hillslope and watershed scales (Flanagan and Nearing, 1995; Licciardello et al., 2007). *WEPP* is based on fundamentals of infiltration, surface runoff, plant growth, residue decomposition, hydraulics, tillage, management, soil consolidation, and erosion mechanics (Nearing et al., 1989).

The *WEPP* erosion model is a continuous simulation computer program which predicts soil loss and sediment deposition from overland flow on hillslopes, soil loss and sediment deposition from concentrated flow in small channels, and sediment deposition in impoundments (Flanagan and Nearing, 1995). The model simulates detachment and transport processes explicitly and reorganizes that runoff is a factor determining soil loss. The equations of sediment continuity, detachment, deposition, shear stress in rills, and transport capacity are employed by the *WEPP* model to simulate soil detachment, transport processes, and deposition within rills (Foster et al., 1995). A simple means for predicting the location of EG initiation is needed by *WEPP* (Flanagan and Nearing, 1995), and the model doesn't account for changes in hillslope morphology when gulley erosion occurs. The WEPP model offers more advantages as compared to the *USLE* and *RUSLE* models which include: ability for predicting spatial and temporal distributions of net soil loss, the capability to better predict off-site delivery of sediment, including particle size information (Nearing and Nicks, 1998)

Ephemeral gully modeling

Modeling of processes leading to formation of EGs can take physical, empirical or combination of both approaches. A physical approach usually involves comparing of soil sheer stresses applied on bottom and side walls of an EG, while an empirical includes analysis of gully data and developing conclusions depending on statistical results. Though EG erosion was given little attention in the past, today different tools and approaches have been developed to estimate soil loss due to EG erosion on cropland fields.

Topographic index models

Topographic index (TI) models have been used in the physical interpretation of processes leading to formation of EGs mainly because of their simplistic nature (Vandekerckhove et al., 1998). The previous advancements in studying of EGs have depended on topographical factors of slope and contributing area as indicators of the potential areas for EG formation (Daggupati et al., 2013; Desmet et al., 1999; Moore et al., 1988; Poesen et al., 2003; Prosser and Abernethy, 1996). The identification of areas with high potential for EG development is often performed using

spatially derived stream power estimates from topographic indices of contributing area (A) and slope (S) (Momm et al., 2013; Moore et al., 1988; Prosser and Abernethy, 1996). Moore et al. (1988) predicted the location of the entire EG trajectory using two topographical indices relating to subsurface and overland flow measured using AS and ln(A/S).

Montgomery and Dietrich (1988) observed strong inverse relationships between contributing area and slope at channel heads from field measurements over several catchments. The catchment area alone, however, does not define the EG network well, as it over predicts channels on the low-gradient foot slopes (Prosser and Abernethy, 1996). The SA model (Moore et al., 1988) was introduced as a measure of erosive power of flowing water based on assumption that discharge is proportional to specific catchment area. The model predicts net erosion in areas of profile convexity and tangential concavity, and net deposition in areas of profile concavity (Fotheringham and Wegener, 1999; Wilson and Gallant, 2000).The slope area power, AS^2 model, (Montgomery and Dietrich, 1992), measures the variation of stream-power when predicting the locations of headcuts of first-order streams (i.e., channel initiation).

The wetness topographic index (WTI), (Moore et al., 1988) represented by, (ln (A/S).), assumes steady-state conditions and uniform soil properties. The index predicts zones of saturation encountered along drainage paths and in zones of water concentration in landscapes. The correlation of slope and catchment area can be considerably strengthened by including additional information on planform curvature (Vandekerckhove et al., 1998). The compound topographic index model (CTI) was introduced by (Thorne et al., 1986) as a measure of the power of streams to erode soils within the watershed. CTI considers topographic attributes such as upstream drainage area, slope, and plan of curvature as topographic controls in the formation process of EGs (Daggupati et al., 2014).

There are modifications to TI methodology that have been made to include factors relating to soil properties such as hydraulic conductivity, critical shear stress, and depth to restrict layer, and resistance to overland flow (Dietrich et al., 1992; Dietrich et al., 1993; Prosser and Abernethy, 1996). McCuen and Spiess (1995) introduced the kinematic wave approach as indicator of locations within the catchment where sheet flow changes into concentrated flow. The kinematic wave equation (nLS) and modified kinematic wave equation (nLSCSS) are closely associated with soil and overland flow characteristics of the catchment. These models determine the occurrence of the transition from overland flow into concentrated flow, and thus can be used to locate areas with

higher erosion potential, possibly where EGs are likely to begin forming (Bennett et al., 2000; Kim, 2006). A threshold concept is used for predicting EG initiation points using topographical information such as digital elevation model (DEM) (Vandekerckhove et al., 1998). Montgomery and Dietrich (1988) suggested a requirement of a threshold over which EGs form, however, obtaining that threshold value for each model is still a subject understudy up to now.

The main morphological characteristics of EG include length, width, and depth (Capra, 2013). Casali et al. (1999) classified EG occurring in the same field in Spain based on EG characteristics of top width, bottom width, depth, length, and width-to-depth ratio. EG characteristics such as length serve as useful parameter in process based models such as *EGEM* (Nachtergaele et al., 2001a). Nachtergaele et al. (2001b) showed that *EGEM* cannot be used to predict EG volumes since EG length is among the input parameters. Souchere et al. (2003) showed relevance of developing models which are able to predict location, length and cross-sectional area of EGs. The critical EG length is interpreted as a requirement to generate a boundary shear stress of hortonian overland flow sufficient to overcome surface resistance to scour (Prosser and Abernethy, 1996). In addition, length analysis provides a better understanding of soil volume that can be transported within a channel (Nachtergaele et al., 2001b). The length analysis approach is further used to simulate EG erosion using Annualized Agricultural Non-Point Source (*AnnAGNPS*) model (Gordon et al., 2007; Taguas et al., 2012).

TI models have been widely applied to predict the locations of channel initiation points within the catchment, however, few studies have been conducted to comprehend the prediction of EG length using TI (Daggupati et al., 2013). In addition, predicting EG location lacks a direct methodology for comparison and evaluation of the predictive potentials of threshold conditions for EG initiation, and thus an optimal prediction has to be a conciliation between the total numbers of predicted pixels where EGs are located (Desmet et al., 1999). TI application is further exacerbated by variation of model thresholds from one watershed to another, or on the small scale from, from catchment to catchment, mainly due to variation in topographic factors from one point to another within the catchment (Daggupati et al., 2013). The choice of model type to be used is uncertain as models exhibit different accuracies at prediction of EG characteristics within the watershed.

The variation of model accuracy is attributed to factors such as geology, soils, climate and vegetation of the watersheds (Vandekerckhove et al., 1998). The setbacks to application of TI in

identifying EG location and related EG characteristics can be solved by using automated geospatial tools such as *ArcGIS* which reduce time and uncertainties involved in evaluating TI thresholds (Momm et al., 2012). Thus, accurate prediction of EG location and length requires optimization of TI model thresholds for each catchment within the watershed.

EG Process-based models

Modeling of process leading to formation of EGs can take physical approach, empirical approach or combination of both approaches. A physical approach usually involves comparing of soil sheer stresses applied on bottom and side walls of an EG, while an empirical includes analysis of gully data and developing conclusions depending on statistical results. One possible approach is simplifying the modeled hydrological processes and representing the key catchment attributes, such as topography, soils, land use, and drainage network, in some skillful manner (Ivanov et al., 2004).

There are increasing requirements for predictive models of distributed hydrological processes, often to be the basis for further predictions of water quality, erosion, or the effects of different localized management strategies (Quinn et al., 1991). Distributed models can serve to elucidate the complexity of hydrologic processes interacting in time and space. The current generation of operational hydrological models lag in the use of information describing the interior watershed structure and in the representation of processes in a spatially distributed form (Ivanov et al., 2004).

Limburg Soil Erosion Model (LISEM)

LISEM is an event based spatially physical distributed model that has been used to model changes in EG geometry characteristics, and also to determine potential areas of channel initiation within a catchment (Jetten and de Roo, 2001) The model simulates splash erosion within a catchment basing on kinetic energy of rainfall, while flow erosion and deposition are simulated basing on the transport capacity of flowing water. The unit stream power approach is used to compute the available energy for transport of soil particles. The areas within a catchment that are susceptible to erosion are predicted using the wetness topographic index model.

The model assumes a rectangular cross section of the gullies, and erosion is distributed equally over channel perimeter. In addition, the simulated incisions are considered gullies if their cross section exceeds 929 cm^2. The model further assumes that lateral erosion takes place relative

to partitioning of soil strength if a soil subsurface layer with a higher bulk density exists. The model requires the DEM as main data input along with a soil parameters such as saturated hydraulic conductivity and depth to restrictive layer. The model over predicts erosion rates on fields with high vegetation cover (Takken et al., 1999)

Ephemeral Gully Erosion Model (EGEM)

EGEM is a two dimensional physical model that has been used to simulate channel incision along a transect (Woodward, 1999). The model is a modification of the Agricultural Research Service Ephemeral Gully Estimate Computer model, developed to address EG erosion on agricultural fields. The model simulates the development of ephemeral gullies through incision and head cut migration in spatially varied and unsteady flows, while addressing sediment transport and deposition, gully widening, and gully reactivation due to subsequent runoff events (Gordon et al., 2008; Gordon et al., 2007).

EGEM uses the NRCS curve number, drainage area, watershed flow length, average watershed slope, and 24 hour single rainfall and standard NRCS temporal rainfall distributions and physical equations to compute the width and depth of EGs. The erosion from concentrated flow is driven by the peak discharge and runoff volume within the watershed. The mechanics of erosion within the model were copied from *CREAMS* model. The regression equations are used to estimate initial channel width depending on duration of runoff. Like other models, *EGEM* assumes a rectangular cross section of the channel, with narrowing in the upstream direction. The channels erode up to a more resistant soil layer, and to a maximum channel depth of 18 inches. The model requires soil data, watershed data, rainfall data, and identification information as inputs. In addition, the model requires the input of landscape positions where the initiation of an EG is expected so as to model conservation planning requirements.

Annualized Agricultural Non-Point Source model (AnnAGNPS)

AnnAGNPS is a continuous, distributed parameter model, simulating surface-runoff volume, peak flow rate, sediment and pollutant transport from an agricultural watershed (Bingner et al., 2009). The model is the continuous version of the single event Agricultural Nonpoint Source model, AGNPS. *AnnAGNPS* was developed to facilitate assessment of watershed and landscape processes affecting agricultural areas. The basic modeling components are hydrology, sediment,

nutrient, and pesticide transport, although the present study was concerned only with the hydrology and sediment modules (Taguas et al., 2012).

The primary strength of *AnnAGNPS* lies in its ability to simulate runoff, sediment yields, and pollutant transport on hillslopes as affected by agricultural activities and best management practices through the use of well-established numerical methods and techniques (Gordon et al., 2007). Within *AnnAGNPS*, the watershed is divided into cells that have uniform slope, soil type, land use, and land management, and the model uses the soil erosion routines of the Revised Universal Soil Loss Equation (*RUSLE*) to predict soil loss for each cell.

The minimum spatial units where the main physical processes are modeled are represented by the cells of a watershed that are defined as land area with homogeneous bio-geophysical properties, used to provide spatial variability in the landscape and determined from climate, land use, soil properties and topographical information. The topographical parameters "critical source areas" and "minimum source channel lengths" are required by TOPAGNPS to represent landscape in cells and streams. The constituents are routed from their origin within the cells and are either deposited within the cells, the stream channel system, or transported out of the watershed (Bingner et al., 2009).

Recently, modifications and development have been made within the *AnnAGNPS* model to include processes relating EG formation. A tillage-induced EG erosion module (*TIEGEM*) is implemented in *AnnAGNPS* to estimate changes in EG geometry and also predict sediment yield from EGs. *TIEGEM* is based on modification of *REGEM* (Gordon et al., 2008; Gordon et al., 2007), which incorporates plunge pool formation and headcut retreat but with plunge pool depth restricted by a non-erodible layer (Alonso et al., 2002). *TIEGEM* operates within single or multiple storm events in unsteady, spatially varied flow with watershed contributing area determined as described by (Theurer et al., 1996).

TIEGEM has five optional EG width algorithms, and determines sediment delivery to the mouth of the channel, and therefore the flow transport capacity, using HUSLE (Hydro-geomorphic Universal Soil Loss Equation) procedures (Dabney et al., 2010). Both *CREAMS* and *TIEGEM* discretize sediment into five particle-size classes, assume a permanently non-erodible layer exists at some depth that is commonly taken as either the deepest or last tillage depth, and allow for gully repair and reset when fields are tilled.

Revised Ephemeral Gully Erosion model (REGEM)

REGEM was developed to address two problems that *EGEM*, *CREAMS*, and *WEPP* models were facing (Gordon et al., 2006). The problems include: for any material to be detached, the amount of sediment carried by the water must be below transport capacity, thus deposition cannot be simulated; and (2) soil particle diameter and specific gravity were simplified to some dominant value, the soil material delivered to the mouth of the ephemeral gully contains the same ratios of clay, silt, sand and aggregates as the soil in situ (Gordon et al., 2006).

REGEM incorporates analytic formulations for plunge pool erosion and headcut retreat within single or multiple storm events in unsteady, spatially-varied flow at the sub-cell scale (Dabney et al., 2010). The model employs sediment continuity equations for five soil particle-size classes to predict gully evolution and transport capacity. The event-based simulations demonstrate the model's utility for predicting the initial development of an EG channel, while continuous simulations allow the channel to evolve over multiple runoff events accounting for seasonal variations in management operations and soil conditions (Dabney et al., 2010; Gordon et al., 2006).

Four fundamental improvements were integrated within *REGEM* to overcome major limitations of current technology. They include: (1) storm events as unsteady, spatially-varied flows; (2) addressing the upstream migration of a headcut, thereby removing the EG length as an input parameter; (3) determining channel width from discharge, allowing channel dimensions to be explicitly predicted at any point in time and space; and (4) routing five distinct particle-class sized (clay, silt, sand, and small and large aggregates) through the gully and the downstream sorting of these sediments.

Chemical, Runoff, and Erosion from Agricultural Management Systems Model (CREAMS)

CREAMS simulates EG erosion through a procedure that takes into account detachment of soil due to shear of flowing water, sediment transport capacity, and changing channel dimensions (Knisel, 1980). It was one of the first models that have been widely used. In *CREAMS*, EG erosion is calculated through a procedure that assumes soil detachment occurs from the shear force and unsatisfied transport capacity of flowing water in a flat-bottomed but enlarging channel. The equations that describe change in channel dimensions were developed by (Foster and Lane, 1983). Haan et al. (1994a) provide a derivation of the channel erosion theory represented by the process based equations used in *CREAMS* to describe EG erosion.

The theory is based on several assumptions: (1) that Manning's equation applies, (2) that the shear stress distribution around the cross section of a channel can be represented by a hard-coded dimensionless distribution, (3) that the soil consists of a uniform erodible layer with characteristic erodibility and critical shear stress values overlying a non-erodible layer at a specified depth, (4) that potential detachment rate is proportional to excess shear stress, (5) that actual detachment is proportional to the unsatisfied transport capacity of a steady-state runoff rate, (6) that transport capacity can be determined by the set of equations proposed by Yalin (1963), and (7) that deposition occurs if sediment load exceeds transport capacity.

TIN-based real-time integrated basin simulator *(tRIBS)* model

tRIBS is a physically-based, distributed hydrological model that uses triangulated irregular network (TIN) in spatial discretization of hydrologic parameters (Ivanov et al., 2004). TINs offer the flexibility required for treating large watersheds while capturing the basin hydrologic features efficiently (Francipane et al., 2012; Vivoni et al., 2004). The model stresses the role of topography in lateral soil moisture redistribution accounting for the effects of heterogeneous and anisotropic soil (Francipane et al., 2012; Lepore et al., 2013). *tRIBS* explicitly considers spatial variability in precipitation fields and land-surface descriptors, with a potential to resolve basin hydrologic response at very fine temporal (hourly) and spatial (1 to 100 m) scales.

tRIBS includes parameterizations of rainfall interception, evapotranspiration, infiltration with continuous soil moisture accounting, lateral moisture transfer in unsaturated and saturated zones, and runoff routing (Ivanov et al., 2004). The improvements to the *tRIBS* model include modeling of hillslope and channel processes related to erosion formation processes. A geomorphic component was incorporated into *tRIBS* model to simulate main erosive processes of hillslopes (raindrop impact detachment, overland flow entrainment, and diffusive processes), and channel (erosion and deposition due to the action of water flow) (Francipane et al., 2012). The model computes sediment transport discharge and changes in elevation, which are updated in hydrological dynamic part of the model through local changes of terrain slope, aspect, and drainage network configuration.

The process of infiltration is simulated by postulating gravity-dominated flow in a sloped, vertically heterogeneous and anisotrospic soil. The unsaturated and saturated zones are coupled together accounting for the interaction of moving infiltration front with a variable water table. The

magnitude of lateral moisture transfer in unsaturated zone is controlled by topography and soil. Runoff generation is made possible via four mechanisms: saturation excess (Dunne and Black, 1970), infiltration excess (Horton, 1933; Loague et al., 2010), perched subsurface stormflow (Weyman, 1970), and groundwater exfiltration (Hursh and Brater, 1941). The runoff is obtained by tracking the infiltration fronts, water table fluctuations, and lateral moisture fluxes in the unsaturated and saturated zones. Currently, runoff is assumed to propagate downstream within the step of one hour, which limits the scale of application of the model to headwater catchments.

Soil detachment due to rain drop impact is simulated considering the influence of rainfall and soil characteristics, ground and canopy cover, and water flow depth over soil. The conceptual approach of Wicks and Bathurst (1996) is used to assess the rate of soil detachment by raindrop, Rain action is split between the action due to the direct raindrop impact and the effect of leaf drip. The overland and channel erosion processes of transport and deposition are modeled using the shear stress-based formulations for the entrainment and transport of sediment by runoff discharge (Nearing et al., 1999).

The calculation of erosion starts at the voronoi cell with the highest elevation and proceeds downstream to the basin outlet cell: For each computational element, the rate of soil detachment by raindrop and entrainment capacity rate, and transport capacity rate are calculated. For each cell a potential rate of transport-limited erosion is computed using the control volume approach of mass continuity equations, while detachment/entrainment-limited erosion rates are calculated based on the sum of detachment and entrainment capacity rates. Finally, the two rates are compared to determine changes in elevation due to deposition and erosion. At the hourly scale, the model updates the elevation of each voronoi element and re-computes slopes, azimuthal aspects, flow directions, and drainage areas of the entire voronoi polygon network, as well as re-sorts nodes following the topography-dictated network order. The latter is determined based on local maximum surface slopes and thus leads to a continuously updated drainage pattern. An update of all of the above terrain elements contributes to response from geomorphic processes of erosion and deposition to the watershed hydrological dynamics. More information about the *tRIBS* model and its structure can be obtained from (Francipane et al., 2012; Vivoni et al., 2004).

Foster and Lane model

Foster and Lane (1983) formulated an EG model to simulate changes in EG geometry for steady state flow though extensions to varying flow rates. The model assumes the changes in EG dimensions to be correlated to factors of flow rate, hydraulic roughness, soil surface slope, soil erodibility, and critical shear stress (Nachtergaele et al., 2002). The model stipulates that the shear stress is distributed equally over the channel wetted perimeter, with the maximum shear stress at the center of the channel bed, and minimum shear stress at the intersection of the channel wall and the water surface. During the simulation of erosion process, a channel is assumed to be rectangular in shape, and continue to erode till it reaches a non-erodible layer. Thereafter, the channel starts to widen laterally depending on factors relating to detachment and flow rates within the channel as indicated in Figure 2-1. The model comprises of four components: (1) an equilibrium channel width component, (2) a component for conveyance function, (3) channel erosion component l prior to reaching a non-erodible layer, and (4) a channel erosion component after reaching a non-erodible layer.

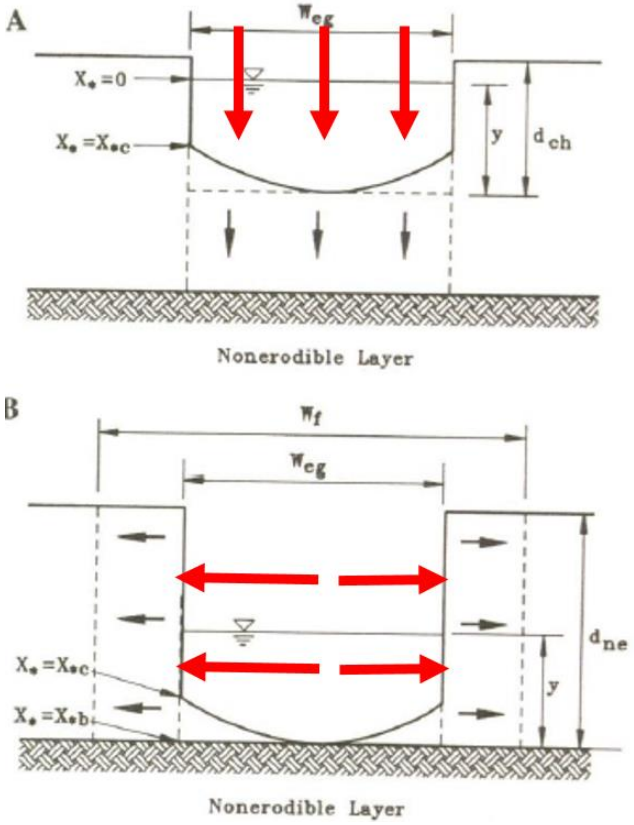

Figure 2-1: Description of transitions in channel cross section assumed by Foster and Lane model.

A description of all model components and associated equations is presented in Appendix F. The model computes the soil detachment rates based on Eq. (F-1) as a function of computed shear stresses within the channel. The distribution of shear stress within the channel is assumed to be symmetrical (Figure 2-1) and the symmetrical distribution of shear defined by Eq. (F-2). The potential stream power to erode channel particles was calculated using the conveyance function at the center of the channel in Eq. (F-3). Prior reaching to the non-erodible layer, the channel is assumed to erode vertically with an equivalent width and potential erosion rate is calculated Eq. (F-4). By knowing the erosion rate and computing the shear stress (from Eq. (F-5)) at this point, the maximum rate downward movement is estimated using Eq. (F-6). The potential rate of widening at this channel stage is computed using Eq. (F-7) with an equilibrium width defined by Eq. (F-8).

Chapter 3 - Methods and Materials

This chapter describes procedures that were used to obtain the results of this study. The tools and approaches that were used are also presented. In what follows is a detailed description of each process.

Study area

This study was conducted in Running Turkey watershed and Dry Turkey watershed, two watersheds in the Little Ark River watershed, South-Central Kansas. The watersheds are located in McPherson County, and characterized by the geological conditions of Arkansas River lowlands. These two paired watersheds receive an average precipitation of 831 mm annually. The average snowfall is 43 cm and annual temperatures range from 6 ^{0}C to 19.6 ^{0}C. The monthly variations in precipitation and temperature within the study area are illustrated in Figure 3-1.

The Kansas Department of Health and Environment (KDHE) drafted watershed plans aimed towards implementing BMPs to address impairments from nutrients, sediment, atrazine, and bacteria in both watersheds (KDHE, 2015). Grassed waterways, terraces, and vegetative buffers are some of the BMPs that KDHE suggested to gain reasonable amounts of pollution load reduction per each dollar spent from these watersheds. KDHE targets 52% reduction in total suspended solids (TSS), and 73% reduction in total phosphorus (TP). It's expected that meeting these BMP targets will result into TP and TSS load reductions by about 2,000 kg/year and 22,000 kg/year, respectively. These KDHE water restoration plans that motivated us to conduct a study aimed at improving the understanding and quantifying EG erosion processes on cultivated croplands in Midwestern watersheds.

Running Turkey watershed

Running Turkey watershed occupies approximately 9,137 ha. The land uses within the watershed are: agriculture (79%), developed land (7.3%), wetlands (0.4%), forests and shrubs (13%), and water (0.2%) as illustrated in Figure 3-3. Grassed waterways and terraces are two structural best management practices that are used to control EG erosion within the watershed. The survey conducted in 2014 estimated EGs to cover more than 3% of the watershed area under agricultural production, and occur at slopes ranging from 0.02% to 6.65%. The dominant soils in the watershed are silt clay loam and silt loam. The major crops are corn, wheat, and sorghum. The

dominant soil management conservation is conventional tillage though varies depending on the season.

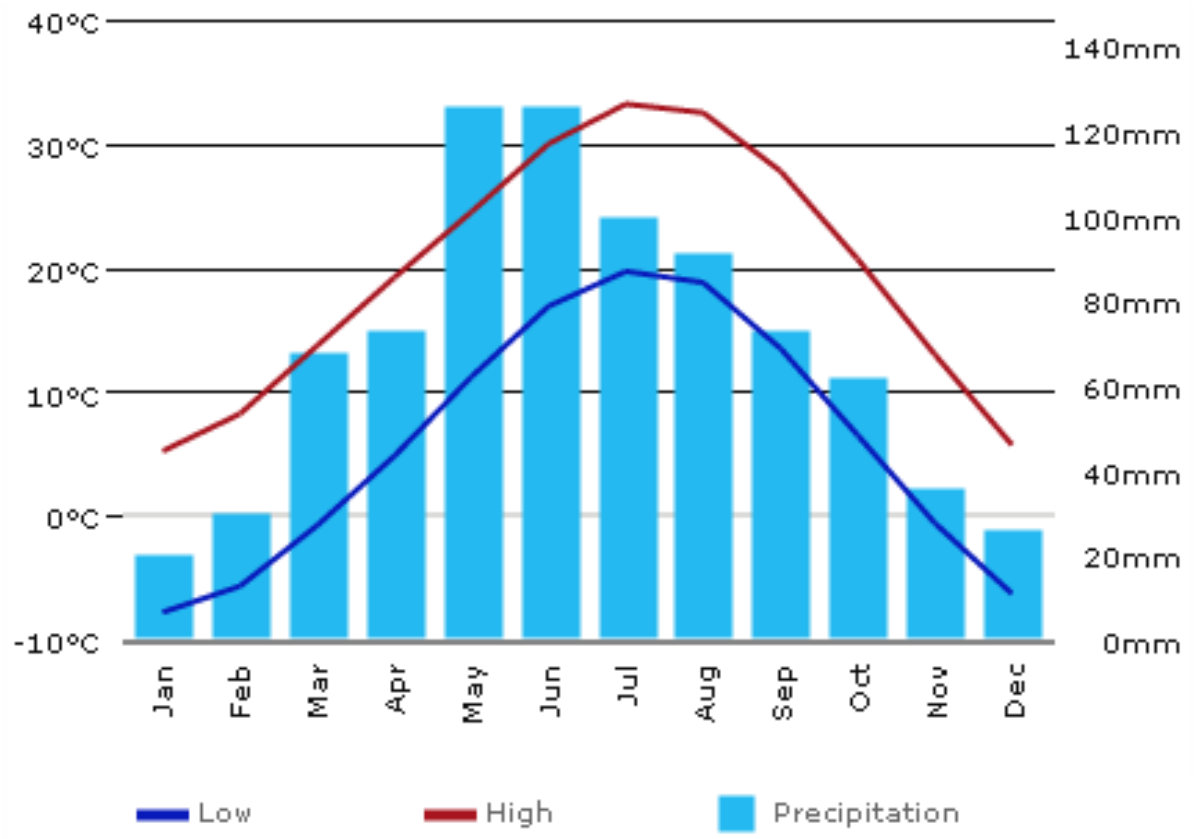

Figure 3-1: Monthly variation of precipitation and temperature for McPherson county for the year 2014 – 2015.

Dry Turkey watershed

The watershed covers approximately 9,525 ha. The land uses in the watershed are; agriculture (77%), grassland (11%), and developed land (6%), forest (4 %), and other land uses (2%) as shown in Figure 3-4. The dominant soils within the watershed are silty clay loam, silt loam, and loam soils. The watershed has 513 terraces and 94 grassed waterways according to the survey carried out in 2014, and EGs occur at mean slopes of 1.62%. Major crops planted in the watershed include: corn, wheat, soybeans, sorghum, and alfalfa.

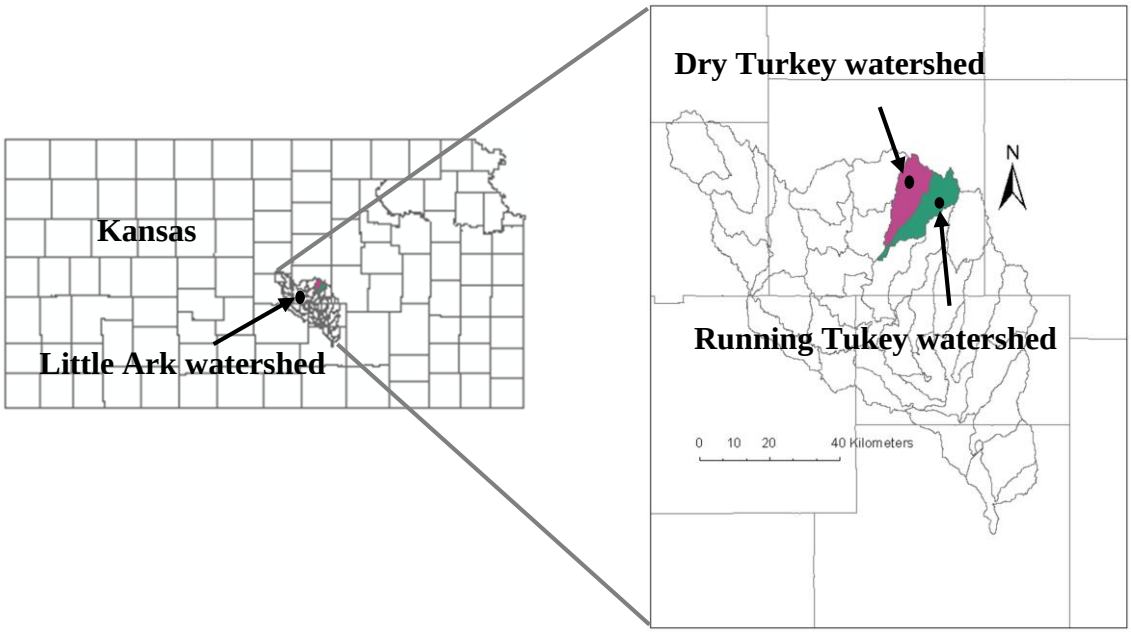

Figure 3-2: Map of the study area showing the location of Running Turkey and Dry Turkey watersheds.

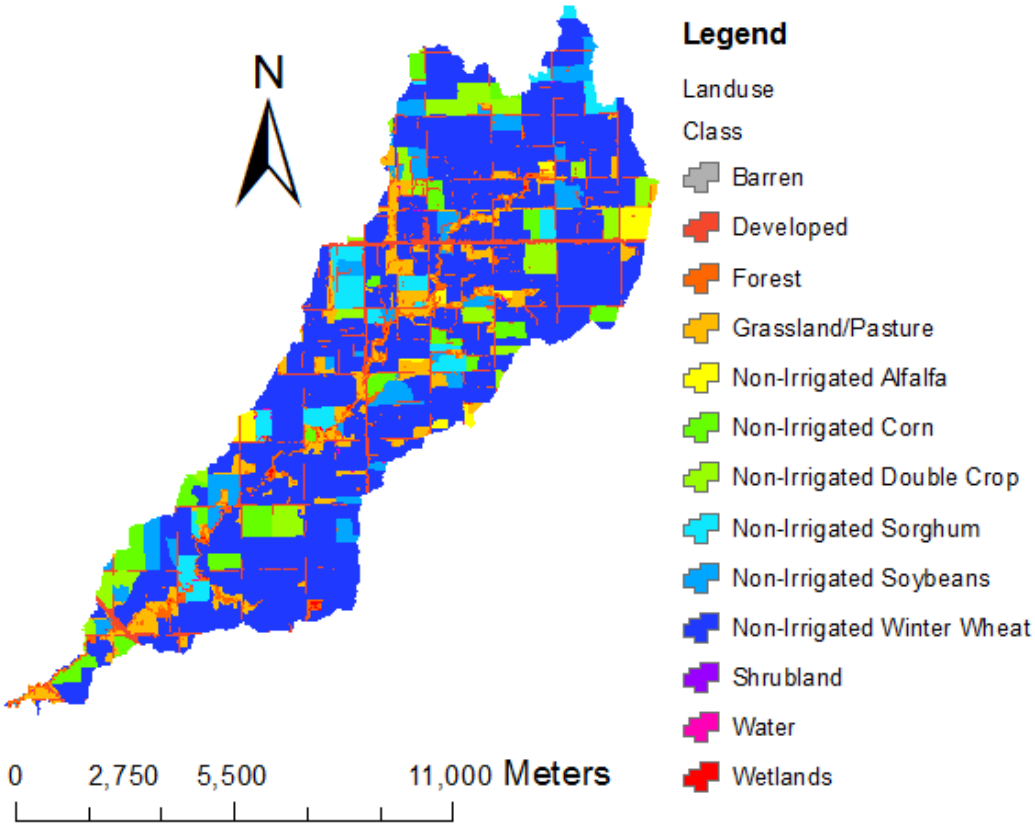

Figure 3-3: Land use classes in Running Turkey watershed.

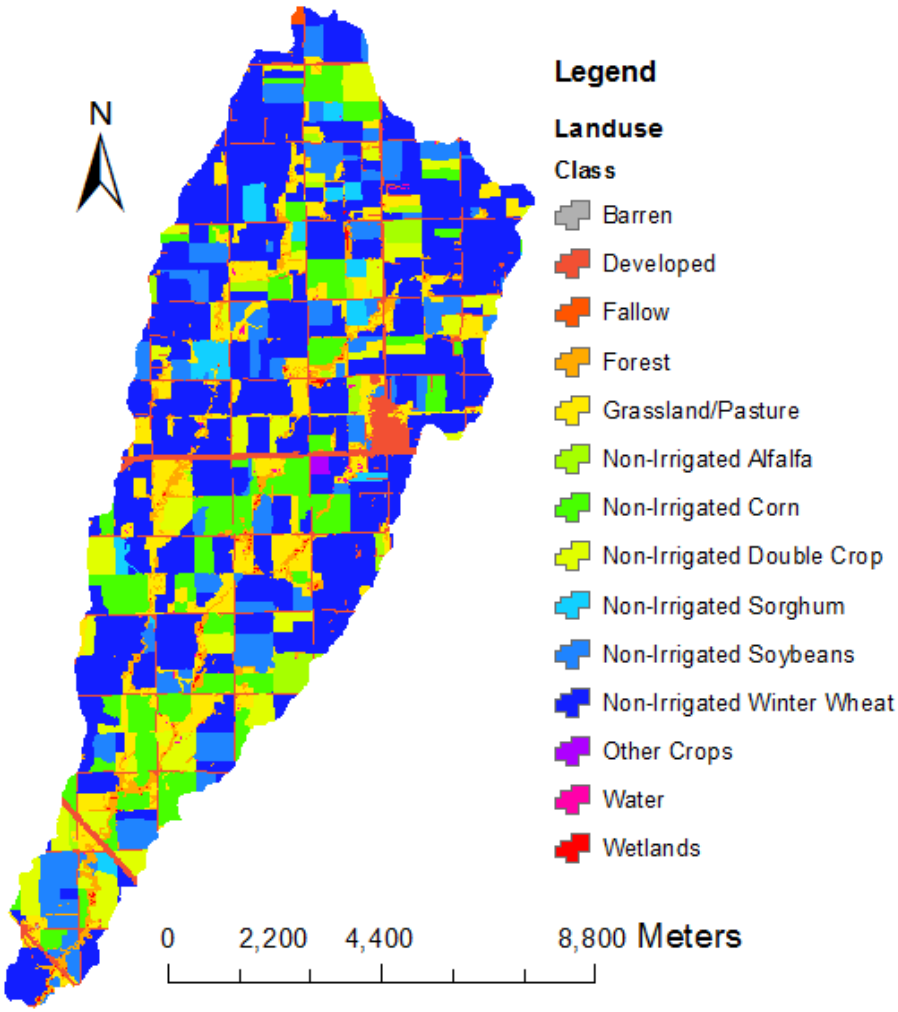

Figure 3-4: Land use classes in Dry Turkey watershed.

Observed EG identification

The high resolution (30 cm) historical imagery from 2003 to 2014 from Google Earth (2014) were used to track locations where EGs have been forming within the time period (Figure 3-5). Aerial images of each field were reviewed for presence/absence of any EGs. A geographical information systems (GIS) from Environmental System Research Institute (ESRI, 2012) was used to create an attribute layer of digitized EGs. The starting and ending points of the EG were identified depending on connectivity in color change from green (or light gray) to darker color of bare soil. The color change was further supplemented by expert judgment of the author and shaded hillslope maps from 1-m LIDAR dataset. There were cases when visualizing the location of EGs was impossible due to dense plant canopy. In such instances, the presence of EGs was confirmed by reviewing EG presence for the years when no cultivation was being done. After observed EG

identification, the observed EGs were intersected with catchments to obtain the total number of catchments with observed EGs.

Field reconnaissance was conducted to confirm the location of field EGs, natural streams, grassed waterways, and culverts within the watershed. This was accomplished by driving along the main roads and streets and confirming EG locations with the map of digitized EGs. Thereafter, the field data were compiled and the shapefile of digitized EGs was updated to include culverts, terraces, grassed waterways, and natural streams. The developed GIS dataset was used to generate maps of erosion risk fields within the watershed. The mapping process involved computing the total length of EGs within each filed. A natural breaks (Jenks) reclassification method provided in ArcGIS was employed to create three (low, medium, and high) erosion risk classes. It is important to note that the agricultural fields with no EGs and classified as low or no-risk may have classic and/or rill channels. This methodology was applied to both watersheds, and summaries of each watershed were generated.

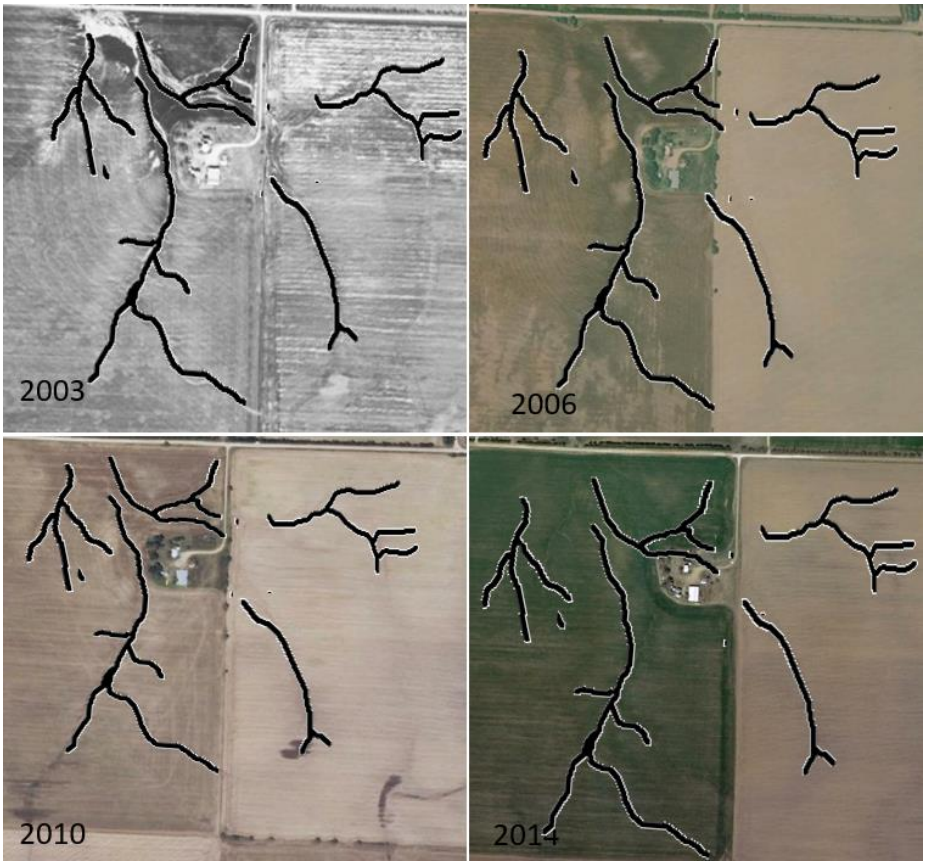

Figure 3-5: Field digitizing of EGs for different years.

The maps of culvert locations generated during this process were used to pre-process the digital elevation model (DEM) by burning streams at spots where culverts were located. The culvert locations in this contest also refer to points where streets and roads restrict flow from fields even if points might lack physical culverts. A dataset of natural streams that were identified during the digitization process was compared with the National Hydrography Dataset (NHD) from the United States Geological Survey (USGS). An updated layer of natural streams was generated to be used in the final refinement of predicted EG location datasets from topographic index models.

DEM pre-processing:

A 3 meter digital elevation model (DEM) acquired from National Resources Conservation Service- Geospatial Data Gateway (USDA NRSC, 2014) was used in the study. The DEM was preprocessed before any geospatial computations were conducted. The process involved burning of streams at points which had culverts as indicated in Figure 3-8 and Figure 3-9. This facilitates continuous routing of flow from any point within any catchment to watershed outlet. The method also provides accurate determination of contributing area for EGs that cross streets and fields. In addition, this method eliminates the effects of "digital dams" within the catchment that might lead to low accuracy at computation of TI values. "Digital dams" (Figure 3-7 A) are usually formed in areas where there is restriction of flow due to presence of culverts, roads, streets, or forest buffers. A GIS model **(**Figure 3-6) was set up in ArcGIS Model Builder to process all the necessary computations to alleviate this problem. The pre-processed DEM (Figure 3-7 B) was then used in the proceeding steps of parameter derivation required in computation of TI values by TI models.

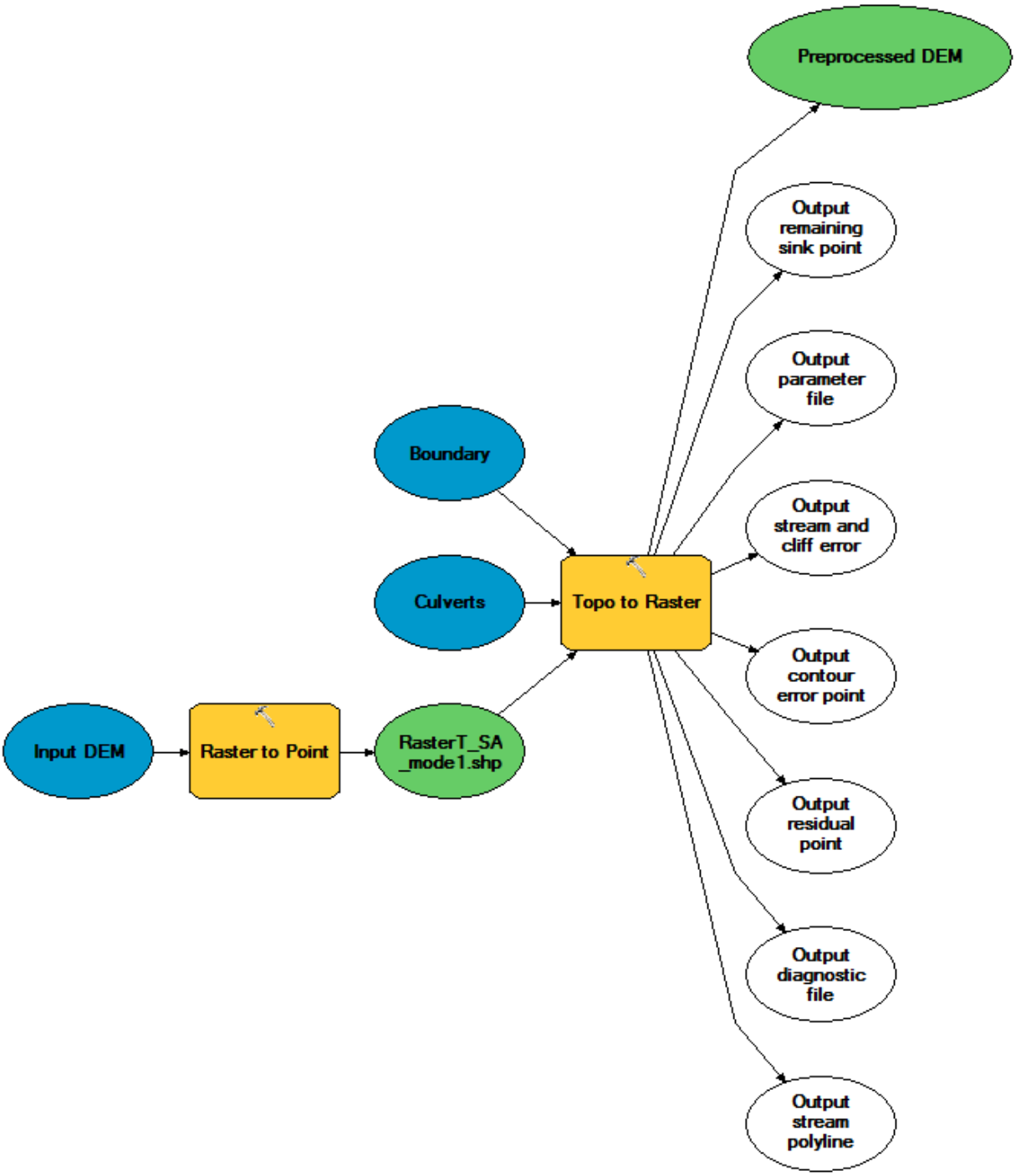

Figure 3-6: Flowchart of DEM pre-processing procedure.

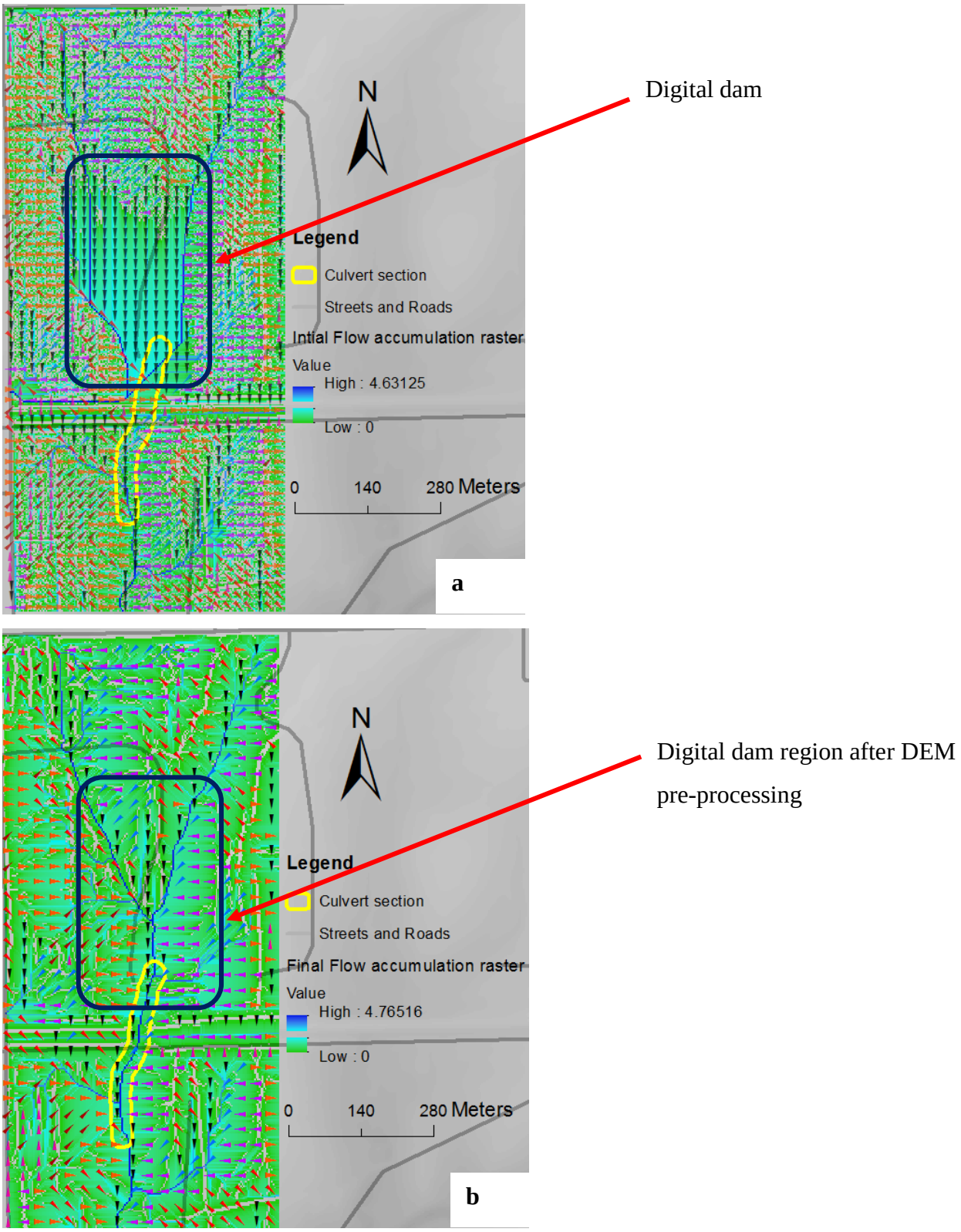

Figure 3-7: Changes in flow accumulation grid before (a) and after (b) DEM pre-processing. The arrows of different colors indicate flow directions.

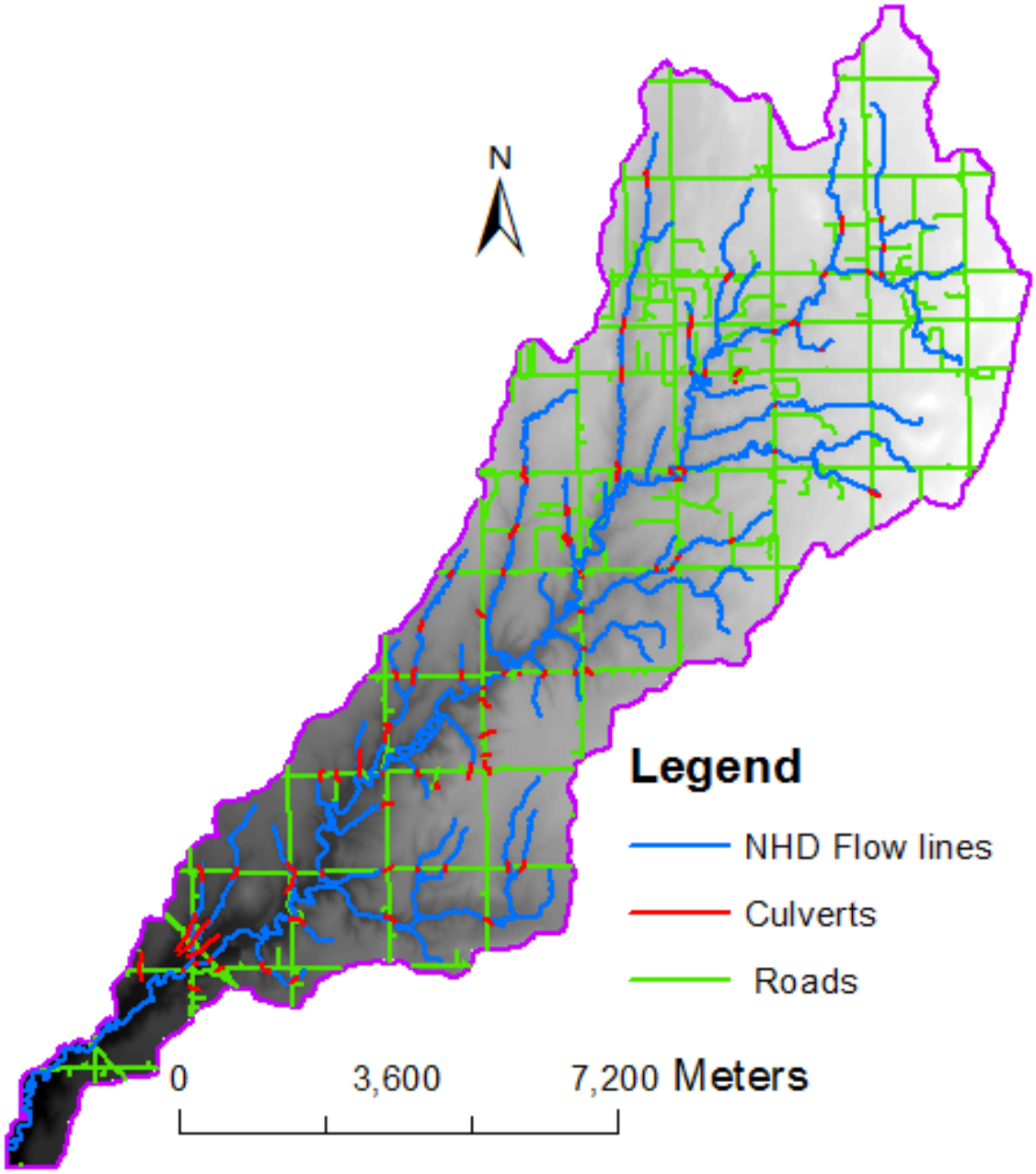

Figure 3-8: Map of culvert locations in Running Turkey watershed.

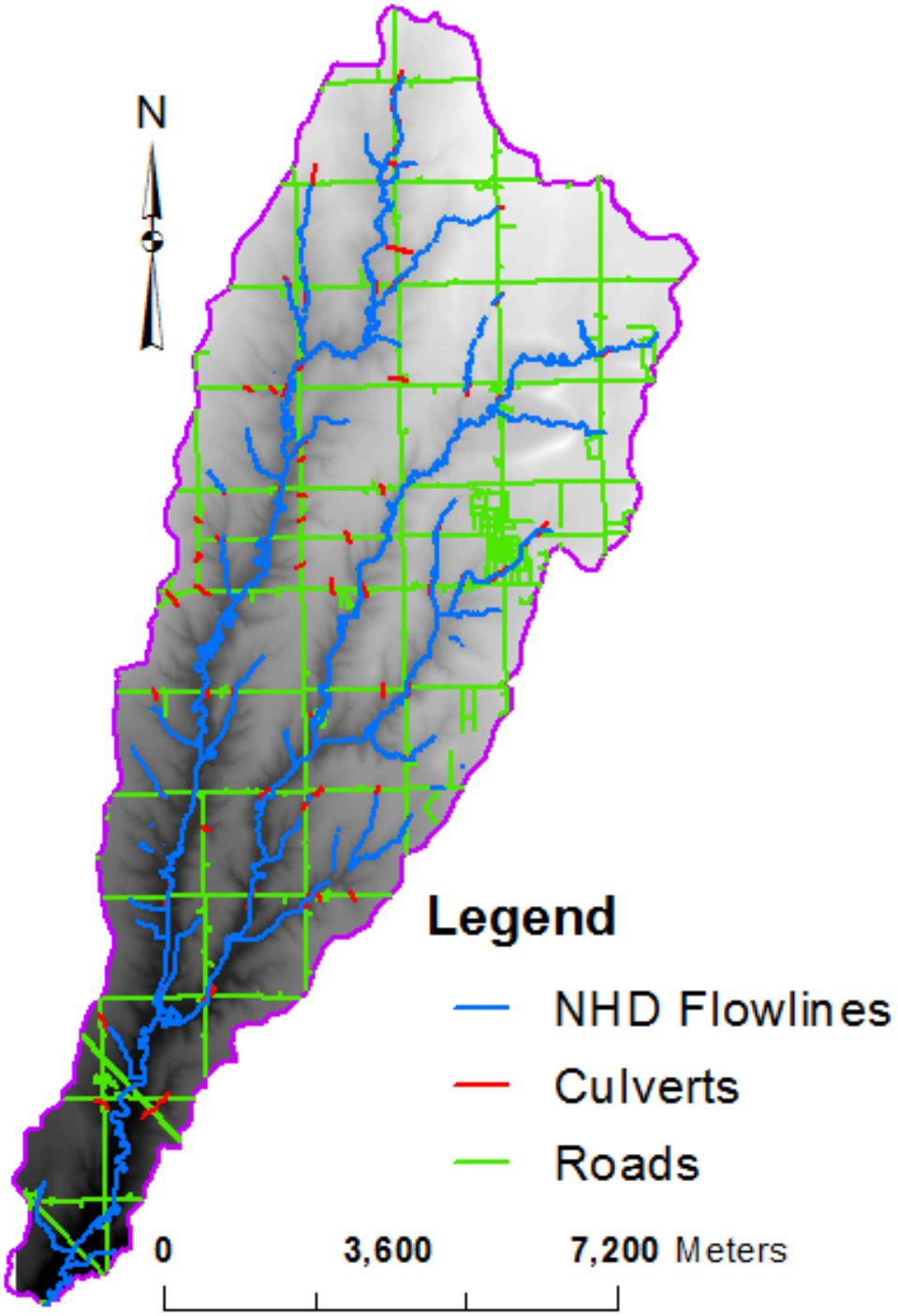

Figure 3-9: Map of culvert locations in Dry Turkey watershed.

Topographic Index (TI) models

Six TI models were utilized to predict location and length of EGs (Table 3-1). The TI model depends on the topographic index calculated at each pixel within a watershed according to the equation presented in Table 3-1. An EG is determined to exist at each point (or pixel in DEM) having an index greater than a specified critical threshold. All points within a field that have index exceed the threshold value identify an area that contributes or belongs to an EG. For different critical TI thresholds EG coverage may change, and for lower TI thresholds the EG coverage is normally larger than for smaller TI thresholds. The smaller TI thresholds allow gully network to be longer and extend into areas of higher elevation, while higher TI thresholds normally identify gullies of smaller length in areas at lower elevations, possibly main channels.

The TI model selection depends on the contributing factors such as topography, overland flow, land cover, and soil properties of the watershed. The list of factors encompassed by each model is shown in Table 3-1. The factors of slope, contributing area, and flow length were derived from elevation data using ArcGIS. The values of the Manning's coefficient for each land cover were obtained from Chow (1959) and spatially assigned to each land use class

The raster grid of Manning's roughness coefficient values was then spatially distributed by resampling to cater for changes that may exist due to change from one land use to another. The values of the critical shear stress were calculated based on soil texture using a method presented by Elliot (1990). The proportions of clay, sand, and silt obtained by querying the gSSURGO database and the resultant raster datasets were generated as indicated in Appendix D. An ArcGIS model shown in Figure 3-10 was set up to compute the value of critical shear stress at each pixel within each watershed. The resultant raster grid was used in computation of topographic values by the nLSCSS model.

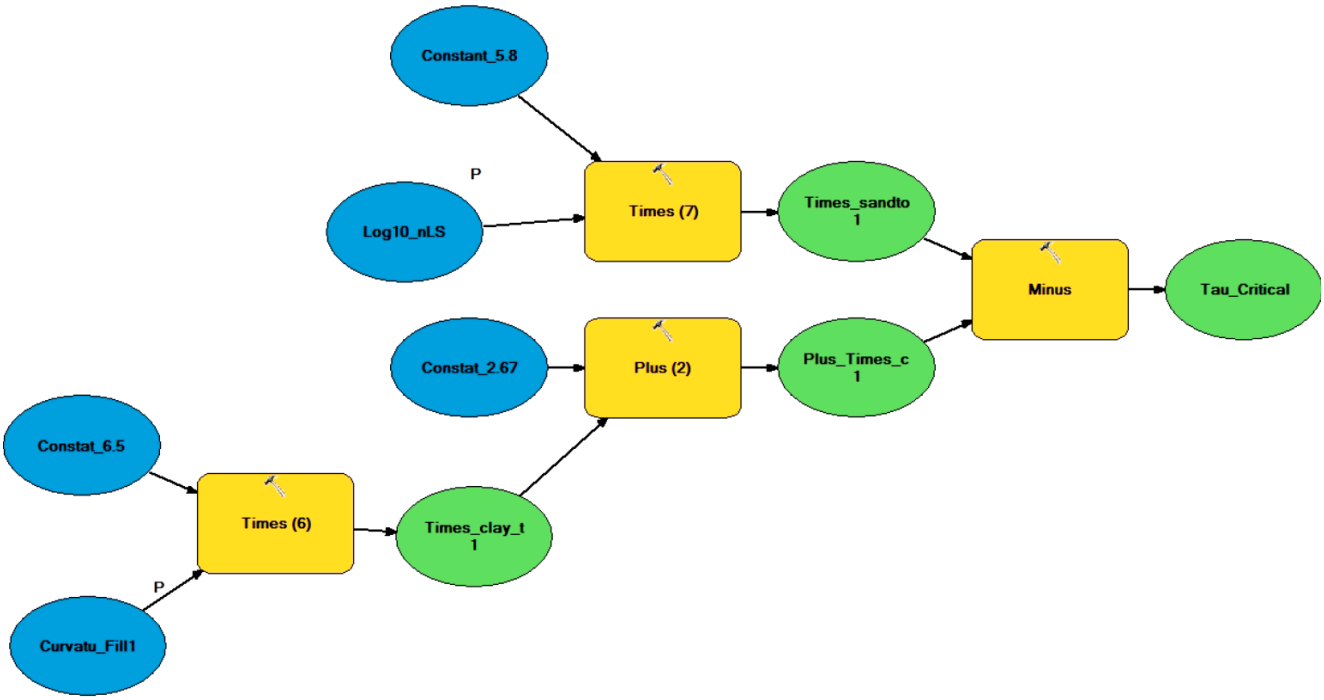

Figure 3-10: ArcGIS model for computing critical shear stress of the soils.

Predicting EG location and length with TI models.

A DEM was used to derive both catchment parameters and TI values for each TI model. The TI values for each model were computed at each pixel within the catchment using equations presented in Table 3-1. All pixels at which the TI value exceeded the critical threshold were recorded and mapped for each TI threshold. The resultant output was further refined by erasing pixels of grassed waterways, terraces, natural streams, roads, and streets. After all refinements, a geospatial vector file was assumed to constitute a map of predicted EGs.

Each EG is located inside a corresponding sub catchment. To generate a map of all sub catchments in two watersheds, the ArcSWAT watershed delineation module was employed with a minimal drainage area set at 1.5 acres. A geospatial model in ArcGIS was constructed to automate the above processes (Figure 3-11 and Appendix I). To obtain the number of catchments containing predicted EGs, the shapefile of predicted EGs was intersected with sub-catchment layer and the cumulative length of predicted EGs within each sub catchment was recorded. The entire process was repeated for each critical TI threshold.

Table 3-1: A list of six topographic index models used in this study

Model	Equation	Parameters	Reference
CTI	$C.S.A$	C = plane curvature S = slope (m/m) A = contributing Area (m^2/m) n = manning's coefficient L = length of overland flow (m) τ_c = Critical shear stress	(Thorne et al., 1986)
WTI	$\ln\left[\frac{A}{S}\right]$		(Moore et al., 1988)
nLS	$\left[\frac{3.3nL}{\sqrt{S}}\right]$		(McCuen and Spiess, 1995)
nLSCSS	$\left[\frac{3.3nL}{\tau_c\sqrt{S}}\right]$		Critical shear stress computed using a method of (Elliot, 1990; Kim, 2006)
AS^2	$S^2.A$		(Montgomery and Dietrich, 1992)
SA	$S.A$		(Moore et al., 1988)

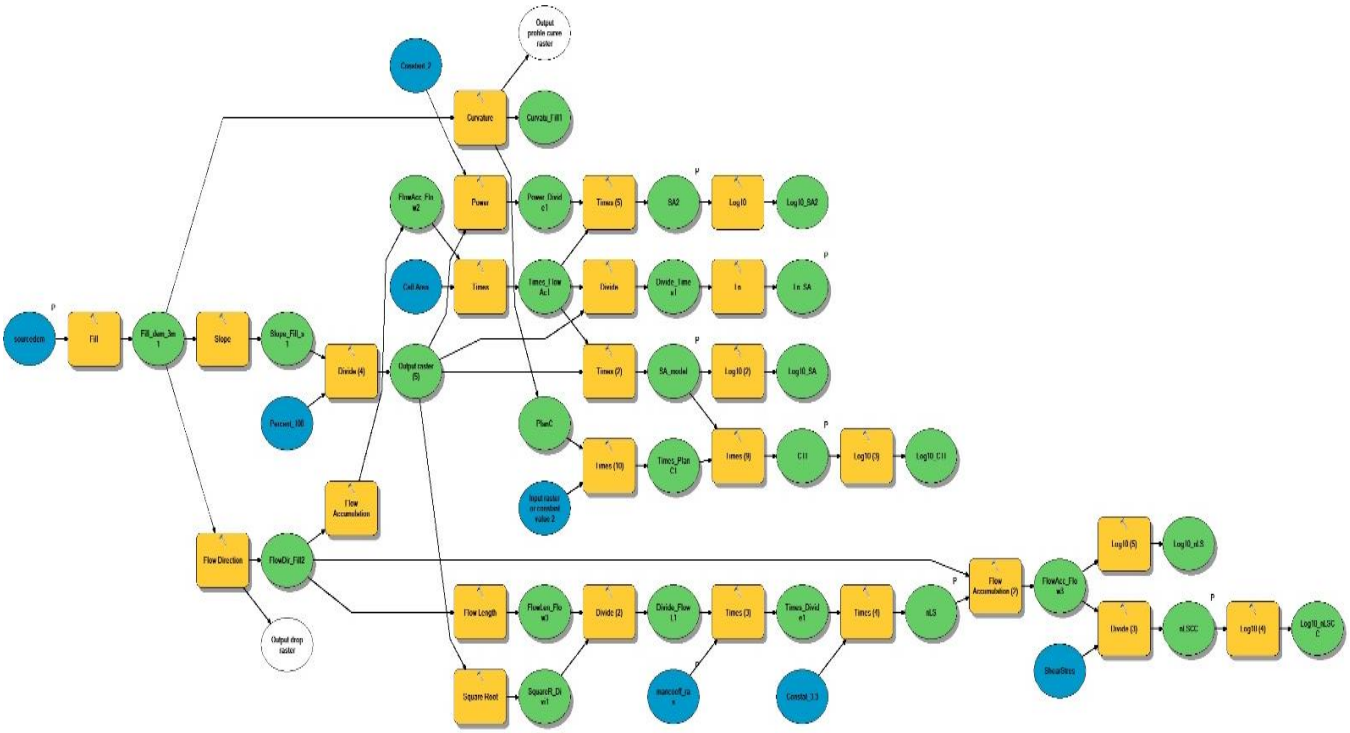

Figure 3-11: Constructed model for computing TI values for each TI model.

Statistical analysis

The statistical approaches applied in this study were objected towards evaluating the performance of different TI models at predicting observed EGs within the watershed. This measurement of agreement was assessed using different approaches as described in the proceeding sections.

EG location analysis

Model thresholds for location approach were obtained by using the concept of error matrix (Kohavi and Provost, 1998; Visa et al., 2011). The error matrix approach was used to track the efficiency of predicting EG catchments for each TI threshold. The interaction of predicted and observed EG catchments is illustrated in the layout of error matrix in Table 3-2. For each sub catchment, EGs from predicted and observed maps were compared for EG absence or presence. Four possible scenarios are recorded:

- True positive (TP): EG is predicted and observed.
- False positive (FP): EG is predicted but not observed.
- False negative (FN): EG is not predicted but observed.
- True negative (TN): EG is neither predicted nor observed.

The value of Cohen's Kappa (Eq.3-1) was selected as measure of agreement between the actual number of catchments and predicted number of catchments with EGs (Cohen, 1960). The values of Kappa are in range one to negative infinity. High value of Kappa (Kappa = 1) indicates good model performance at predicting actual number of catchments with EGs. Two additional statistics were used to evaluate the performance of EG predictions: Precision (P) and Accuracy (TA). The accuracy evaluated by (Eq.3-2) indicates how good the results are at assessing accuracy of correct predictions (TP and TN) versus all predictions (TP + TN+FP+FN) within the error matrix. The precision statistics in (Eq.3-4) evaluates correct identification of EGs (TP) versus total positive identification (TP and FP). The process of calculating Kappa, Accuracy, and Precision was repeated for each TI threshold applied to a watershed following the flow chart in Figure 3-12. The optimum values of these statistics were sought to reach the best TI threshold in EG location identification. The same methodology was applied to both watersheds in the study.

Table 3-2: Illustration of error matrix

Predicted catchments	Observed catchments		
	Present	Absent	
Present	True positive (TP)	False positive (FP)	TP + FP
Absent	False negative (FN)	True negative (TN)	FP + TN
	TP + FN	FP + TN	

$$\text{Kappa} = \left[\frac{\text{TA} - \text{RA}}{1 - \text{RA}}\right] \quad \text{Eq. 3-1}$$

$$\text{TA} = \frac{\text{TP} + \text{TN}}{\text{TP} + \text{TN} + \text{FP} + \text{FN}} \quad \text{Eq. 3-2}$$

$$\text{Random accuracy (RA)} = \frac{[(\text{TN} + \text{FP}) * (\text{TN} + \text{FN})] + [(\text{FN} + \text{TP}) * (\text{FP} + \text{TP})]}{[\text{TP} + \text{TN} + \text{FP} + \text{FN}] * [\text{TP} + \text{TN} + \text{FP} + \text{FN}]} \quad \text{Eq. 3-3}$$

$$\text{P} = \frac{\text{TP}}{\text{TP} + \text{FP}} \quad \text{Eq. 3-4}$$

EG length analysis

For the length analysis, Root Mean Square Error (RMSE) and Nash-Sutcliffe Efficiency (NSE) statistics were employed to evaluate the accuracy of each model threshold at predicting the length of EGs within all catchments. The values of NSE and RMSE were calculated for each TI threshold in six TI models according to Eq. 3-5 and to Eq. 3-6, respectively. The optimum threshold value was selected to be when NSE reached the maximum value (close to 1) and RMSE reached the minimum value (RMSE close to zero).

The drainage density provides a measure of the length of gullies per unit square of an area. The drainage density was calculated for all predicted and observed EGs. Comparing drainage density of predicted and observed EGs, the absolute error in drainage density (DDE) was computed for all catchments in the watershed using Eq. 3-7. This statistics combines the accuracy of predicting the location of EGs with the differences in EG length estimations in each catchment. Thus, the optimum TI threshold can be seen as the one that yields the minimum of drainage density error.

$$\text{NSE} = 1 - \frac{\Sigma(L_d - L_p)^2}{(L_d - \overline{L_d})^2} \quad \text{Eq. 3-5}$$

$$RMSE = \sqrt{\frac{\sum (L_d - L_p)^2}{N}} \quad \text{Eq. 3-6}$$

$$DDE = \left| \frac{L_p - L_d}{L_p} \right| \quad \text{Eq. 3-7}$$

L_d = Digitized length

L_p = Predicted length

$\overline{L_d}$ = Mean digitized length

N = Total number of catchments

Where L_d is digitized length of EG in a catchment, L_p is predicted length of EG in a catchment, $\overline{L_d}$ is average digitized length of EGs, and N is total number of catchments.

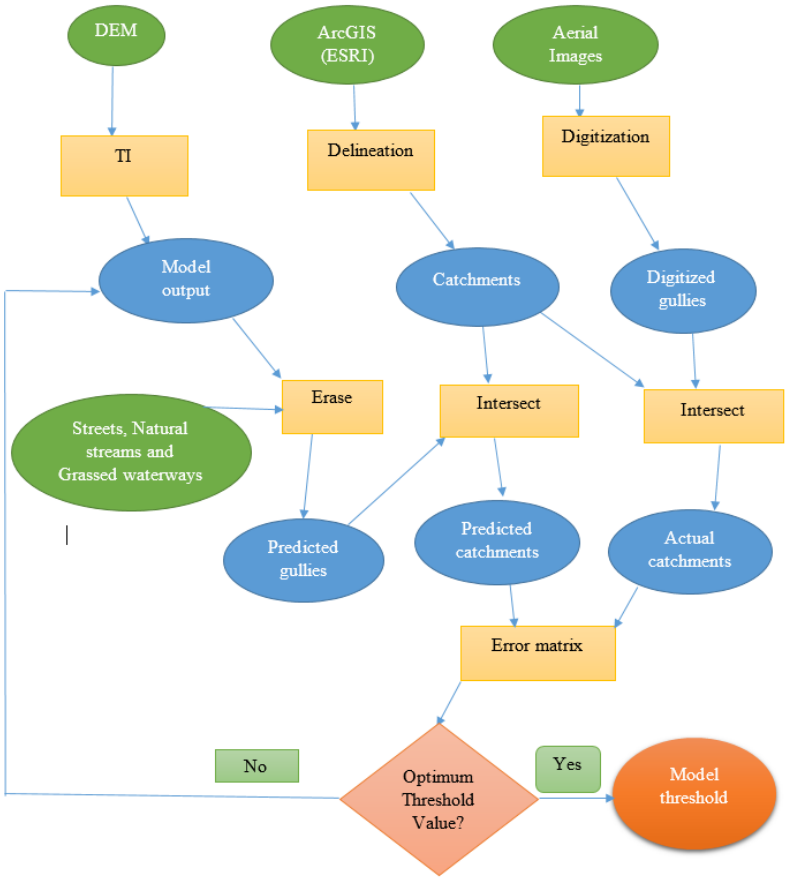

Figure 3-12: Flow chart of procedure for model thresholds using error matrix approach.

tRIBS model input overview

The *tRIBS* model is designed to take inputs from various types of data formats ranging from text tables, grid data, point data, and TIN data as depicted from the model structure in Figure 3-13. The grid data supplied to the model can be time-varying such as rainfall and weather grids or time-invariant for example soil and land use grid data. The point data characterize the values of time-varying parameters that are available at specified points within the watershed such as meteorological and rainfall data. The resampling routines are available for geographically overlaying the grid or point data onto the Voronoi polygon mesh.

tRIBS model setup

The *tRIBS* model was tested on one of the agricultural fields within Running Turkey watershed shown in Figure 3-14. The field has a total area of 40 ha. The field has an EG running through it as shown in Figure 3-14. Currently, the *tRIBS* model doesn't have a well-developed interface for inputting and uploading all the data required by the model. A text input file is prepared specifying the format of the data to be input into the model.

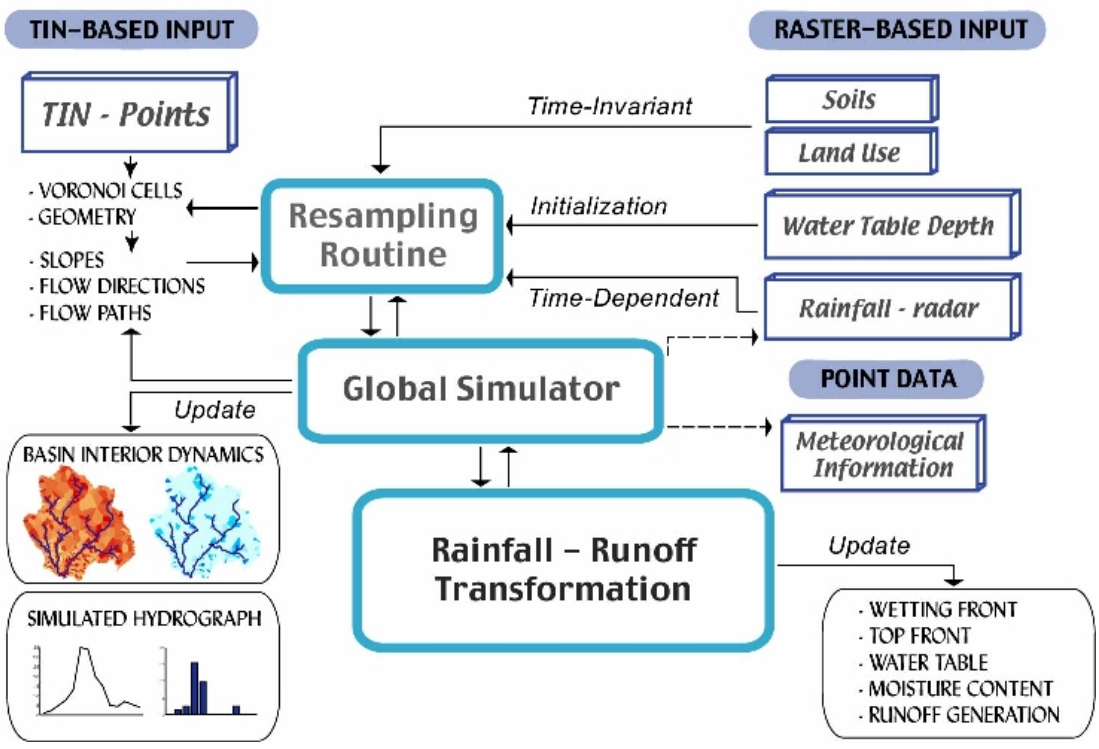

Figure 3-13: General framework of the *tRIBS* model (Ivanov et al., 2004).

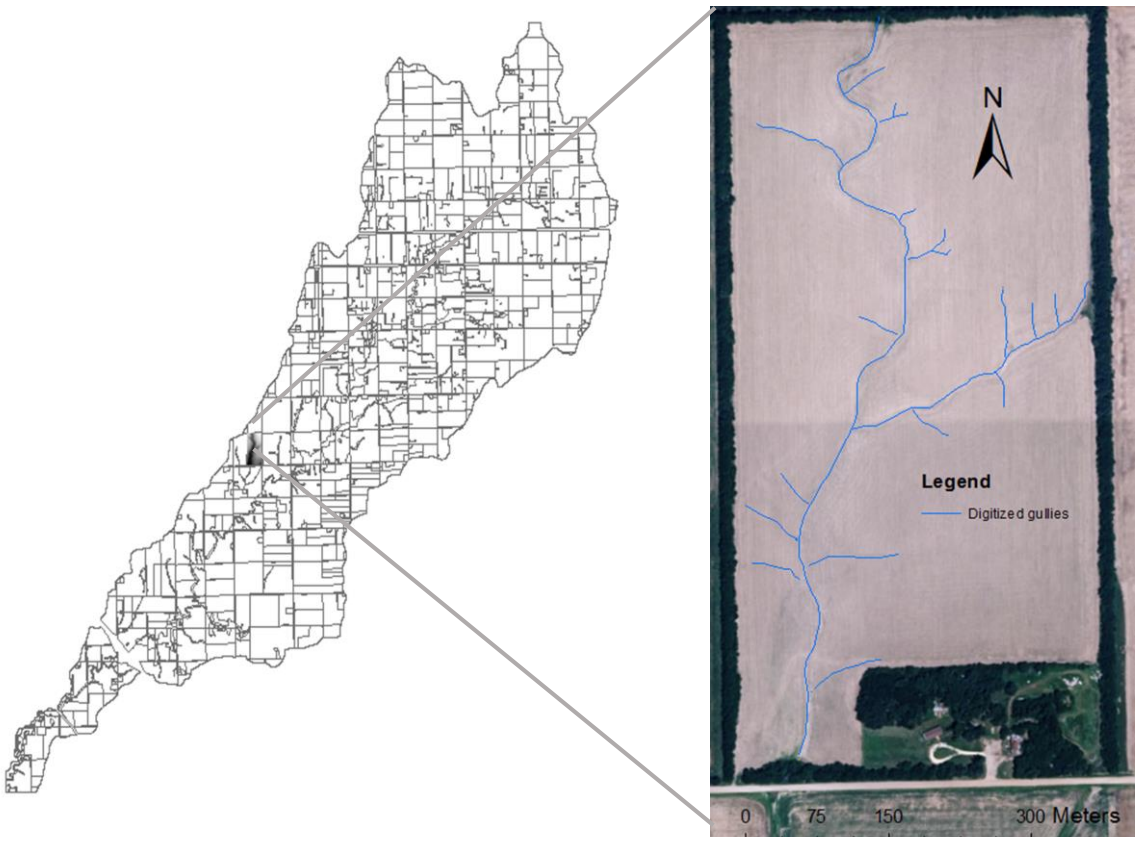

Figure 3-14: A map of the studied gully field for *tRIBS* modeling.

Data preparation

The elevation data in form of a DEM, soil, and land use data were downloaded from the USDA – NRSC geospatial data gateway. The DEM was converted into a point file representing the latitude, longitude, and elevation of each point in the study field. The ArcGIS tools from ESRI were employed to accomplish the process of adding geographical coordinates of the study area. The python scripts were written to arrange the data in the proper format accepted by the *tRIBS* model. The soil and land use types within the field were represented by codes that are read by the *tRIBS* model as shown in Appendix E.

The land use data were further used to generate raster grids of soil roughness and vegetation percentage values. The values of soil roughness were obtained by matching the land use type and values of manning's roughness coefficients listed in Chow (1959) and Steichen et al. (2008). The soil, land use, soil roughness, and vegetation raster data were exported to ASCII grids that are

acceptable by the model. McPherson county weather and rainfall data for the month of July were obtained from Kansas Mesonet website (http://www.ksu.edu/mesonet). After obtaining and formatting all the required data, the input text file was customized for model run depending on the required scenarios.

tRIBS model scenarios

The model scenarios set aimed at assessing the effects of different conservation practices at reducing both upslope and EG erosion rates. The conservation practices that relate to model scenarios include; grassed waterways, vegetated channels, crops residues, and cover crops. The conditions under which model scenarios were run are shown in Table 3-3. The estimated erosion rates from each run were obtained to draw conclusions on how these practices reduce soil erosion on agricultural lands.

Table 3-3: Three simulated model scenarios.

Scenario		**Surface roughness coefficient (n)**	**Vegetation cover (%)**	***tRIBS* channel width (m)**	**Channel roughness ($s/m^{1/3}$)**
1	Baseline	0.01	0.3	0.5	0.01
2	Vegetated channel	0.04	0.5	2	0.04
3	Grassed waterway	0.1	0.9	5	0.1

Foster and Lane model setup

The Foster and Lane (1983) model requires peak discharge rates, runoff volume, surface roughness, and soil detachment coefficients as inputs. These data were obtained from the *tRIBS* model outputs. The python scripts (Appendix J) were written following the procedures outlined in Foster and Lane (1983). These methods were applied at each pixel along the channel to compute the erosion rates and changes in channel geometry. It should be noted that the trajectory of EGs in the studied field was identified using TI models. Thus, at each pixel along the EG trajectory, erosion rate and channel geometry are computed according to Foster and Lane (1983) model.

Chapter 4 - Results and Discussion

This chapter highlights the findings of the study. TI Model threshold is represented as tenth power of the threshold value in all graphs and tables within this chapter. A field refers to an area within Common Landuse Unit (CLU) field boundaries. What follows is a presentation of each model performance at prediction of EGs. The limits under which each model yields better results are presented.

Mapping erosion risk areas

Maps and datasets of digitized gullies were generated for two evaluated watersheds. The location of EGs digitized in this study had good agreement with EGs digitized by the Kansas Department of Health and Environment (KDHE) as shown in Figure 4-2. Using maps of digitized gullies for each watershed, erosion risk fields were ranked depending on the total length of EGs in each field (Figure 4-3 and Figure 4-6). The structural best management practices (BMP) implemented within each watershed were also identified. This observatory study showed that Dry Turkey watershed had higher number of grassed waterways than Running Turkey watershed. It was also observed that the total number and length of EGs reduced due to implementation of terraces and grassed waterways. From Table 4-1, it can be seen that the total number of EGs within the Dry Turkey watershed was almost half of those in Running Turkey watershed.

It can be noted that EGs within both watersheds span from lengths of 3 m to 100 m, and could extend from one field to another. These EGs form mainly on upslope crop fields rather than in downslopes areas such as along creeks and natural streams. This was in agreement with the classification method which is used to identify EGs from rills, which normally is expected to occur along natural streams and creeks. Although some BMPs were already implemented to reduce EG erosion, it was observed that actually some grassed waterways convey runoff to fields which led to EG formation. This situation is common to areas where one farmer implemented BMPs on the upslope field but his neighbor, usually downslope, didn't implement any BMPs. This situation doesn't affect EG predominance on croplands, however, it impacts the proper evaluation of changes in water quality indexes due to implementation of BMPs within the watershed since such fields act as active minute sources of sediments and nutrients.

Table 4-1: Summary description of EG intensity in the study area.

Parameter	**Running Turkey watershed**	**Dry Turkey watershed**
Total Cropland fields	476	584
Number of Cropland fields with EGs	109	115
Number of EGs identified	700	477
Total EG length on fields (m)	22,600	8,543
Mean EG length (m)	22	15
Total length of grassed waterways (m)	179	379
Number of cropland fields with grassed waterways	48	85
Total length of Terraces (m)	525	1900
Number of cropland fields with Terraces	25	95

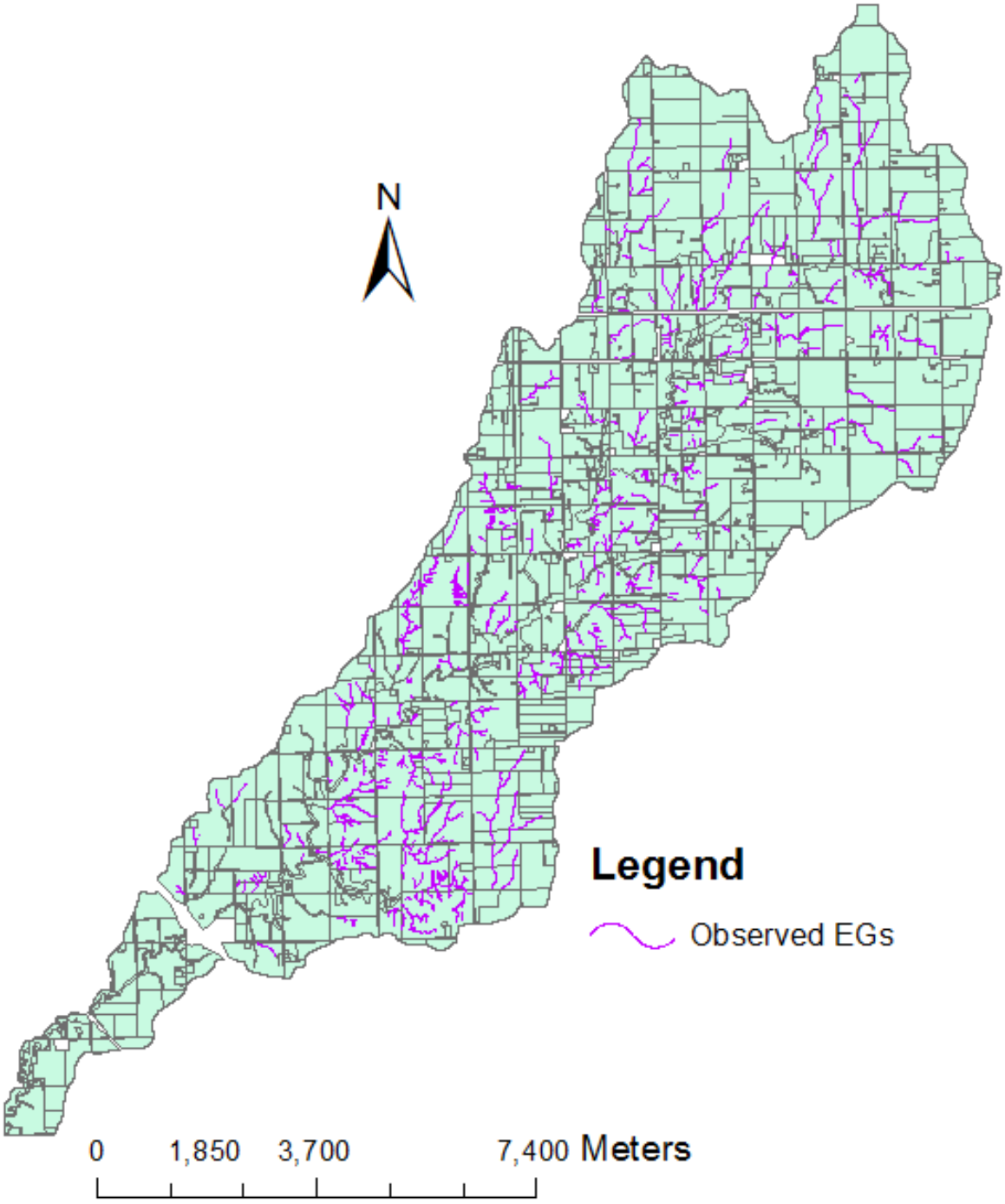

Figure 4-1: Map of observed EGs within Running Turkey watershed.

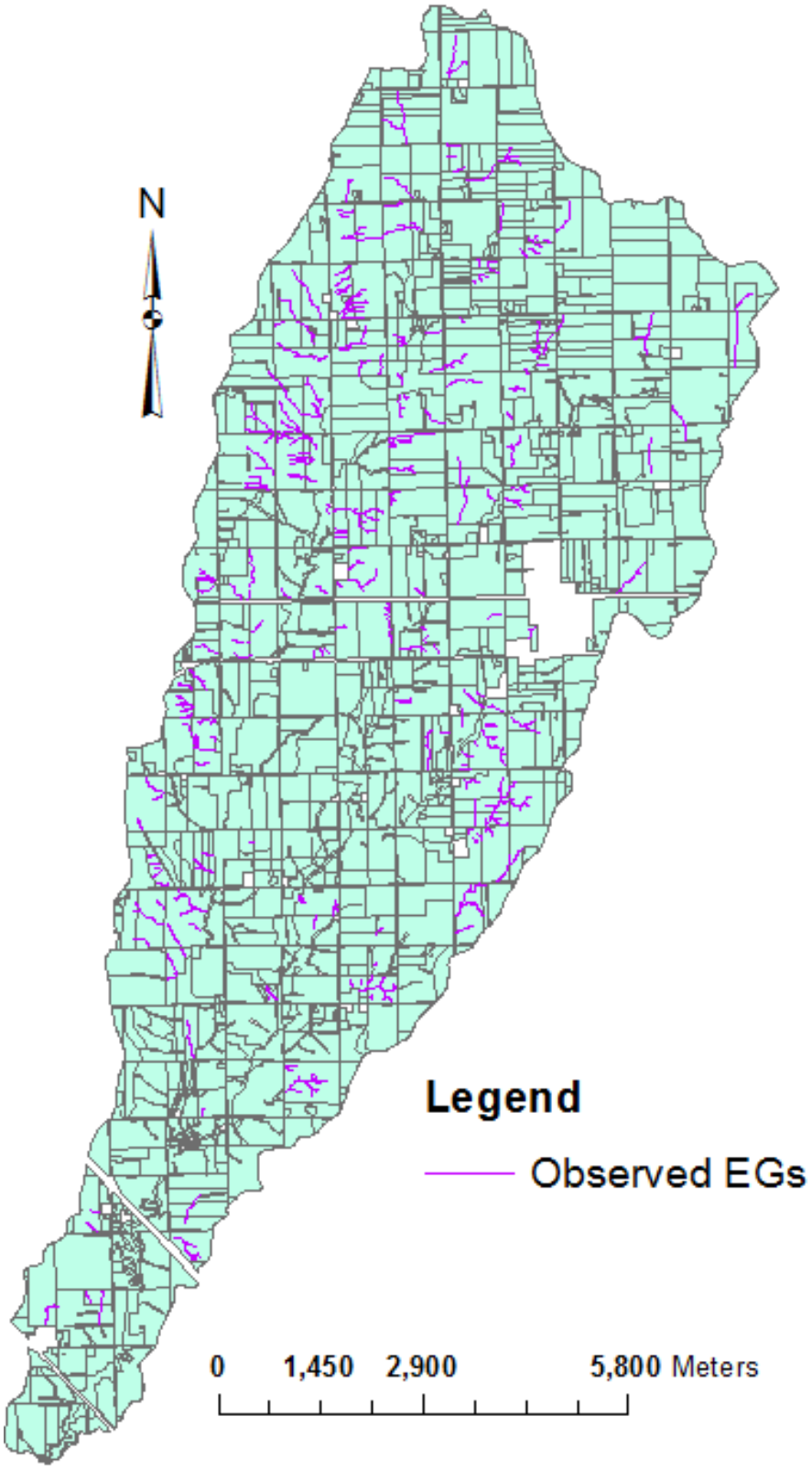

Figure 4-2: Map of observed EGs within Dry Turkey watershed.

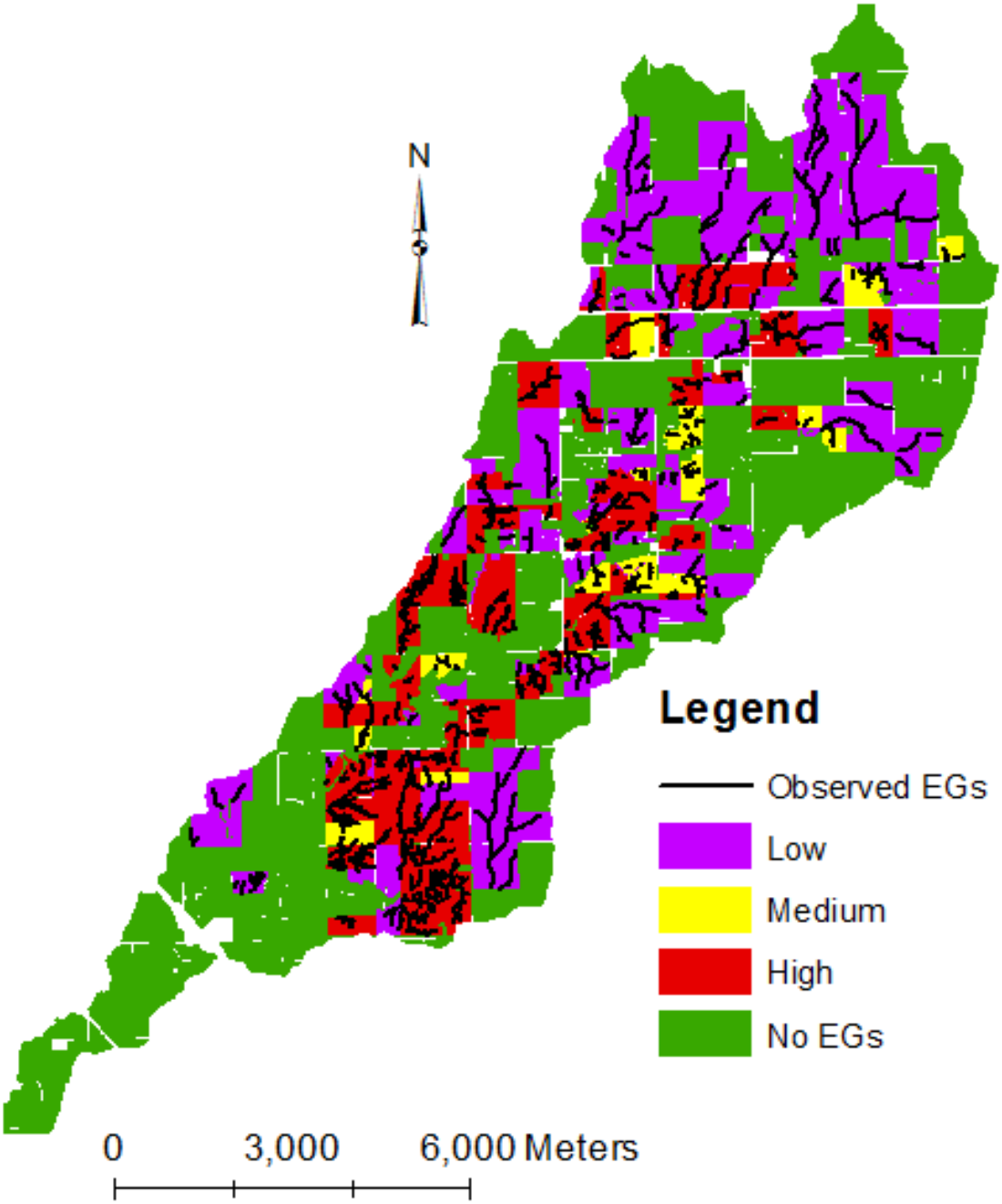

Figure 4-3: Map of erosion risk field ratings in Running Turkey watershed

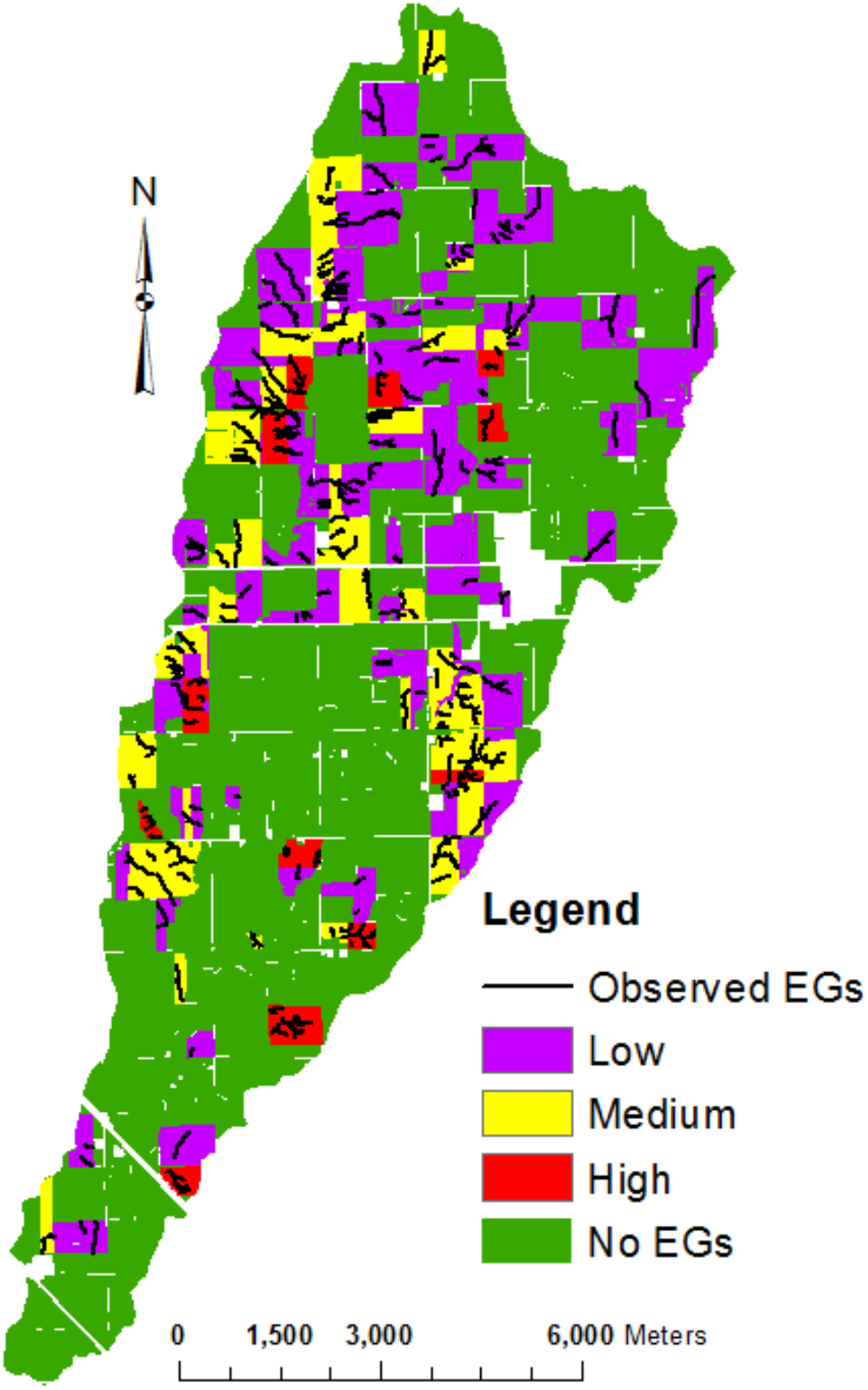

Figure 4-4: Map of erosion risk field ratings in Dry Turkey watershed

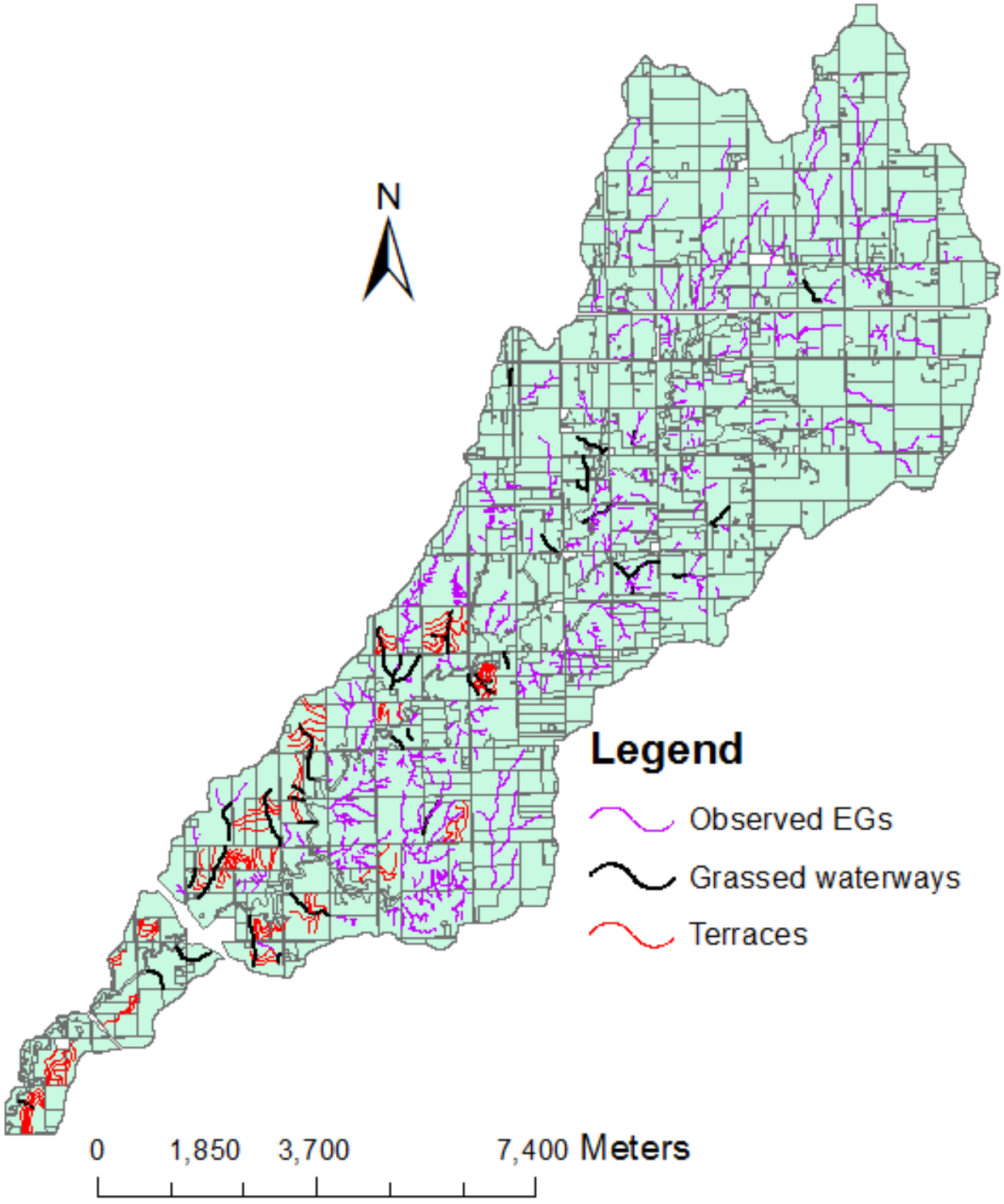

Figure 4-5: Terraces and grassed waterways identified within Running Turkey watershed

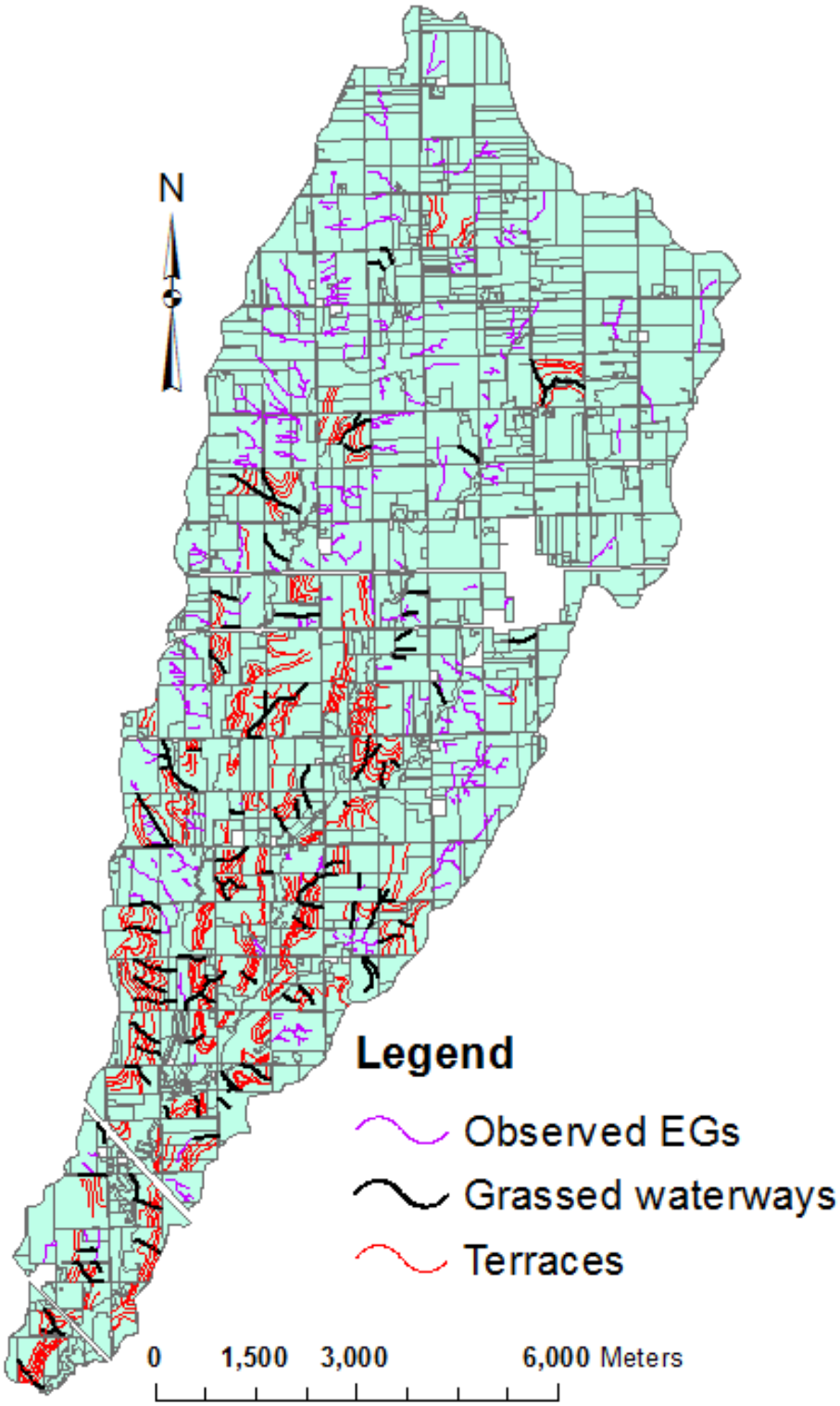

Figure 4-6: Terraces and grassed waterways identified within Dry Turkey watershed.

EG prediction by TI models

The raster maps of TI values computed by each model are presented in Figure 4-7 and Appendix C. The observation of the predicted EG raster maps shows that there is a variation in the prediction of initiation points over which EGs form. Hence, it's of great importance to evaluate the optimum thresholds over which each TI model predicts EGs better. The evaluation of thresholds over which TI models predict EGs better was assessed on both catchment and watershed scales using the methods for EG location and length described in Chapter 3.

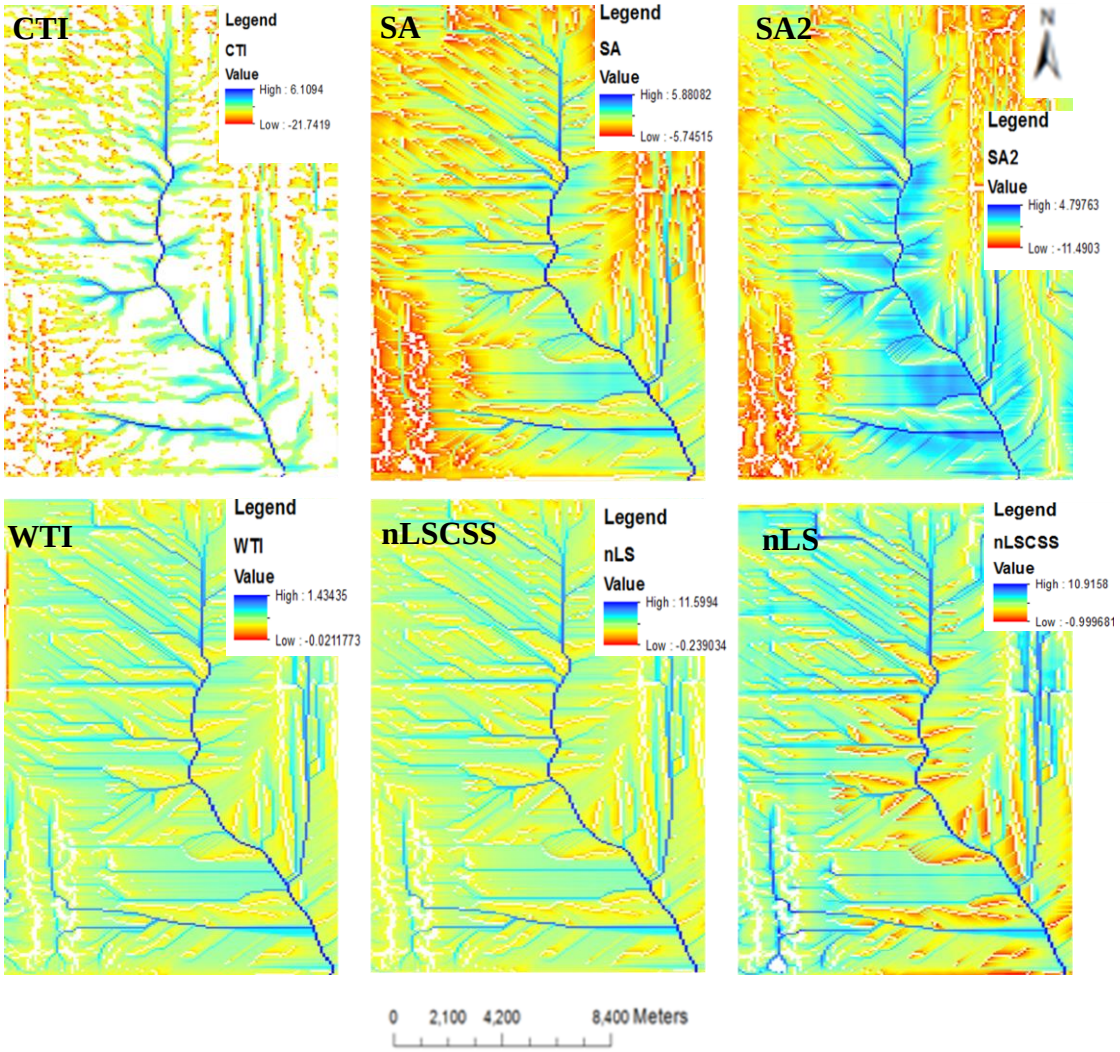

Figure 4-7: Raster maps of predicted EGs by different TI models in Running Turkey watershed.

EG Location analysis

The location analysis discussed in Chapter 3 was applied to studying EG locations within all catchments in the two watersheds. The statistical analysis results (Figure 4-8) indicate that none of TI models predicted catchments with EGs exceptionally well. The values of kappa, all below 0.3, show that all six TI models over predicted the total number of catchments with EGs. The optimum thresholds for predicting catchments with observed EGs within Running Turkey watershed were for: CTI = 1.4, SA = 2.2, SA2 = 0.05, WTI = 1.22, nLSCSS = 8, and nLS = 9.2. The CTI model ($\kappa = 0.29$) outperformed all other models at prediction of EGs, with the SA model ($\kappa = 0.26$) slightly trailing behind the results of the CTI model.

In Dry Turkey watershed, the best thresholds for each model as depicted in Figure 4-9 were for: CTI = 1.9, SA = 2.7, SA2 = 0.3, WTI = 1.25, nLSCSS = 9.4, and nLS = 9.6. The CTI model ($\kappa = 0.31$) still outperformed all other the other TI models similarly to the Running Turkey watershed. The nLS and nLSCSS models performed better in prediction of EGs within Dry Turkey watershed as compared to Running Turkey watershed. There were general improvements in the performance of TI models in Dry Turkey watershed as compared to Running Turkey watershed considering the close proximity of watersheds to each other.

Parker et al. (2007) applied the CTI model with thresholds ranging from 0.69 to 1.88, and they attributed CTI model performance to its capability to differentiate more clearly the limits of EG locations than other topographic index models that do not include the influence of planform curvature and managing to recognize that EGs are not present in other areas despite upstream area and slope values being high. Desmet et al. (1999) reported values of 1.8 and 1.4 for SA model; (Moore et al., 1988) reported values of 0.83 and 1.3 by WTI and SA models respectively, and (Kim, 2006) reported values of 1.02 and 0.54 for WTI and SA2 models respectively. Generally, the threshold values obtained in this study were within the range or very close to the values reported in the literature.

CTI model performance was attributed to the addition of plan curvature coefficient to two other topographic factors of S and A that were also included in SA and SA2 models. The WTI model exhibited poor performance in predicting EGs in both watersheds. Although, the model has capability to predict saturated areas within the catchment, it was not able to distinguish the pathway where EG would form. The nLS and nLSCSS models showed low levels of accuracy. This can be attributed to errors encountered at precise computation of the Manning's coefficient and critical

sheer stress values at each pixel within catchments. These results indicate that incorporation of contributing area into the kinematic wave models might improve their efficiency at predicting EGs within agricultural fields.

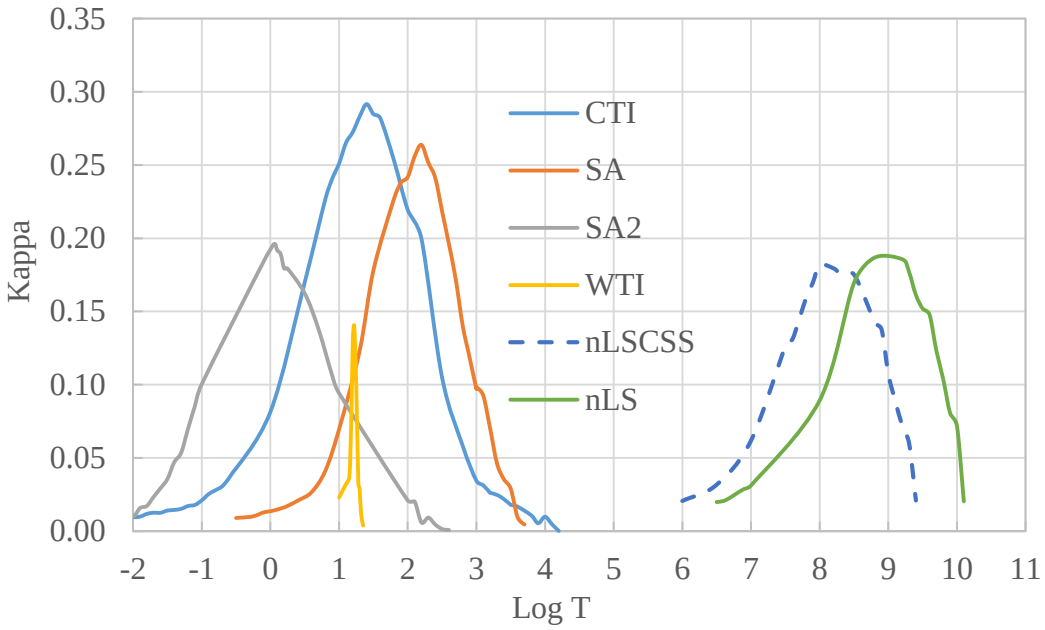

Figure 4-8: Kappa versus TI threshold for six TI models in Running Turkey watershed.

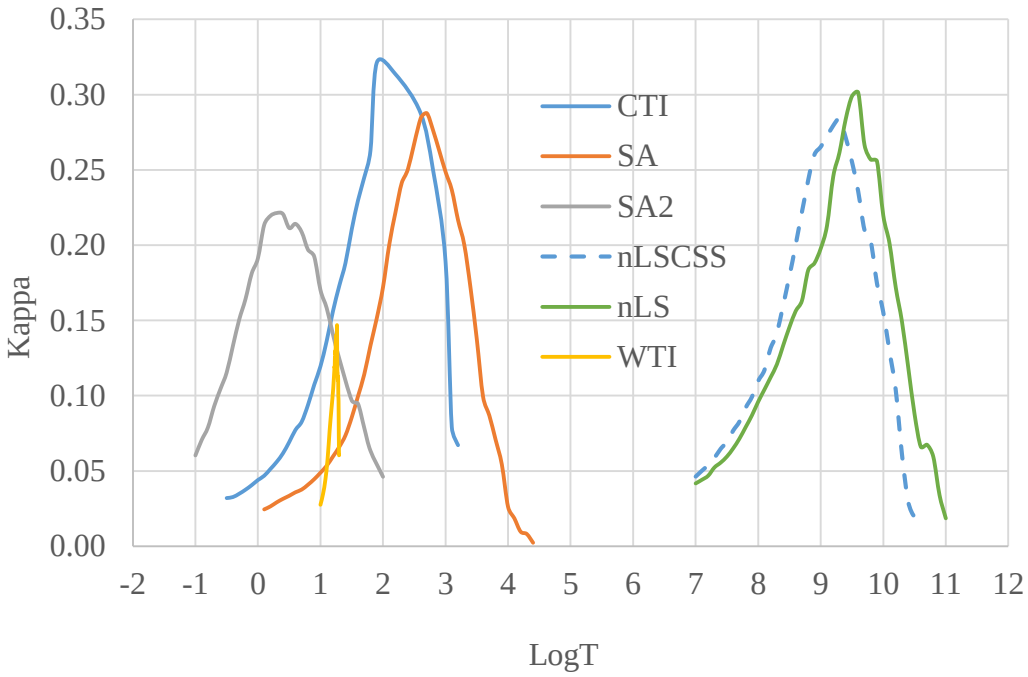

Figure 4-9: Kappa versus TI threshold for six TI models in Dry Turkey watershed.

Accuracy of TI models

The accuracy statistics were computed from the results of error matrix. All TI models had similar trends in the variation of precision and accuracy as indicated in Appendix A. It can be reported that for both watersheds, the efficiency of TI models was less than 70%. The accuracy and precision of the models increases gradually to some degree and remains relatively constant at high model thresholds (Figure 4-10). It would be anticipated that models have the highest accuracy at the optimum threshold, however, this was not the case. Model accuracy and precision increases to some extent and remain stagnant as model thresholds are increased.

These trends in accuracy and precision could be due to gradual decrease in prediction of true values (true positive rate) and an increase in missing of true values (false negative rate) by the models as indicated in Figure 4-10. At higher thresholds, models exhibit great potential to miss catchments with observed EGs as shown by the trend of the false negative rate curve. It can also observed that no specific value of threshold can be used to draw conclusions over the best threshold. Thus, the optimum thresholds over which TI models predict EGs better is always an interaction between the miss rate and true positive rate of the TI model. The error matrix for the CTI model over which these optimum interactions occurred is presented in Table 4-2.

The trends in variations of true positive rate and false negative rate were similar to those reported by Gali et al. (2014) and Daggupati et al. 2013. Gali et al. (2014) obtained a change of 7.14 % in false negative rate as CTI model thresholds were varied from 0 to 1.7. Daggupati et al. (2013) reported a decrease in false positive rate from 54% to 10% and an increase in the false negative rate from 21% to 38% for SA model as thresholds were changed from 0.6 to 1.6. All the reported trends in literature indicate that a low value of false negative rate is always obtained at low thresholds. In which ever circumstance, it’s always desirable to have a wide variation between true positive and false negative rates for a high accuracy of the TI models.

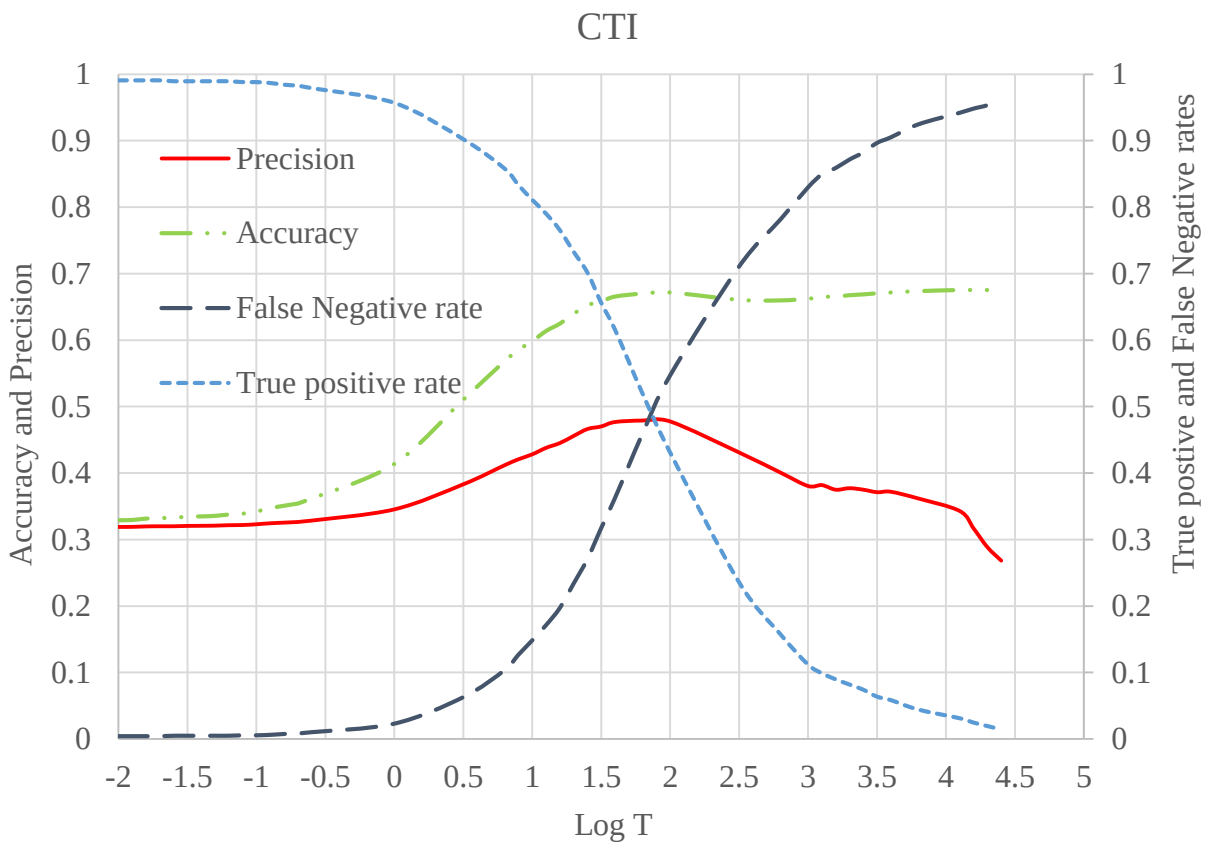

Figure 4-10: Accuracy and precision statistics for CTI Model in Running Turkey watershed.

Table 4-2: An error matrix composed for Log T = 1.5 for CTI Model in Running Turkey watershed.

		Observed catchments	
Predicted catchments	Present	Absent	Total
Present	504	568	1072
Absent	264	1097	1361
Total	768	1665	2433

EG length analysis

The thresholds for the EG length analysis were evaluated on watershed scale. The variation in threshold performance at prediction of EG length within Running Turkey watershed is illustrated in Figure 4-11. The optimum thresholds for predicting EG length in Running Turkey watershed are: CTI = 1, SA = 1.7, SA2 = -0.1, WTI = 1.18, nLSCSS = 7.86, and nLS = 8.57. The CTI model had the highest performance (NSE = 0.552 and RMSE = 0.134 m) at prediction of EG length. The thresholds obtained are in close proximity to those reported by; (Gali et al., 2014) for CTI = 1.5; (Daggupati et al., 2013) CTI = 1.8 to 2, SA = 1.3, and SA2 = -0.5 to 0.

In Dry Turkey watershed, the trends in threshold performance at prediction of EG length shown in Figure 4-12. The optimum thresholds for predicting EG length in Running Turkey watershed are: CTI = 2, SA = 2.6, SA2 = 0.5, WTI = 1.3, nLSCSS = 9.9, and nLS = 10.2. Like in Running Turkey watershed, the CTI model had the highest performance (NSE = 0.42 and RMSE = 0.087 m) at prediction of EG length as compared to other models. It should be noted all models performed poorly at prediction of EG length within Dry Turkey watershed as compared to their performance within Running Turkey watershed. The models overestimated the EG length within Dry Turkey watershed. This is attributed to the presence of many grass waterways and terraces within watershed that break EG length within each catchment. The TI models could predict flow lengths within the catchment well but since grassed waterways and terraces are erased during the analysis, this refinement reduces the efficiency of TI models at prediction of EG trajectory.

Though grassed waterways and terraces affect TI model performance at accurate prediction of EG length, the defects in DEM also affect the proper prediction of EG length by the TI models. These defects normally contribute to discontinuities in EG trajectory thus compromising the accuracy of TI models. Parker et al. (2007) stated that inclusion of parameters such as plan curvature in TI models, mainly CTI lead to discontinuity in the model EG output. This same problem was further highlighted by (Daggupati et al., 2013). In this study we proposed a methodology to reduce the variation of TI pixel values by transforming the TI value thresholds at a logarithmic scale. In this way, discontinuity in EG trajectory posed a minimal menace to performance of TI models at prediction of EG length.

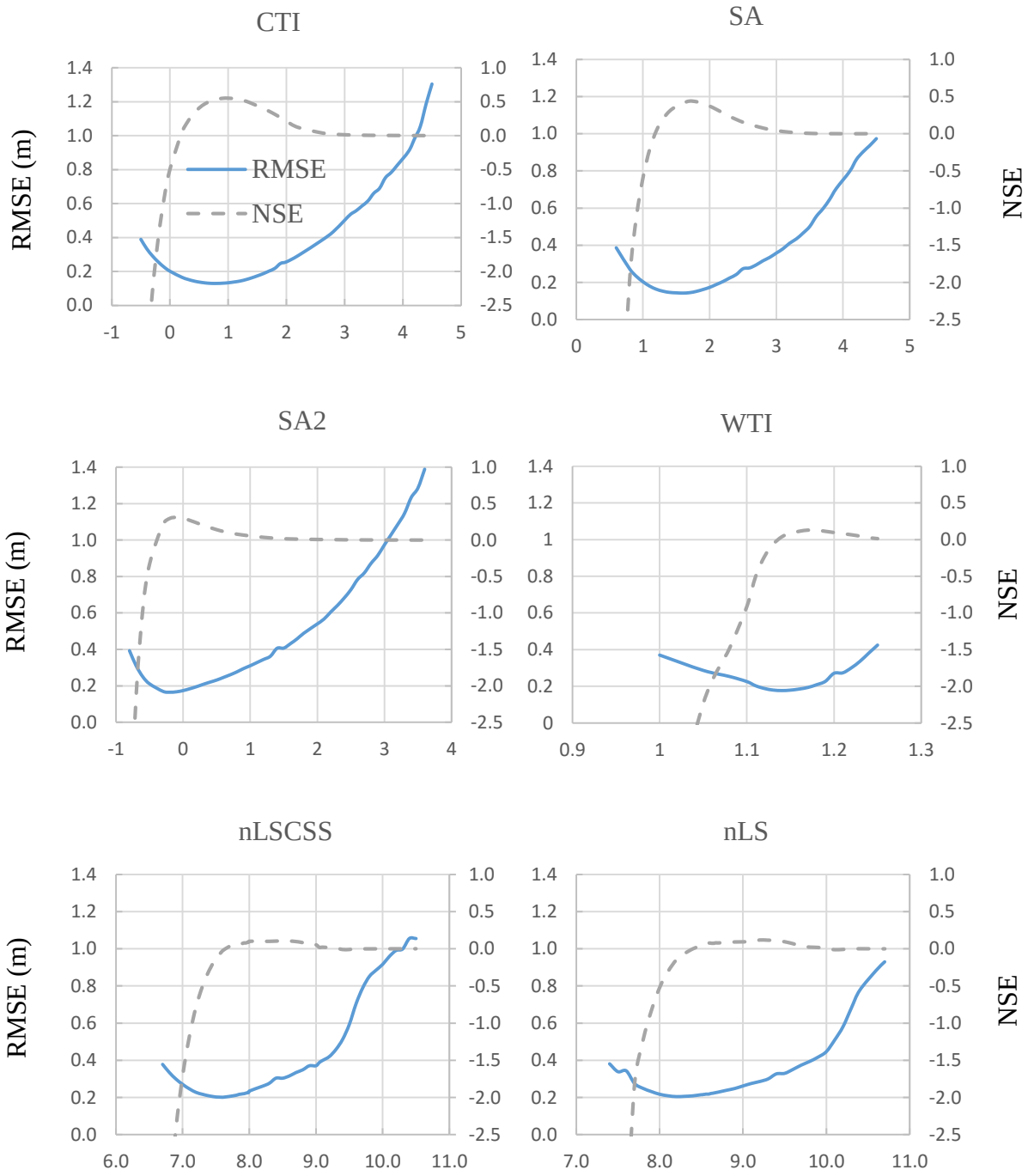

Figure 4-11: Statistics for EG length analysis for six TI models in Running Turkey watershed.

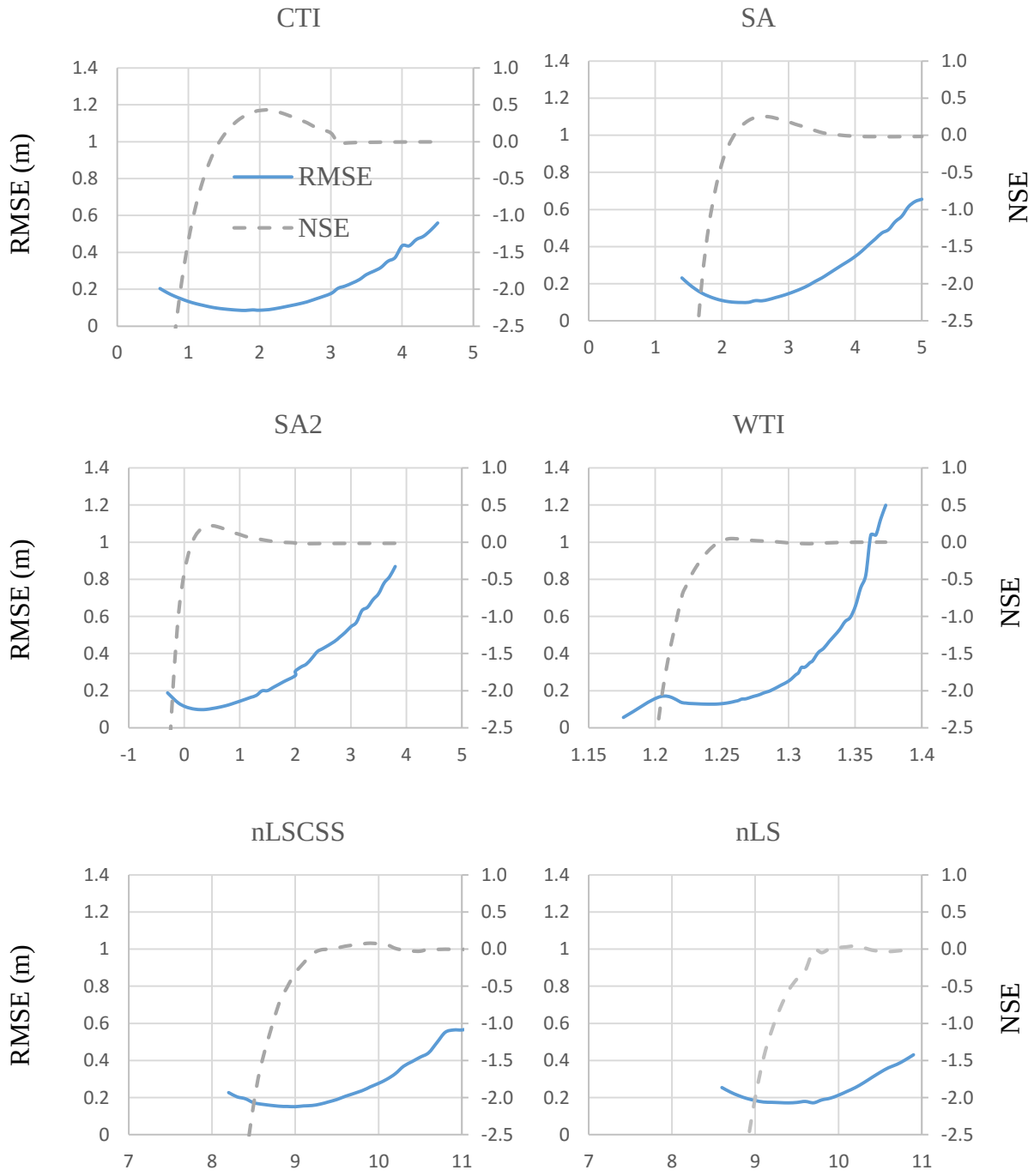

Figure 4-12: Statistics for EG length analysis for six TI models in Dry Turkey watershed.

Spatial visualization

The outputs (Figure 4-13) for observed EGs and CTI show that length thresholds predict EG better than location thresholds. These variations between length and location thresholds were the same for all other TI models. The thresholds of location in all instances under estimate EG trajectory, and this might be the reason why length thresholds might be better predictors of observed EGs on field than the location thresholds. The assessment of model threshold values for length exhibits small discontinuities as compared to location threshold values. This comparison gives a glimpse over some possible sources of error at prediction of EGs by TIs. The discontinuities in EG trajectory usually led to deviations and noise within the data thus reducing model accuracy. The comparison of thresholds indicate that the model threshold value from length analysis suits all TI models. Thus, it can be concluded that model thresholds obtained using length analysis are efficient at prediction of EGs by the TI models.

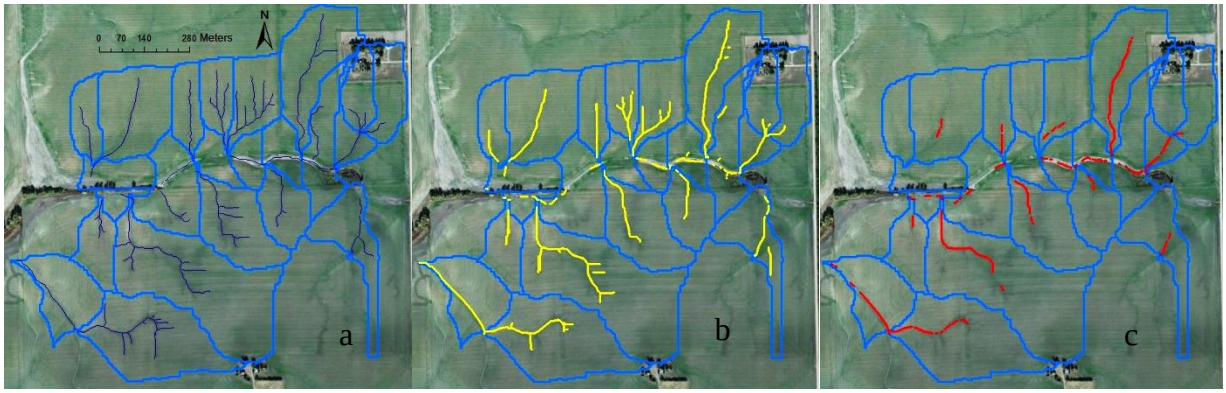

Figure 4-13: Spatial visualizations of (a) digitized gullies, (b) CTI length threshold, and (c) CTI location threshold.

Comparison of location and length thresholds

The comparison of the effectiveness of TI models at prediction of EGs on agricultural fields was evaluated using the obtained values of Kappa and NSE from both watersheds. A high value of Kappa and NSE for the TI model indicates its effectiveness at prediction of EGs. The values of Kappa and NSE outlined in Table 4-3 show that the CTI model outperformed all the assessed TI models at prediction of both the location and length of EGS. The WTI model exhibited poor performance of prediction of EG length and location. This could be attributed to WTI capability to predict the proximity of EGs but cannot specifically predict the critical points where EGs form. This phenomenon might be attributed to the small range of TI values over which the WTI model

predicts EGS (Figure 4-8 and Figure 4-9). The proper identification of pixels by the TI model where EGs form requires a wide difference in the values of pixels predicted by each model. This wide variation leads to less similarity between pixel values, thus maximizing the difference among them. This classification makes an easy distinction between the pixels that belong to an EG and those outside the EG locality. Thus, a model like CTI and SA which exhibits a wide range of thresholds would predict EGs better as compared to its counterparts which possess small deviations. These small attributions of each TI model formulation might some of the reasons for the difference in performance of each TI model at prediction of EGs.

Table 4-3: Comparison of model thresholds of location and length.

	Running Turkey watershed		**Dry Turkey watershed**	
TI model	**kappa**	**NSE**	**kappa**	**NSE**
CTI	0.29	0.55	0.32	0.42
SA	0.26	0.44	0.29	0.25
SA2	0.21	0.31	0.22	0.22
WTI	0.14	0.12	0.15	0.05
nLSCSS	0.18	0.16	0.28	0.08
nLS	0.19	0.18	0.3	0.04

Drainage density analysis

A range of TI thresholds at which the model performance is acceptable (see Figures 4-9 and 4-10) or the difference in the values of best critical threshold found by location and length analyses (see Table 4-2) indicates that a close look at driving factors in TI models is needed. It can be stressed that an interpretation of physical processes related to infiltration, drainage, and channel characteristics within the catchment may be required for better assessment of critical TI threshold within each watershed.

Drainage density, a ratio of total EG length within a catchment to the total catchment area (Tucker and Bras, 1998), was used to correlate thresholds of location and length approaches. The drainage density was computed for each catchment in the watershed for each simulation run as well as for the observed EG network. The error in matching the observed drainage density was calculated for each catchment, and absolute drainage density errors were plotted for each model

threshold as shown in Figure 4-15 and Figure 4-16. The CTI model was used as a core TI model for drainage density analysis.

For the drainage density analysis we classify all catchments according to channel ordering scheme. The catchments with EGs (or channels) of the first order will be called headwater (HW) catchments, while catchments containing higher order channels from the EG network will be called the main-stem (MS) catchments. Figure 4-14 (see Appendix B) illustrates a watershed division into HW and MS catchments.

Studying the drainage density error curves, it was observed that MS catchments maintain a relatively constant absolute value over a wide range of thresholds as shown in Figure 4-16, while the HW catchments exhibit more gradual changes with increase of TI threshold (Figure 4-15). It can be stipulated that an increase in the TI model threshold would tend to predict catchments with classic gullies other than EGs, however, a decrease in model thresholds tends to predict more rills and regions of sheet flow paths. The transitions over which these forms of erosion occur can be explained by the scenarios where catchments of high and low order streams are predicted at low and high thresholds respectively.

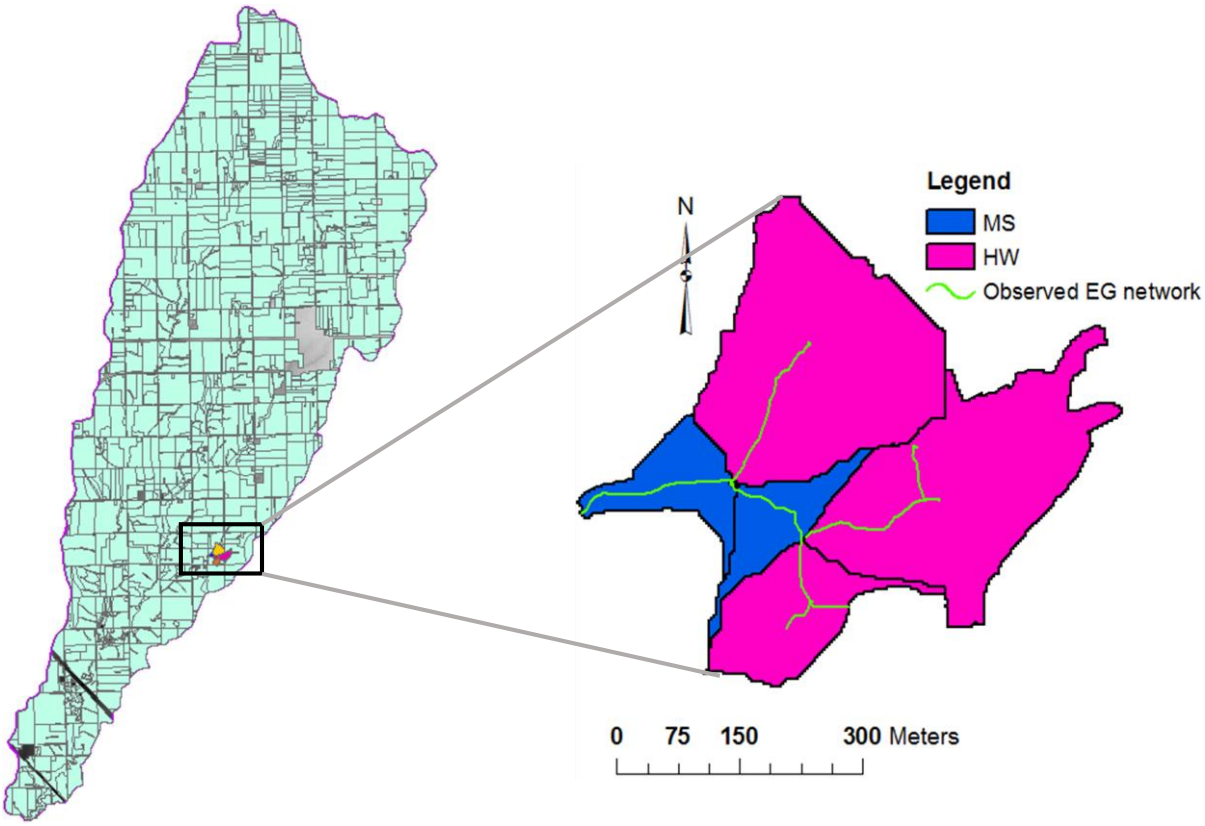

Figure 4-14: Illustration of MS and HW catchments along a gully trajectory

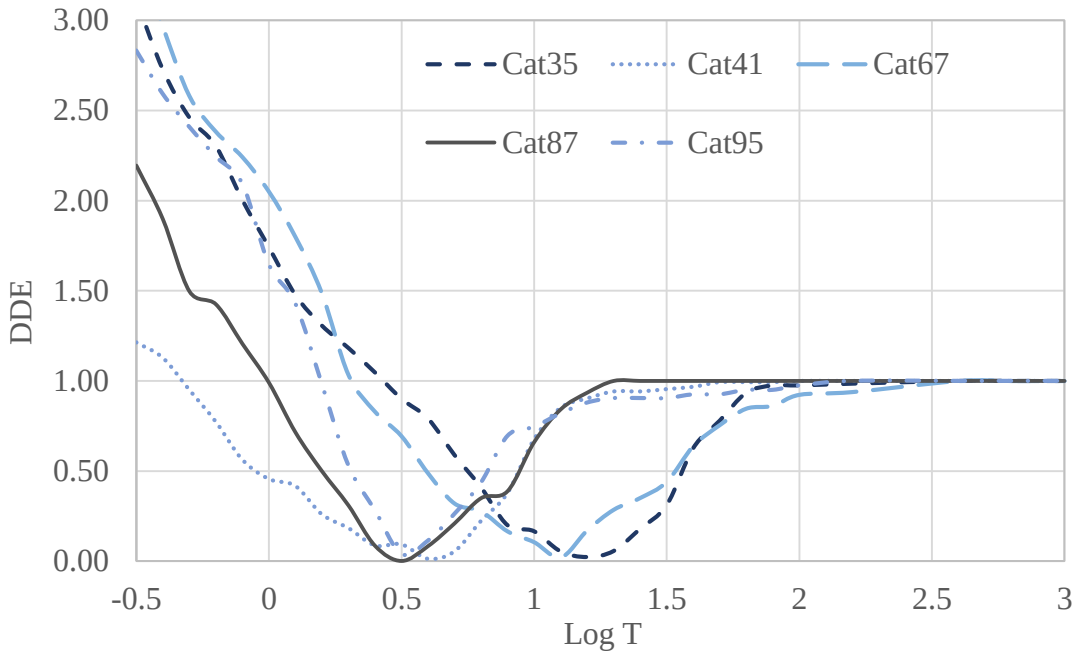

Figure 4-15: DDE as function of TI model threshold for headwater catchments in Running Turkey watershed.

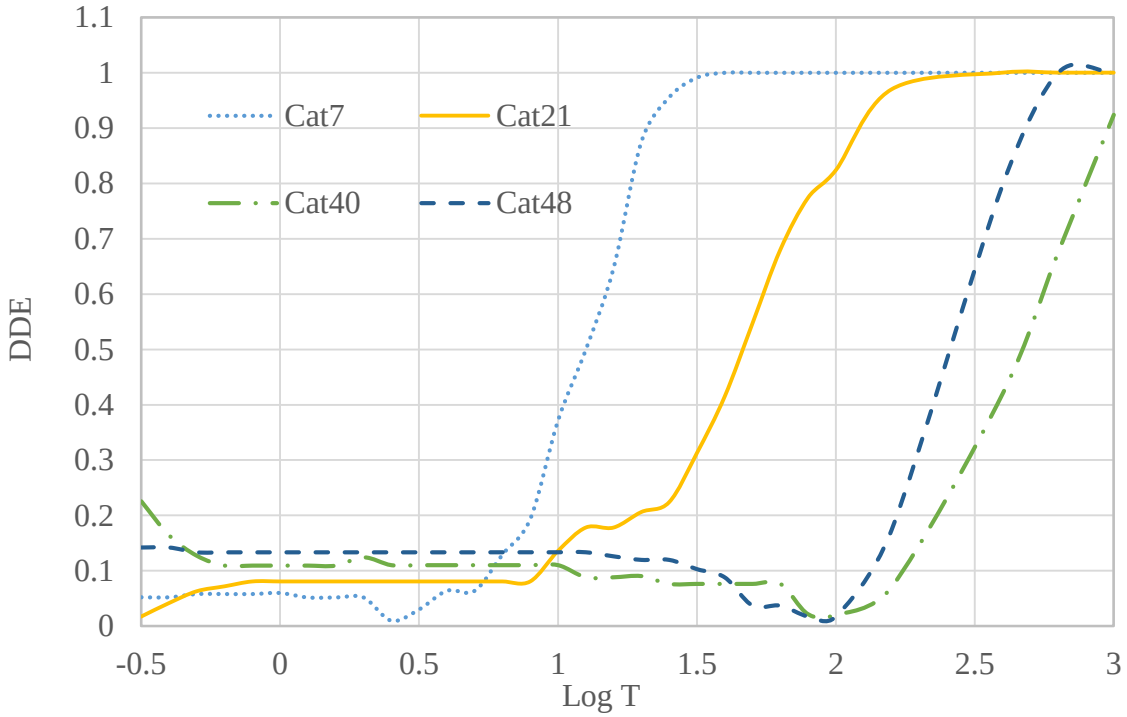

Figure 4-16: DDE as function of TI model threshold for main stem catchments in Running Turkey watershed.

Drainage density thresholds

The mean drainage density error (DDE) was computed for each TI threshold for HW, MS, and all catchments in Running Turkey and Dry turkey watersheds. The zero value of the error yields the best thresholds over which EGs will form. Within Running Turkey watershed, zero error was obtained at threshold of 1.4 for all catchments (Figure 4-17). This value of threshold was not much different from the one obtained from length and location analyses. This is a confirmatory result that indicates that the best threshold for EG initiation within Running Turkey is 1.4 for the CTI model.

Within Dry Turkey watershed, there was a disagreement in the minimum threshold value of the DDE for HW, MS, and total catchments within the catchment. The minimum error values of error were obtained at 2.3 for MS catchments, 2.9 for total catchments, and 3.1 for HW catchments. Thus, it can be stipulated that MS threshold value present the best value close to thresholds found in location and length analyses. Generally, no specific threshold value of DDE can be deduced from the analysis except a range of threshold values (2.3 to 3.1). The disagreement of threshold values for HW, MS and total catchments can be attributed to the presence of structural BMPs (terraces and grassed waterways) within the Dry Turkey watershed.

In general, the errors found in computation of DDE for HW catchments are higher than those for MS catchments. This is evidenced by the trend of curves in Figure 4-17 and Figure 4-18 which indicate that always the variation of DDE in HW catchments is skewed to the right and one for MS catchments is skewed to the left from the curve representing all catchments. This difference indicates a higher possibility of EG head cut and channel migration within HW as compared to MS catchments.

The trends in Figure 4-18 indicate that EGs form at lower thresholds in MS catchments, although from previous analysis we concluded that EGs in MS catchments form at higher thresholds than in HW catchments. This result can be explained by the fact that grassed waterways and terraces were removed within the EG network during the refinement process of predicting EGs by the TI models. Consider Figure 4-19, removing grassed waterways and terraces from the flow network turns typical MS catchments into HW catchments. This shift from MS catchment to HW catchment leads to intermittent trends in variation of drainage density within HW catchments. Furthermore, it shows the effect of structural BMPs on reduction of EG erosion. The increase in threshold values indicates a reduction in available stream power, erosion energy, and flow length

available to erode channels, encouraging infiltration and abstraction processes to prevail in such areas. In that way, the rates of erosion and sediment transport are reduced within the watershed.

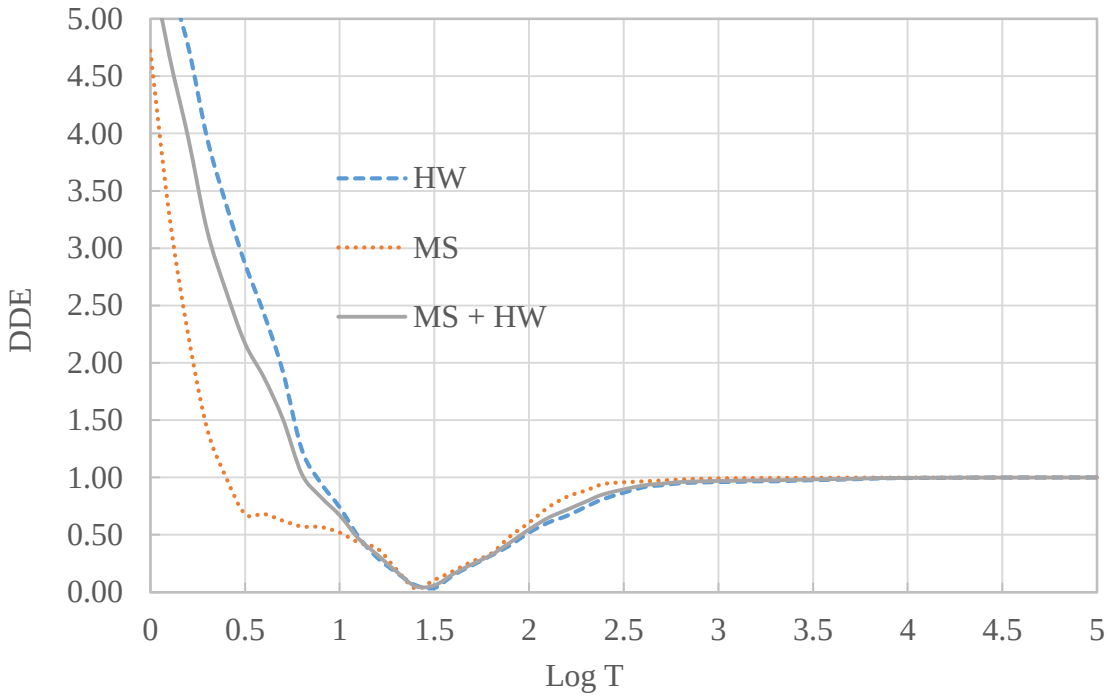

Figure 4-17: DDE as function of TI model threshold for RunningTurkey watershed.

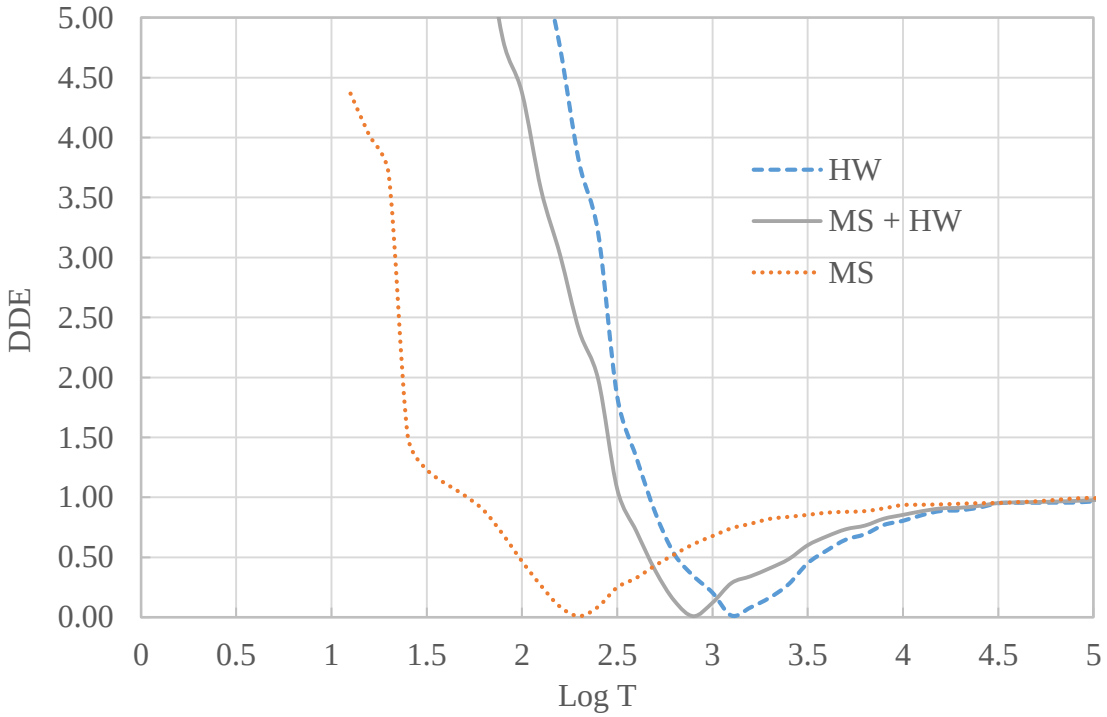

Figure 4-18: DDE as function of TI model threshold for Dry Turkey watershed.

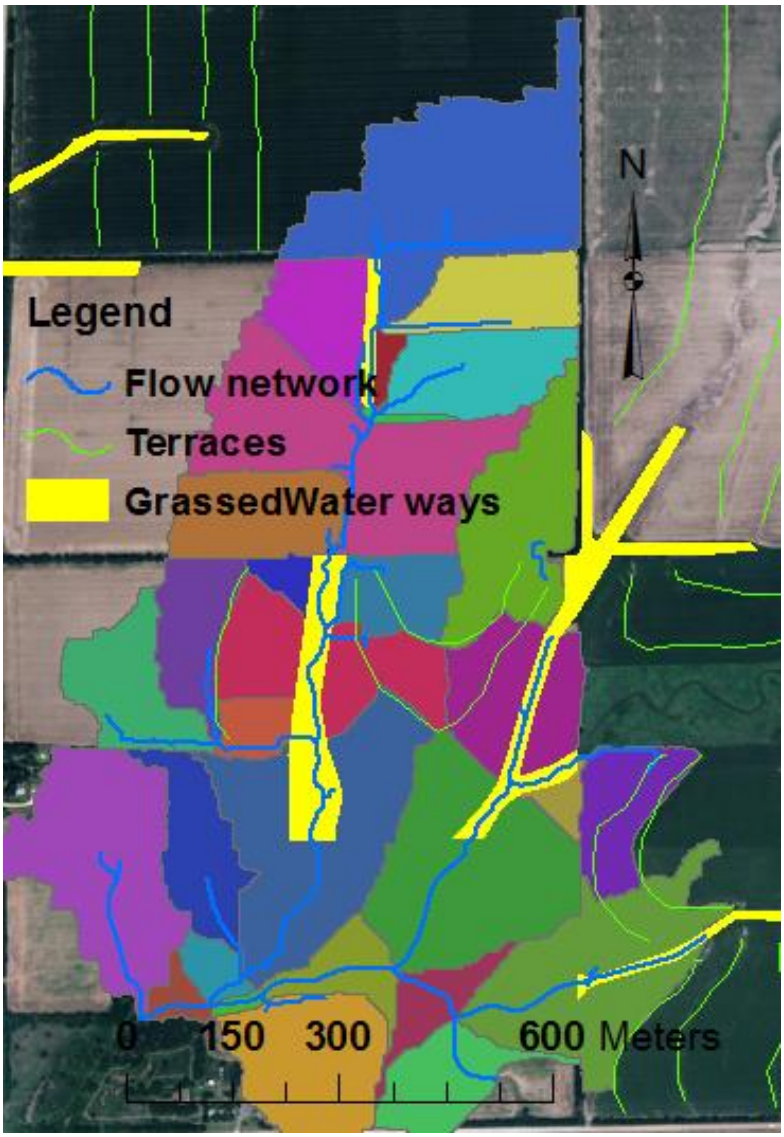

Figure 4-19: Effect of grassed waterways and terraces on EG location.

Effect of watershed features on EG prediction

The effects of watershed features (roads and streets, grassed waterways, terraces, field boundaries, and culvert) were assessed by creating two cases during the refinement process: 1) including features in the TI model EG prediction dataset, and 2) deleting features in the TI model EG prediction dataset. The output datasets were analyzed following the statistical procedures presented above. The removal of watershed features in the EG length analysis by the CTI model increases the Kappa value by 24% in Running Turkey and 65% in Dry Turkey watersheds (Figure 4-20 and Figure 4-21).

The prediction of EG trajectory by the CTI model improved NSE value by 26.03% in Running Turkey and 97.24% in Dry Turkey watershed if watershed features were deleted from the analysis (Figure 4-22 and Figure 4-23). These figures indicate that proper accuracy of TI models can be achieved by employing a holistic approach ranging from preprocessing of elevation data to refinement of EG locations and trajectories within watershed. In addition, hydrological modelling of processes involving application of TI require understanding of watershed features since hydrological processes such infiltration and runoff generation may change along these features.

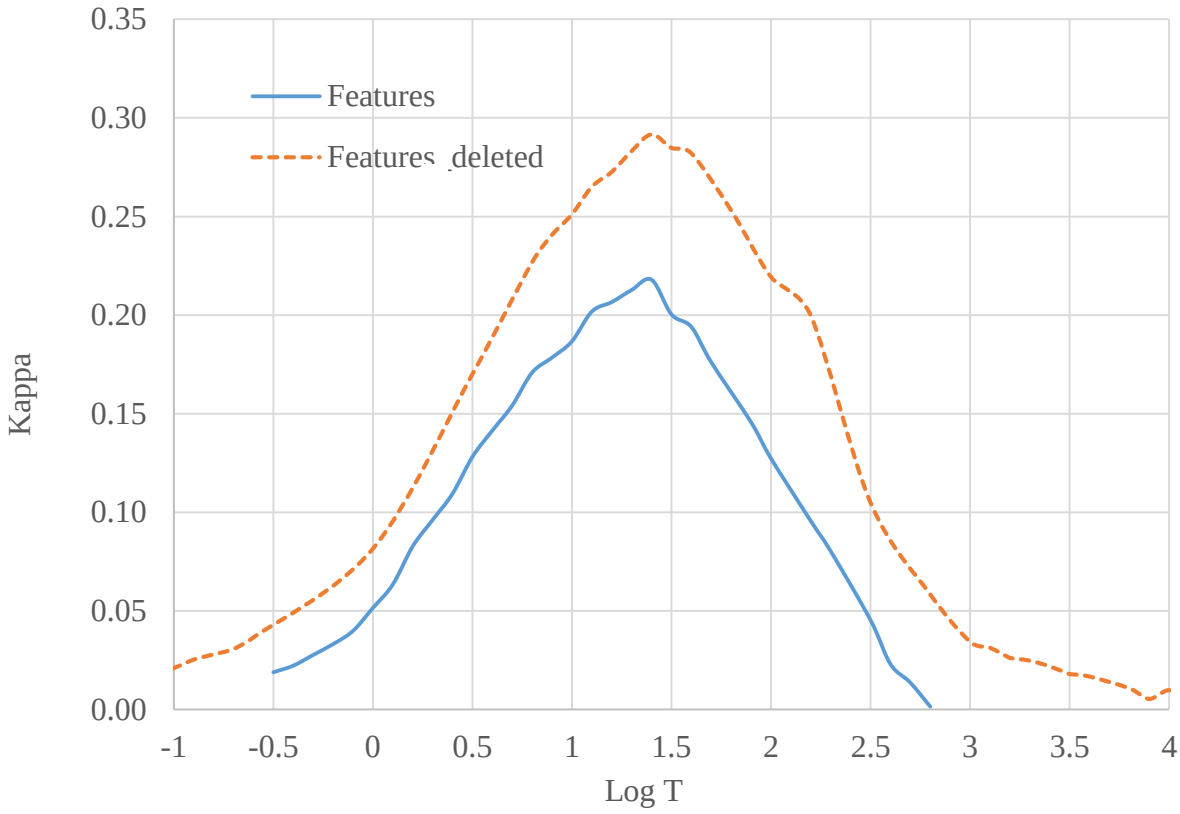

Figure 4-20: Effect of BMPs on EG location in Running Turkey watershed.

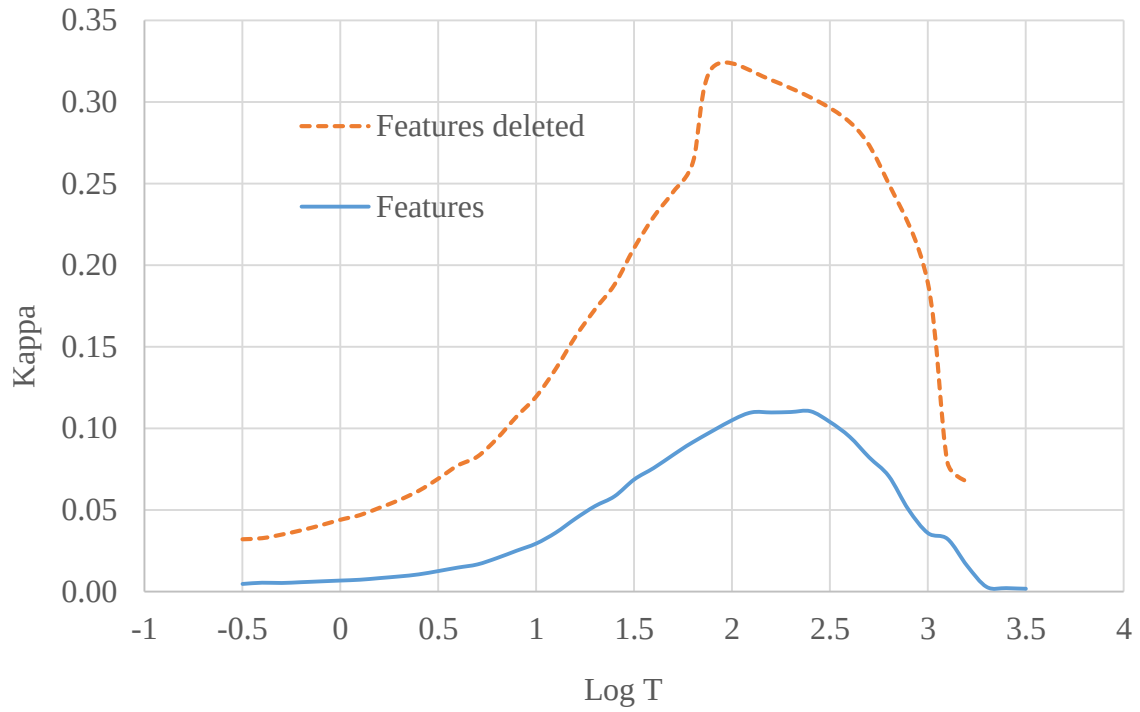

Figure 4-21: Effect of BMPs on EG location in Dry Turkey watershed.

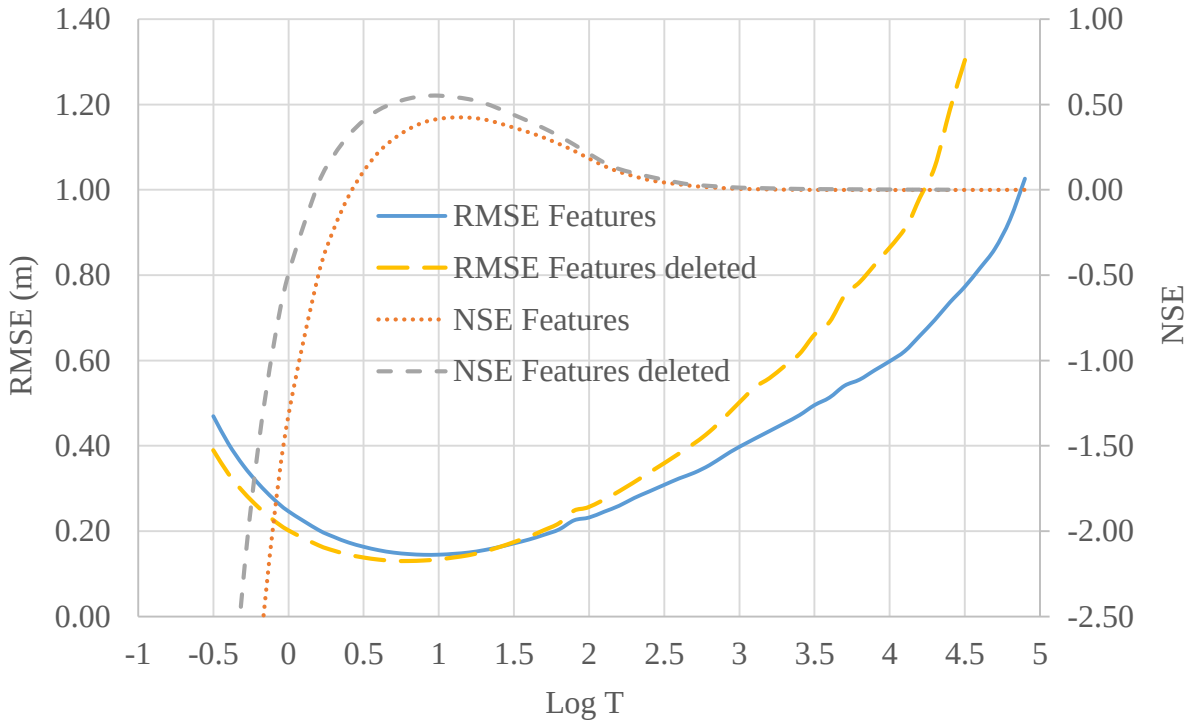

Figure 4-22: Effect of BMPs on EG length in Running Turkey watershed.

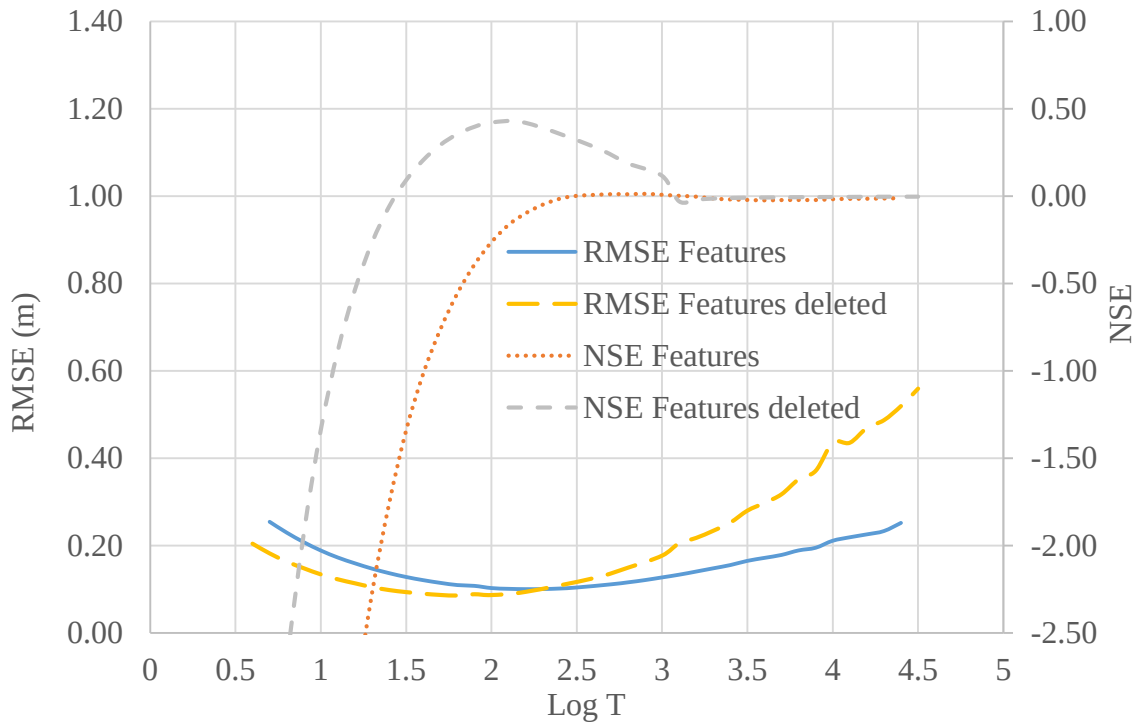

Figure 4-23: Effect of BMPs on EG length in Dry Turkey watershed.

Effect of upscaling from catchment scale to watershed scale on TI thresholds

TI models have been normally applied on catchments to predict the initiation points over which EGs form. In this study we study we applied the CTI model following the same procedures to predict the TI thresholds over which EGs form at both catchment and watershed scales.

Catchment thresholds

An observed EG network was selected within Dry Turkey watershed similar to the one shown in Figure 4-24. Executing the modeling procedure described in Chapter 3 with a set of thresholds applied to the CTI model, we studied a range of thresholds for comparison of observed and simulated EGs. From the trend observed in variations of NSE and RMSE in Figure 4-25, a threshold of 1.3 is seen producing the maximum value of NSE (0.6) and minimum of RMSE (0.07 m). Though a threshold value of 1.3 presented the best performance, the spatial visualizations show that threshold values within the range from 1.2 to 1.5 could still predict EG trajectory quite well with a minimum NSE at 0.55. The variation in the efficiency of threshold at prediction of EGs indicates that, the CTI model could predict EGs well over a range of values other than one single point.

The comparison of CTI thresholds at both catchment and watershed scale show a decrease in model efficiency and thresholds. On catchment scale, the CTI model has a threshold of 1.3 with an efficiency of NSE = 0.6 while on watershed scale the model has a threshold of 1.9 with efficiency of NSE = 0.39. These variations show the need to increase the CTI model catchment thresholds by 0.6 to obtain the thresholds at a watershed scale. However, enough information is required to come up with a concrete scaling factor to be used at both scales. It can be stipulated that at catchment scale, the topographic factors take control of the thresholds over which EGs will form, however, on watershed scale, other factors and features affecting flow come into control. Among the features that control flow are grassed waterways, terraces, culverts, roads, and field boundaries. These features abstract flow leading to changes in the available energy to erode soil particles within the watershed. This can be evidenced by an increase of threshold values from low to high at catchment and watershed scales respectively.

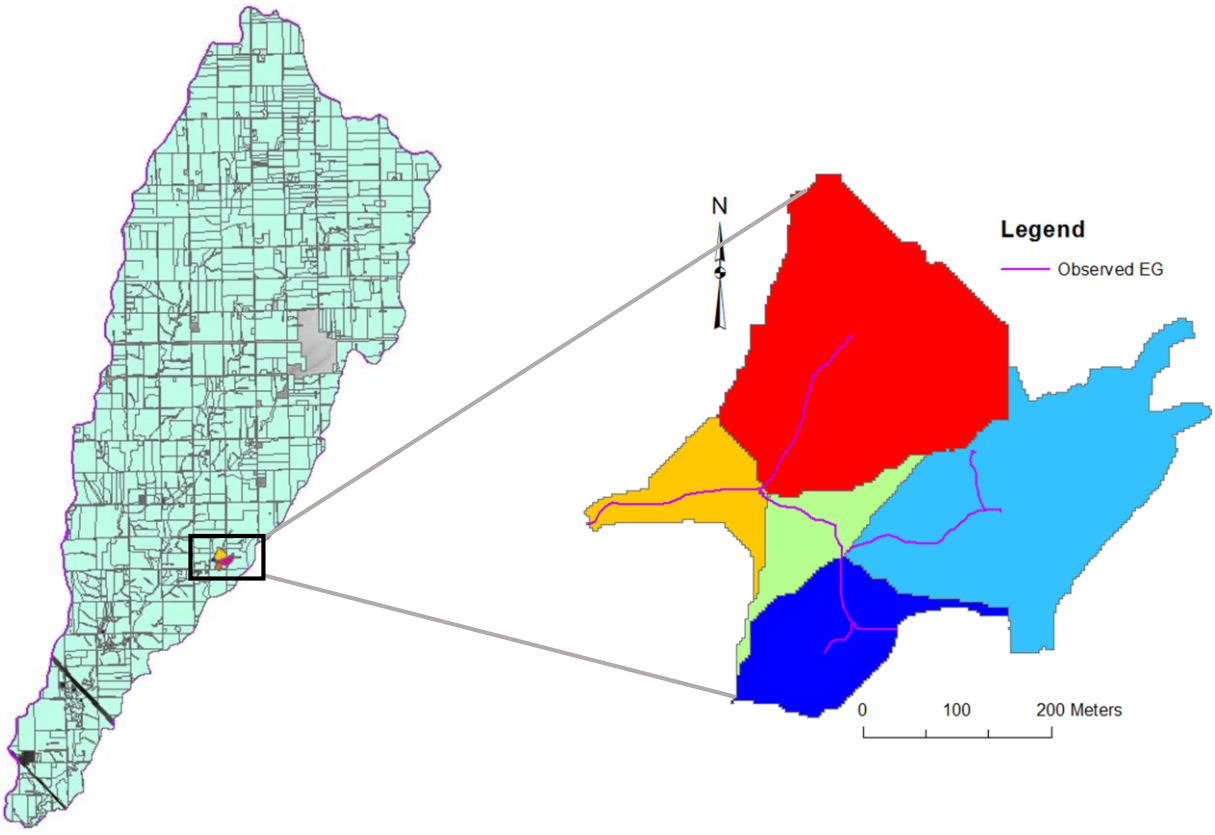

Figure 4-24: A representative map of catchment with observed EGs.

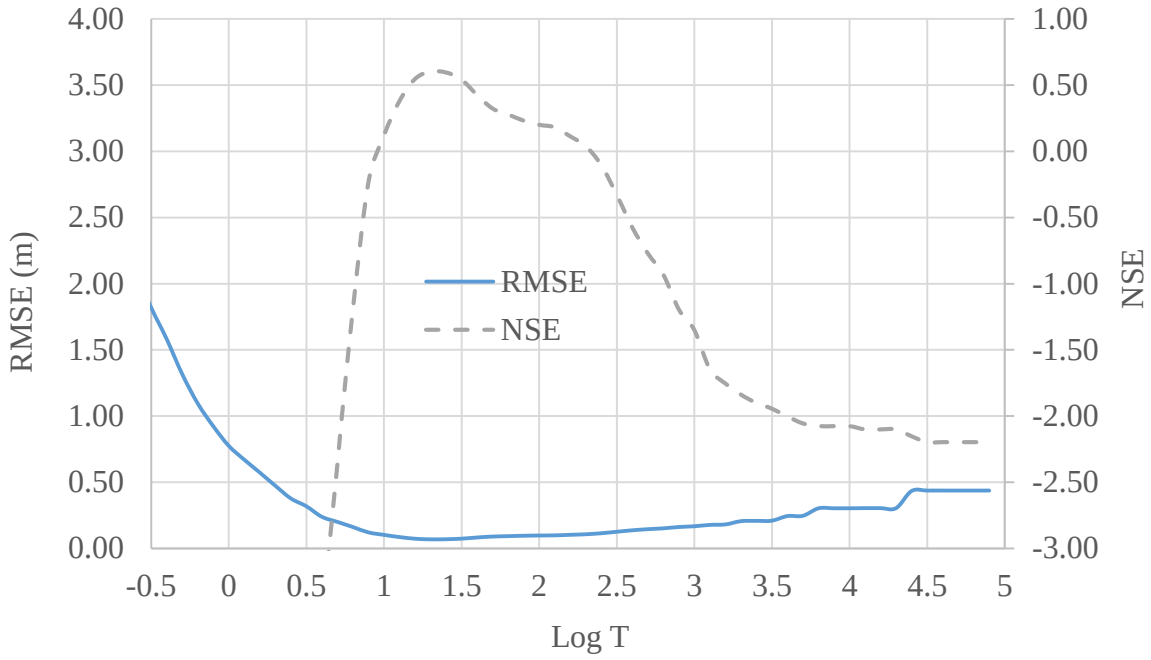

Figure 4-25: Statistics for EG trajectory prediction by the CTI model in Dry Turkey watershed

Effect of physiographic region of the watershed on TI thresholds

TI models have been reported to have limited application due to their need to revalidate thresholds over which they predict EGs. It's known that the geomorphologic factors of mainly slope, contributing area, and curvature determine the range of optimum threshold values over which TI models predict EGs. These geomorphologic factors are usually defined by the physiographic characteristics of the watershed. In this study, the effect of watershed location on TI thresholds was assessed by comparing the TI thresholds obtained in this study with those reported by different authors in literature.

Table 4-4 shows the TI thresholds obtained by different authors, and Figure 4-26 indicates the location of watersheds where the TI thresholds were obtained by each author. The comparison of thresholds indicate that, for the SA model there is a significant difference in the threshold values obtained in this study as compared to those reported in literature. However, the comparison of the WTI model did show any significant differences. It can be deduced that the physiographic location of the watershed impacts the TI thresholds to some extent. Thus, the variation of TI thresholds might be influenced by a combination of factors related to the physiographic location of the

watershed, and activities that alter the topography of the watershed. Activities such tillage, leveling of agricultural fields, and installation of terraces alter the topography of watersheds thus causing the shift in topographic thresholds within the watershed. It can be further stated that, watersheds which have experienced little topographic alternations will merely have the same mean optimum TI thresholds.

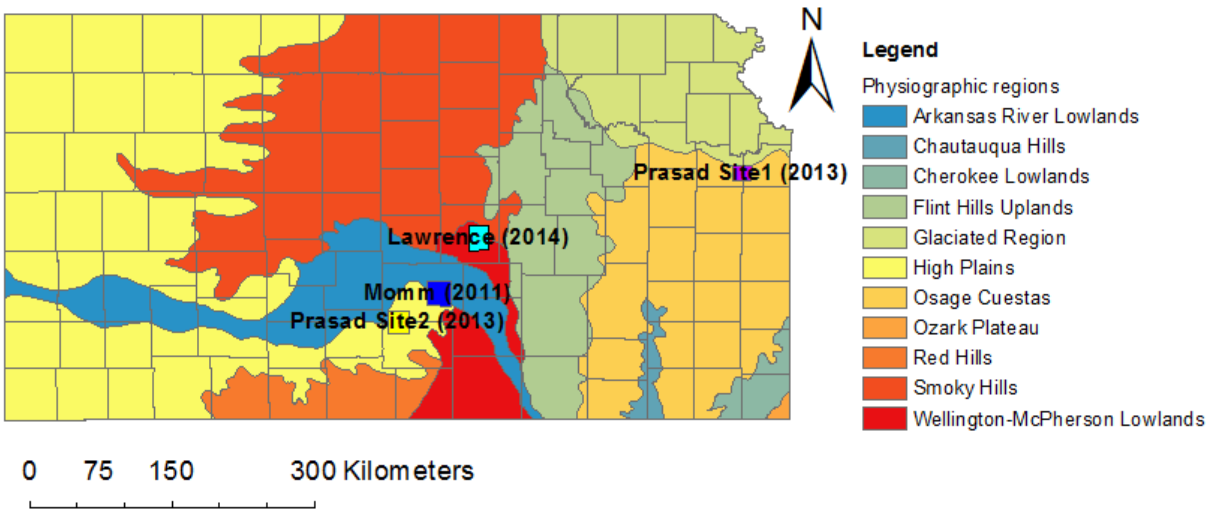

Figure 4-26: Map showing the physiological regions of Kansas, and locations where TI models have been applied by different authors.

Table 4-4: Comparison of topographic thresholds obtained in different physiological regions

Reference	Model Threshold		
	CTI	SA	WTI
Momm et al. (2011), Reno County, KS	-	-	1.2
Daggupati et al. (2013), Douglas County, KS	-	1.5	-
Daggupati et al. (2013), Reno County, KS	-	1.7	-
This study, Running Turkey watershed, KS	1.4	2.2	1.2
This study, Dry Turkey watershed, KS	1.9	2.7	1.3

tRIBS model results

tRIBS model was used to estimate stream flows, runoff and erosion rates under three different scenarios. It should be noted that the *tRIBS* model simulated the hydrological response of the test field well, however, there were inconstancies of the model at prediction erosion rates over the gridded scale of the tested fields. In what follows is the discussion of model output results.

tRIBS Model hydrology

The results of stream flow in Figure 4-27 indicate that increasing vegetation cover and surface roughness leads to a reduction in peak stream flows, time to reach the peak discharge, and shift of the hydrograph from left to right. These fluctuations in stream flows allow the infiltration and dissipation of energy of flowing water thus reducing the chance of occurrence of erosion and sediment transport to downslope receiving streams. It is hypothesized that these scenarios will mimic the changes that occur when grassed waterways are implemented on agricultural fields. The EG locations and trajectories are transformed into low grade, vegetated, and widen waterways referred to as grassed waterways. Thus, its analogue to deduce that grassed waterways impact the rates of sediment transport and erosion by reducing the stream power available to erode channels, and also reducing the peak stream discharges by encouraging infiltration. The impact of vegetation cover and surface cover on runoff rate was minimal in all simulated scenarios. All simulated scenarios had generally the same values of runoff rates as indicated in Figure 4-28. Thus, no proper conclusions can be drawn from these results.

The spatial analysis of stream flows along the channel show that stream flows increase from the upslope points of the channel to downstream points, with the highest values around the channel outlet (Figure 4-29). Similar trends in stream discharges were obtained by Knighton (1999), and he attributed them to slope and curvature of the basin. These variations in stream flows highlight the role of topography, mainly slope at controlling channel discharges, and runoff volumes within the watershed. Thus, areas at low slopes will experience high stream flows making them susceptible to erosion activities. These erosion processes are further intensified by the geomorphology of the landscape. Converging landscapes will led to generation of high stream power, thus more potential to erode channels as compared to diverging or flat landscapes. It is these dynamics in watershed hydrology that make the down slope areas to be the target points for implementation of BMPs aimed towards reducing nutrient and sediment delivery into streams.

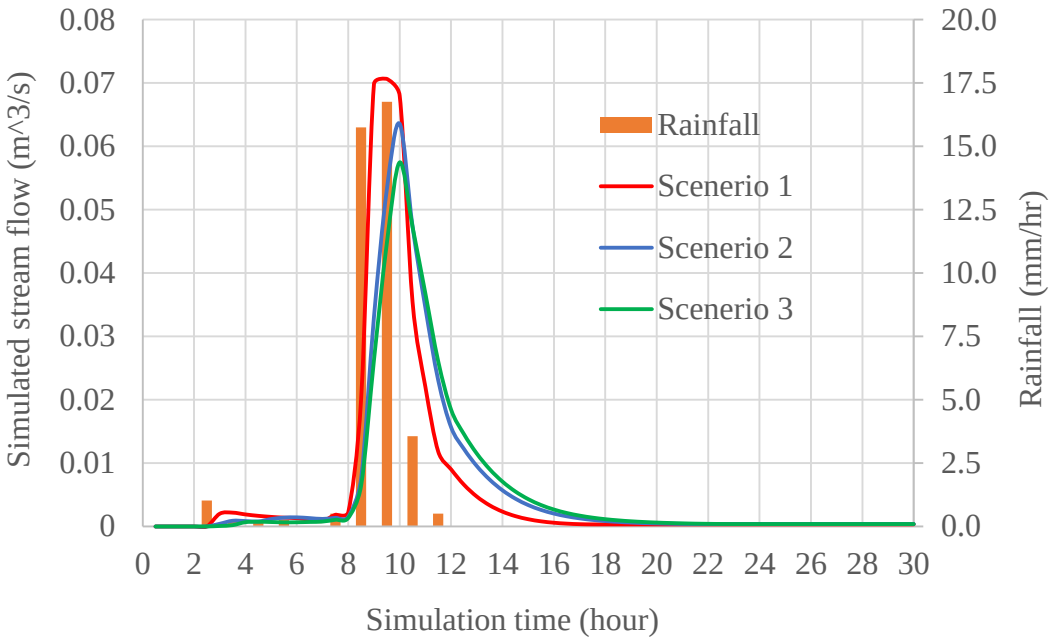

Figure 4-27: Changes in stream flow hydrographs for simulate scenarios.

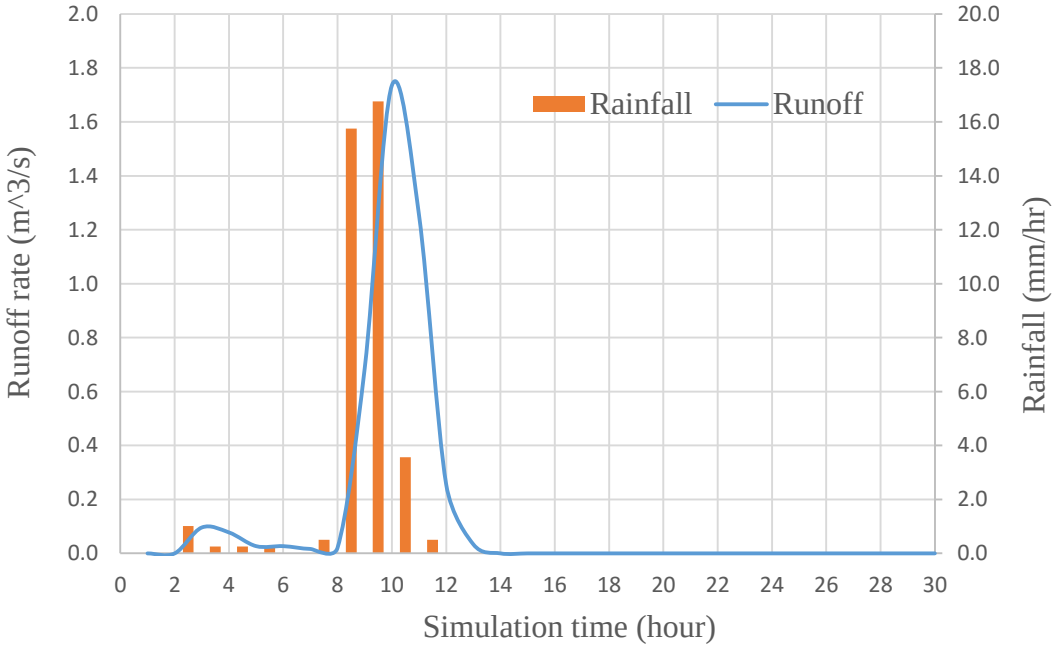

Figure 4-28: Runoff hydrograph for simulate scenarios.

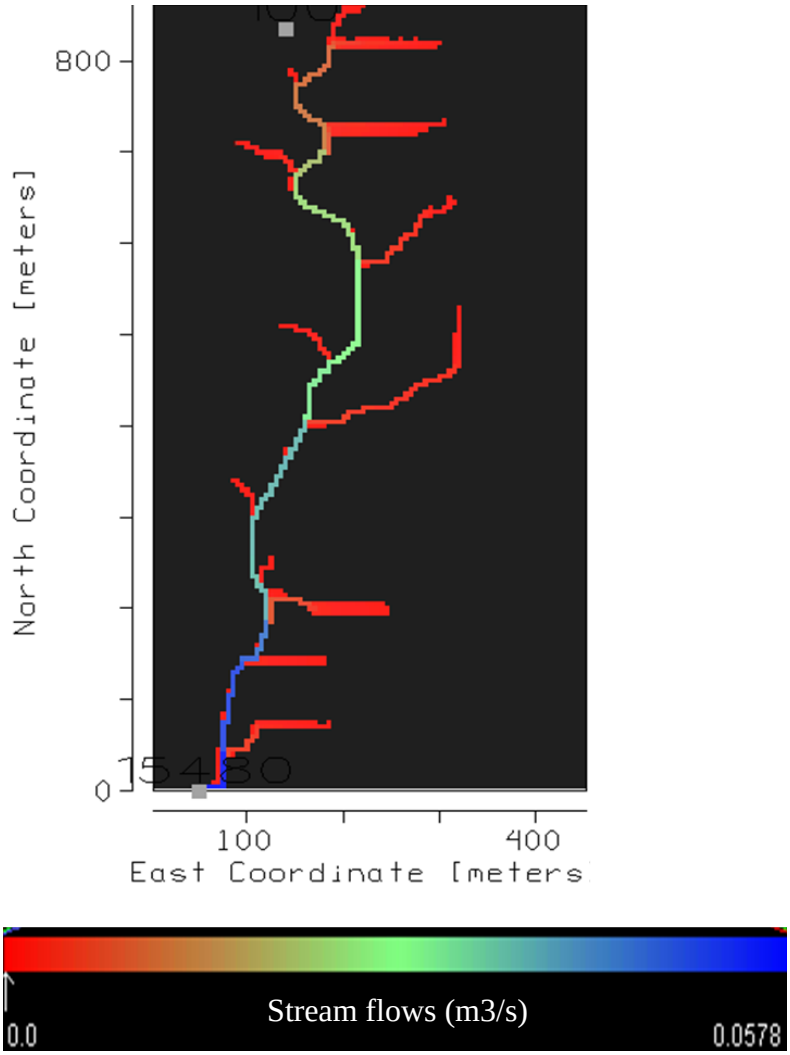

Figure 4-29: Variation of stream flows along an EG for scenario 3.

Foster and Lane model results

The Foster and Lane model was used to compute erosion rates due to EG erosion at outlet of the field and along the EG. Foster and Lane model requires peak discharge rate, slope, Manning's roughness coefficient, and length of the channel to compute the total amount of soil lost within a given period. These data requirements were obtained from the *tRIBS* model outputs. In addition, the *tRIBS* model output such as soil shear stress and detachment rates were used to calculate the sediment transport capacity and sediment loading at different points within the channel. The changes in erosion rates, and channel width at the field outlet and along the channel are presented for all the simulated scenarios.

EG erosion rates at the field outlet

The erosion rates at the channel outlet were computed using the peak values of discharge from Figure 4-27, and a constant Manning's roughness coefficient value of 0.03. The total soil losses for each scenario are presented in Table 4-5. These results indicate that reducing stream flows due to implementation of practices such as grassed waterways can led to reduction of total amount of soil being lost from the field. Further, the rates of change in channel development is also slow down as exhibited by the differences in final channel width for each scenario. Decreasing stream flows through activities such as planting grass within the channel impacts the rates of channel development by reducing water flow velocities, thus impacting the amount of kinetic energy available to erode soil particles. In addition, planting grasses increases infiltration since grass roots possess the potential to penetrate the impermeable soil layers, creating paths for water infiltration into deeper layers of soil. In this way, the time for channels to be eroded is slow down as indicated by the difference in times to reach the non-erodible layer under different scenarios as shown in Table 4-5.

The examination of erosion rate graphs for simulated scenarios show that, for an EG the maximum erosion rates are experienced at the time when channel erosion reaches the impeding layer. Figure 4-30 shows the variations in erosion rates per unit meter length of an EG with time. Initially, the erosion rates are high since channel development is at its early stages of development. The wetted perimeter and hydraulic radius of the channel are at their optimum values, and large number of soil particles are being exposed to water action. At this point, the channel has more potential to generate enough tractive force to detach soil particles, mainly due to reduced channel width, depth, and shear stress. In that way, more soil particles are separated from each other leading to high erosion rates. However at the final stages of channel development, the erosion rates decrease gradually due to reduced stream power of the channel and a decrease in the number of soil particles being exposed to erosion. Under these conditions, the erosion rates are no longer determined by the channel geometry but rather other external erosion recharges from sources such as stream banks, interills, and subsurface flow diffusions.

Table 4-5: Comparison of final width, total erosion, and time to reach the non-erodible layer for all simulated scenarios.

Scenario	Final width (m)	Total erosion (Kg)	Time to reach non-erodible layer (hours)
Scenario1	0.95	173.87	2.88
Scenario2	0.89	156.89	3.06
Scenario 3	0.83	139.77	3.26

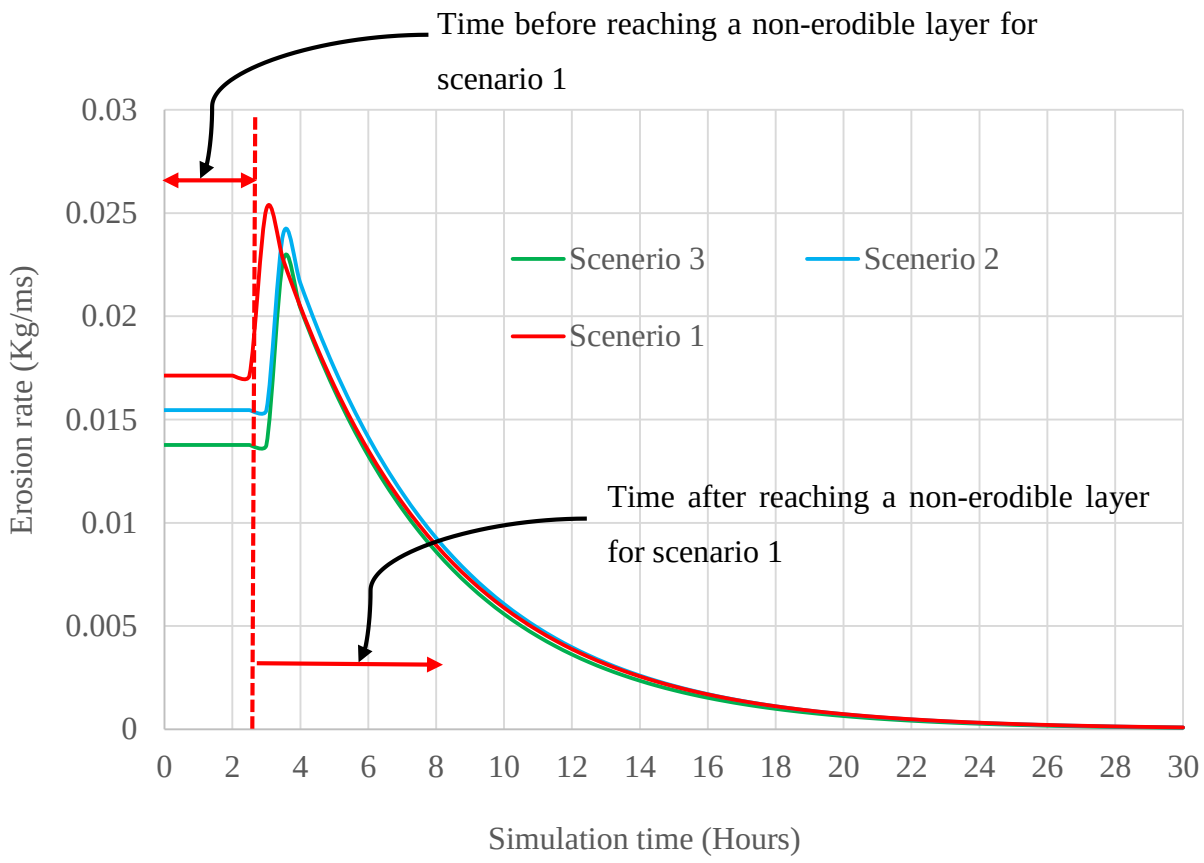

Figure 4-30: Changes in erosion rates per unit length of a 5 m EG at the field outlet.

Spatial variation of erosion rates along an EG

The spatial variations in erosion rates for scenarios 2 and 3 are presented along with the corresponding variations in channel geometry. The total amount of soil eroded for the simulation period was 12848 kg for scenario two, and the maximum channel width attained was 0.14 m (Figure 4-31 and Figure 4-33). For the case of scenario 3, the total soil eroded was 74600 kg with

a maximum change of 0.46 m in channel width (Figure 4-32 and Figure 4-34). It can also be observed that there were high erosion rates in scenario 3 as compared to scenario 2. The high erosion rates in scenario 3 are attributed to the over prediction EG erosion rates by the Foster and Lane model when the Manning's coefficients are increased.

The Foster and Lane model computes the rate of EG erosion by employing factors related to slope, discharge, channel roughness, and shear stress. On the spatial scale, all these factors are variants and thus evaluating their sole effect on the rates of erosion might be peculiar. The resultant effects of all these variables can be expressed using the concepts of sediment transport capacity and sediment loading at each point within the field. The ratio of sediment loading to sediment transport capacity offers the understanding of how much soil can be detached from a point under prevailing conditions. Figure 4-31 and Figure 4-32 shows the variation of erosion rates along an EG in the test field. It is expected that erosion rates would increase from the upslope areas of the channel to downslope points, because that's how the stream power (discharge) varies, however, this was not the case. The intermittent changes in soil loss along the stream might be attributed to fluctuations in sediment loading, sediment transport capacity, curvature of the surface, and changes in channel width. Figure 4-33 and Figure 4-34 show that areas experiencing bigger changes in channel width have the highest erosion rates and occur just upslope of the field outlet as illustrated, by Figure 4-31 and Figure 4-32. This might be attributed to low sediment loading rates, high transport capacity, high slope, and convergence of flow at these points. These conditions can lead to high accumulation of soil in the proceeding downslope points, thus limiting their transport capacity to carry soil particles. The same conditions might also lead to meandering and flattening of the channel (changing the slope and curvature of the surface), which results into reduced stream power. If conditions continue to prevail, the ratio of sediment loading to transport capacity might turn to a unit, and neither erosion nor deposition is occurring at such points. The resultant effect is the creation of "no erosion cells" represented by the gaps along the stream network. The proper prediction of EG erosion rates require a good grasp of erosion processes and dynamics that occur along the channel other than relying on topographic attributes of slope and geomorphology.

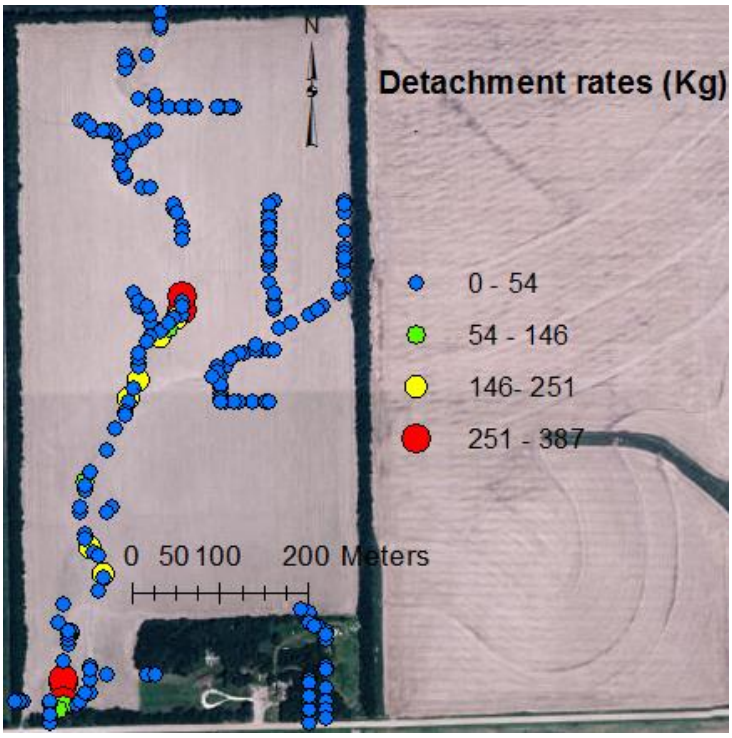

Figure 4-31: Variations in soil detachment rates along an EG for scenario two.

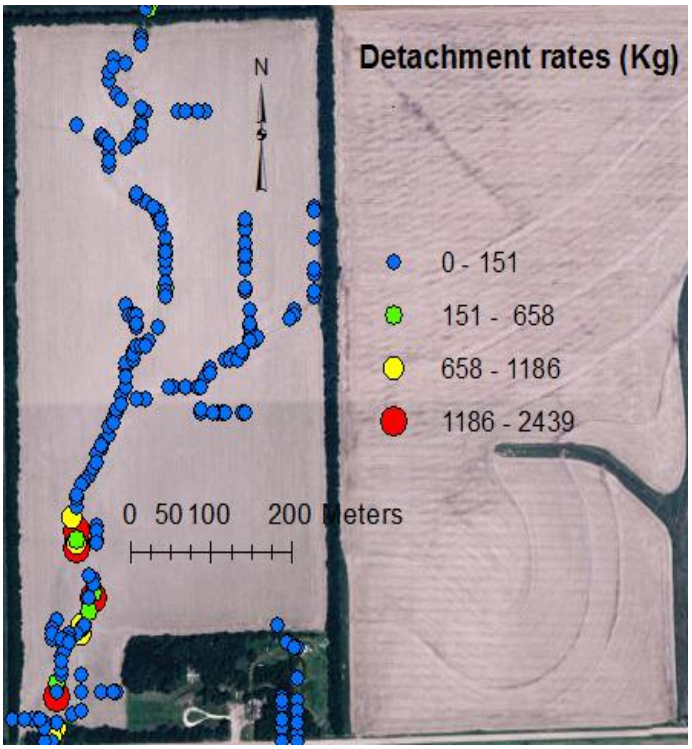

Figure 4-32: Variations in soil detachment rates along an EG for scenario three.

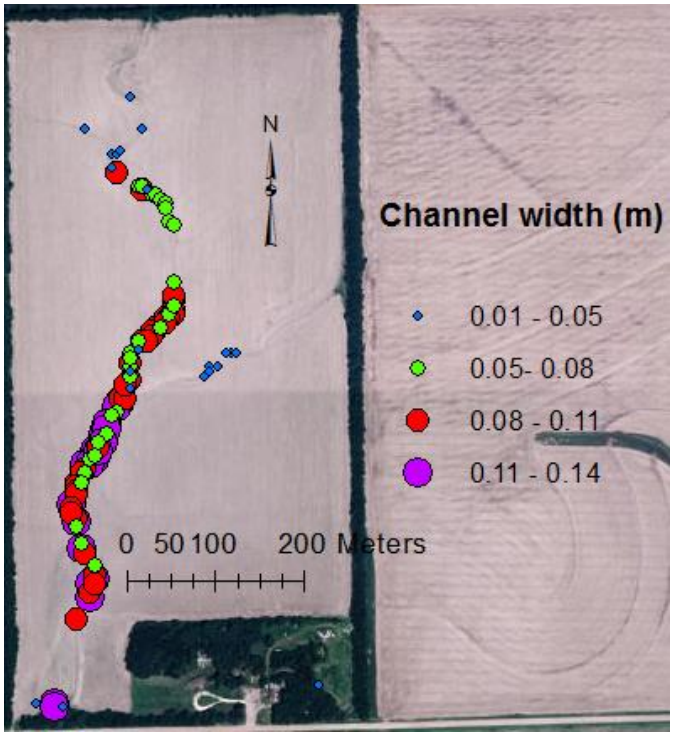

Figure 4-33: Variations in channel width along an EG for scenario two.

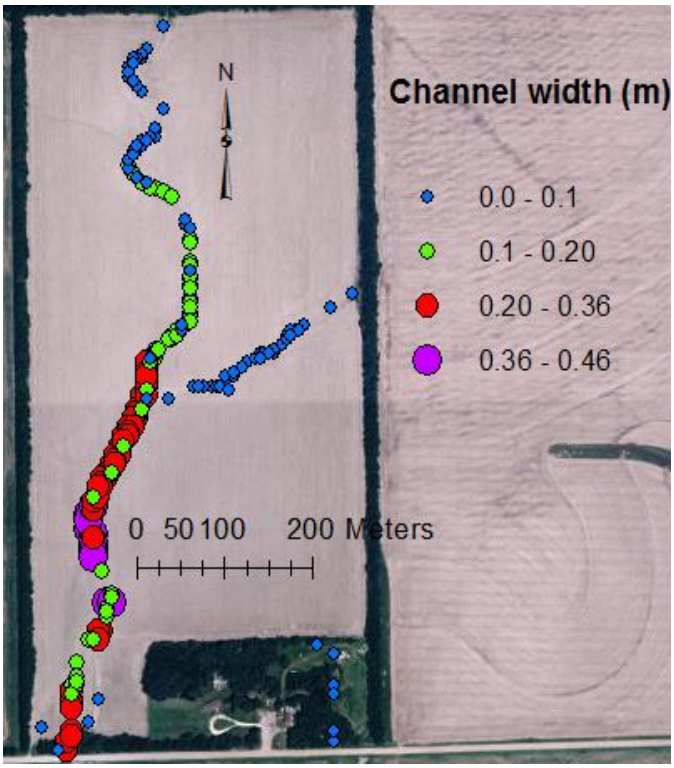

Figure 4-34: Variations in channel width along an EG for scenario 3.

Chapter 5 - Conclusion

TIs provide simple means of predicting the location and trajectory of EGs on agricultural fields. TI models can predict locations of EGs up to a maximum accuracy of 70%. Accuracy of TI thresholds require a holistic approach of considering both EG location and EG length. In addition, the performance of TI models at prediction of EGs is affected by watershed features such as grassed waterways, terraces, and culverts. These watershed features impact both flow and topography of the watershed. CTI model outperformed all the models that were evaluated in this study, mainly due to incorporation of plan curvature coefficient. The variations in TI model thresholds for all the models suggested that TI models can predict EG location and length over a range of thresholds rather than one single value.

The range of values over which TI models predict EGs is determined by scale of the area under study (catchment or watershed scales), physiographic region of the watershed, terraces, and grassed waterways. The concept of drainage density can be used in the identification of head water and main stem catchments, and a confirmatory test to between the EG location and length thresholds. The identification of head water catchments improves the understanding of catchments experiencing head cut migration while identification of main stem catchments highlights regions of well pronounced EGs and natural streams.

Terraces and grassed waterways reduce erosion on field by increasing thresholds over which EGs form. In addition, they also impact the stream power of headwater channels thus impacting kinematic energy available to detach soil particles. Increasing vegetation cover and surface cover of the fields impacts sediment discharge from fields by increasing infiltration and reducing the peak runoff rates thus protecting the soil from erosion process. Though *tRIBS* model, simulates watershed hydrology well, it still needs some improvement to perfectly predict erosion rates over an agricultural field. The combination of process – based approaches exhibits a great potential to assess the erosion rates and effectiveness of BMPs at reduction of EG erosion.

References

Agnew, L.J., S. Lyon, P. Gérard-Marchant, V.B. Collins, A.J. Lembo, T.S. Steenhuis and M.T. Walter. 2006. Identifying hydrologically sensitive areas: Bridging the gap between science and application. J. Environ. Manage. 78:63-76.

Alonso, C.V., S.J. Bennett and O.R. Stein. 2002. Predicting head cut erosion and migration in concentrated flows typical of upland areas. Water Resour. Res. 38:39-1-39-15.

Andraski, T.W. and L.G. Bundy. 2003. Relationships between phosphorus levels in soil and in runoff from corn production systems. J. Environ. Qual. 32:310-316.

Bennett, S., J. Casali, K. Robinson and K. Kadavy. 2000. Characteristics of actively eroding ephemeral gullies in an experimental channel. Trans. ASAE 43:641-649.

Bingner, R., F. Theurer and Y. Yuan. 2009. Agricultural Non–point Source Pollution Model.AnnAGNPS Technical Processes Documentation Version 5.0.

Boll, J., E. Brooks, C. Campbell, C. Stockle, S. Young, J. Hammel and P. McDaniel. 1998. Progress toward development of a GIS based water quality management tool for small rural watersheds: Modification and application of a distributed model. p. 12-16. *In* Progress toward development of a GIS based water quality management tool for small rural watersheds: Modification and application of a distributed model. ASAE annual international meeting in orlando, florida, july, 1998. Citeseer, .

Bruno, C., C.D. Stefano and V. Ferro. 2008. Field investigation on rilling in the experimental sparacia area, south italy. Earth Surf. Process. Landforms 33:263-279.

Capra, A. 2013. Ephemeral gully and gully erosion in cultivated land: A review. Drainage Basins and Catchment Management: Classification, Modelling and Environmental Assessment.Nova Science Publishers, Hauppauge, NY.

Capra, A., C. Di Stefano, V. Ferro and B. Scicolone. 2009. Similarity between morphological characteristics of rills and ephemeral gullies in sicily, italy. Hydrol. Process. 23:3334-3341.

Casalı, J., J. López and J. Giráldez. 1999. Ephemeral gully erosion in southern navarra (spain). Catena 36:65-84.

Chow, V., T. 1959. Open channel hydraulics. McGraw Hill Book Company Inc, New York.

Cohen, J. 1960. A coefficient of agreement for nominal scales. Educational and Psychological Measurement.

Dabney, S., D. Yoder, D. Vieira, R. Bingner and R. Wells. 2010. Scaling a representative storm sequence to estimate ephemeral gully erosion with RUSLE2. *In* Scaling a representative storm sequence to estimate ephemeral gully erosion with RUSLE2. Federal interagency sedimentation conference proceedings, 2010.

Daggupati, P., A.Y. Sheshukov and K.R. Douglas-Mankin. 2014. Evaluating ephemeral gullies with a process-based topographic index model. Catena 113:177-186.

Daggupati, P., K.R. Douglas-Mankin and A.Y. Sheshukov. 2013. Predicting ephemeral gully location and length using topographic index models. Transactions of the ASABE 56:1427-1440.

De Santisteban, L., J. Casalí, J. López, J. Giráldez, J. Poesen and J. Nachtergaele. 2005. Exploring the role of topography in small channel erosion. Earth Surf. Process. Landforms 30:591-599.

Desmet, P., J. Poesen, G. Govers and K. Vandaele. 1999. Importance of slope gradient and contributing area for optimal prediction of the initiation and trajectory of ephemeral gullies. Catena 37:377-392.

Di Stefano, C. and V. Ferro. 2011. Measurements of rill and gully erosion in sicily. Hydrol. Process. 25:2221-2227.

Dietrich, W.E., C.J. Wilson, D.R. Montgomery and J. McKean. 1993. Analysis of erosion thresholds, channel networks, and landscape morphology using a digital terrain model. J. Geol.259-278.

Dietrich, W.E., C.J. Wilson, D.R. Montgomery, J. McKean and R. Bauer. 1992. Erosion thresholds and land surface morphology. Geology 20:675-679.

Dunne, T. and R.D. Black. 1970. An experimental investigation of runoff production in permeable soils. Water Resour. Res. 6:478-490.

Elliot, W.J. 1990. Compendium of soil erodibility data from WEPP cropland soil field erodibility experiments 1987 & 88.

Elliot, W. and J. Laflen. 1993. A process-based rill erosion model. Transactions of the ASAE (USA).

FAO. 2015. FAO says food production must rise by 70%.

Flanagan, D. and M. Nearing. 1995. USDA-Water Erosion Prediction Project: Hillslope Profile and Watershed Model Documentation.

Foster, G.R. 2005. Modeling ephemeral gully erosion for conservation planning. International Journal of Sediment Research 20:157-175.

Foster, G.R. 1986. Understanding ephemeral gully erosion. Soil Conservation:: An Assessment of the National Resources Inventory 2:90.

Foster, G.R., T.E. Toy and K.G. Renard. 2003. Comparison of the USLE, RUSLE1. 06c, and RUSLE2 for application to highly disturbed lands. p. 154-160. *In* Comparison of the USLE, RUSLE1. 06c, and RUSLE2 for application to highly disturbed lands. First interagency conference on research in watersheds, 2003.

Foster, G. and L. Lane. 1983. Erosion by concentrated flow in farm fields. p. 9.65-9.82. *In* Erosion by concentrated flow in farm fields. Proceedings of the DB simons symposium on erosion and sedimentation, 1983. Colorado State University Fort Collins, CO, .

Foster, G., D. Flanagan, M. Nearing, L. Lane, L. Risse and S. Finkner. 1995. Hillslope erosion component. WEPP: USDA-Water Erosion Prediction Project11.1-11.12.

Fotheringham, S. and M. Wegener. 1999. Spatial models and GIS: New and potential models. CRC press, .

Francipane, A., V.Y. Ivanov, L.V. Noto, E. Istanbulluoglu, E. Arnone and R.L. Bras. 2012. tRIBS-erosion: A parsimonious physically-based model for studying catchment hydro-geomorphic response. Catena 92:216-231.

Frankenberger, J.R., E.S. Brooks, M.T. Walter, M.F. Walter and T.S. Steenhuis. 1999. A GIS-based variable source area hydrology model. Hydrol. Process. 13:805-822.

Gali, R.K., M.L. Soupir, A.L. Kaleita and P. Daggupati. 2014. Identifying potential locations for grassed waterways using terrain attributes and precision conservation technologies. Assessing Monitoring and Modeling Approaches to Improve Water Quality in the Hickory Grove Lake66.

Gérard-Marchant, P., W. Hively and T. Steenhuis. 2005. Distributed hydrological modelling of total dissolved phosphorus transport in an agricultural landscape, part I: Distributed runoff generation. Hydrology and Earth System Sciences Discussions Discussions 2:1537-1579.

Gordon, L.M., S.J. Bennett, C.V. Alonso and R.L. Bingner. 2008. Modeling long-term soil losses on agricultural fields due to ephemeral gully erosion. J. Soil Water Conserv. 63:173-181.

Gordon, L., S. Bennett, R. Bingner, F. Theurer and C. Alonso. 2007. Simulating ephemeral gully erosion in AnnAGNPS. Transactions of the ASABE 50:857-866.

Gordon, L., S. Bennett, R. Bingner, F. Theurer and C. Alonso. 2006. REGEM: The revised ephemeral gully erosion model. *In* REGEM: The revised ephemeral gully erosion model. Proceedings of the 8th federal interagency sedimentation conference, 2006.

Haan, C.T., B.J. Barfield and J.C. Hayes. 1994a. Design hydrology and sedimentology for small catchments. Elsevier, .

Haan, C.T., B.J. Barfield and J.C. Hayes. 1994b. Design hydrology and sedimentology for small catchments. Elsevier, .

Horton, R.E. 1933. The role of infiltration in the hydrologic cycle. Eos, Transactions American Geophysical Union 14:446-460.

Hursh, C. and E. Brater. 1941. Separating storm-hydrographs from small drainage-areas into surface-and subsurface-flow. Eos, Transactions American Geophysical Union 22:863-871.

Ivanov, V.Y., E.R. Vivoni, R.L. Bras and D. Entekhabi. 2004. Catchment hydrologic response with a fully distributed triangulated irregular network model. Water Resour. Res. 40:.

Jetten, V.G. and A.P. de Roo. 2001. Spatial analysis of erosion conservation measures with LISEM. p. 429-445. *In* Landscape erosion and evolution modeling. Springer, .

KDHE. 2015. KDHE approved nine element watershed plans. 2015:.

Kim, I. 2006. Identifying the roles of overland flow characteristics and vegetated buffer systems for nonpoint source pollution control. ProQuest, .

Kim, S. and T. Steenhuis. 2001. GRIEROM: Grid-based variable source area soil-water erosion and deposition model. Trans. ASAE 44:853-862.

Knighton, A.D. 1999. Downstream variation in stream power. Geomorphology 29:293-306.

Knisel, W.G. 1980. CREAMS: A field-scale model for chemicals, runoff and erosion from agricultural management systems. USDA Conservation Research Report.

Kohavi, R. and F. Provost. 1998. Special issue on "applications of machine learning and the knowledge of discovery process". Machine Learning 30:.

Leh, M., I. Chaubey, J. Murdoch, J. Brahana and B. Haggard. 2008. Delineating runoff processes and critical runoff source areas in a pasture hillslope of the ozark highlands. Hydrol. Process. 22:4190-4204.

Lepore, C., E. Arnone, L. Noto, G. Sivandran and R. Bras. 2013. Physically based modeling of rainfall-triggered landslides: A case study in the luquillo forest, puerto rico. Hydrology and Earth System Sciences 17:3371-3387.

Licciardello, F., D. Zema, S. Zimbone and R. Bingner. 2007. Runoff and soil erosion evaluation by the AnnAGNPS model in a small mediterranean watershed.

Loague, K., C.S. Heppner, B.A. Ebel and J.E. VanderKwaak. 2010. The quixotic search for a comprehensive understanding of hydrologic response at the surface: Horton, dunne, dunton, and the role of concept-development simulation. Hydrol. Process. 24:2499-2505.

McCuen, R.H. and J.M. Spiess. 1995. Assessment of kinematic wave time of concentration. J. Hydraul. Eng. 121:256-266.

Momm, H., R. Bingner, R. Wells and S. Dabney. 2011. Analysis of topographic attributes for identification of ephemeral gully channel initiation in agricultural watersheds. p. 7-10. *In* Analysis of topographic attributes for identification of ephemeral gully channel initiation in agricultural watersheds. Proceedings of the american society of agricultural and biological engineers international (ASABE), 2011.

Momm, H., R. Bingner, R. Wells and D. Wilcox. 2012. AGNPS GIS-based tool for watershed-scale identification and mapping of cropland potential ephemeral gullies. Appl. Eng. Agric.

Momm, H., R. Bingner, R. Wells, J. Rigby and S. Dabney. 2013. Effect of topographic characteristics on compound topographic index for identification of gully channel initiation locations. Transactions of the ASABE 56:523-537.

Montgomery, D.R. and W.E. Dietrich. 1988. Where do channels begin? Nature 336:232-234.

Montgomery, D.R. and W.E. Dietrich. 1992. Channel initiation and the problem of landscape scale. Science 255:826-830.

Moore, I., G. Burch and D. Mackenzie. 1988. Topographic effects on the distribution of surface soil water and the location of ephemeral gullies. Transactions of the ASAE (USA).

Nachtergaele, J., J. Poesen, A. Sidorchuk and D. Torri. 2002. Prediction of concentrated flow width in ephemeral gully channels. Hydrol. Process. 16:1935-1953.

Nachtergaele, J., J. Poesen, L. Vandekerckhove, D. Oostwoud Wijdenes and M. Roxo. 2001a. Testing the ephemeral gully erosion model (EGEM) for two mediterranean environments. Earth Surf. Process. Landforms 26:17-30.

Nachtergaele, J., J. Poesen, A. Steegen, I. Takken, L. Beuselinck, L. Vandekerckhove and G. Govers. 2001b. The value of a physically based model versus an empirical approach in the prediction of ephemeral gully erosion for loess-derived soils. Geomorphology 40:237-252.

Nearing, M. and A. Nicks. 1998. Evaluation of the water erosion prediction project (WEPP) model for hillslopes. p. 43-53. *In* Modelling soil erosion by water. Springer, .

Nearing, M., G. Foster, L. Lane and S. Finkner. 1989. Erosion prediction project technology.

Nearing, M., J. Simanton, L. Norton, S. Bulygin and J. Stone. 1999. Soil erosion by surface water flow on a stony, semiarid hillslope. Earth Surf. Process. Landforms 24:677-686.

Nearing, M., L. Norton, D. Bulgakov, G. Larionov, L. West and K. Dontsova. 1997. Hydraulics and erosion in eroding rills. Water Resour. Res. 33:865-876.

Nouwakpo, S. and C. Huang. 2010. Pore water effects on soil erodibility and its implication in ephemeral gully erosion modeling.

Parker, C., C. Thorne, R. Bigner, R. Wells and D. Wilcox. 2007. Automated mapping of the potential for ephemeral gully formation in agricultural watersheds. US Department of Agriculture, Agricultural Research Service, National Sedimentation Laboratory Research Report, Oxford, MS.

Poesen, J., J. Nachtergaele, G. Verstraeten and C. Valentin. 2003. Gully erosion and environmental change: Importance and research needs. Catena 50:91-133.

Prosser, I.P. and B. Abernethy. 1996. Predicting the topographic limits to a gully network using a digital terrain model and process thresholds. Water Resour. Res. 32:2289-2298.

Quinn, P., K. Beven, P. Chevallier and O. Planchon. 1991. Prediction of hillslope flow paths for distributed hydrological modelling using digital terrain models. Hydrol. Process. 5:59-79.

Rejman, J. and R. Brodowski. 2005. Rill characteristics and sediment transport as a function of slope length during a storm event on loess soil. Earth Surf. Process. Landforms 30:231-239.

Renard, K.G., G.R. Foster, G.A. Weesies and J.P. Porter. 1991. RUSLE: Revised universal soil loss equation. J. Soil Water Conserv. 46:30-33.

Renard, K.G., G. Foster, G. Weesies, D. McCool and D. Yoder. 1997. Predicting soil erosion by water: A guide to conservation planning with the revised universal soil loss equation (RUSLE). United States Department of Agriculture Washington, DC, .

Rodney, L., Huffman, D.F. Delmar, William J. Elliot and Stephen R. Workman. 2013. Chaptyer 7: Soil erosion by water. p. 145-170. *In* Soil and water conservation engineering. Seventh ed. America Society of agricultural and Biological Engineers, St Joseph Michigan.

Sidorchuk, A. 1999. Dynamic and static models of gully erosion. Catena 37:401-414.

Soil Science Society of America. 2015. Glossary of soil science terms. 2015:.

Souchere, V., O. Cerdan, B. Ludwig, Y. Le Bissonnais, A. Couturier and F. Papy. 2003. Modelling ephemeral gully erosion in small cultivated catchments. Catena 50:489-505.

Steichen, J.M., S.L. Hutchinson, N. Zhang, J. Hutchinson, C. Oviatt, A. Anderson, T. Keane and P.L. Barnes. 2008. Assessing the Impact of Maneuver Training on NPS Pollution and Water Quality.

Taguas, E., Y. Yuan, R. Bingner and J. Gomez. 2012. Modeling the contribution of ephemeral gully erosion under different soil managements: A case study in an olive orchard microcatchment using the AnnAGNPS model. Catena 98:1-16.

Takken, I., L. Beuselinck, J. Nachtergaele, G. Govers, J. Poesen and G. Degraer. 1999. Spatial evaluation of a physically-based distributed erosion model (LISEM). Catena 37:431-447.

Theurer, F.D., C.V. Alonso and Bernard,. 1996. Hydraulic geometry for pollutant loading computer models using geographical information systems to develop input data. p. 8. *In* Hydraulic geometry for pollutant loading computer models using geographical information systems to develop input data. March 1996 1996.

Thorne, C., L.W. Zevenbergen, E. Grissinger and J. Murphey. 1986. Ephemeral gullies as sources of sediment. *In* Ephemeral gullies as sources of sediment. Proceedings of the fourth federal interagency sedimentation conference march 24-27, 1986, las vegas, nevada. 1986.

Tiwari, A., L. Risse and M. Nearing. 2000. Evaluation of WEPP and its comparison with USLE and RUSLE. Trans. ASAE 43:1129-1135.

Toy, T.J., G.R. Foster and K.G. Renard. 2002. Soil erosion: Processes, prediction, measurement, and control. John Wiley & Sons, .

Tucker, G.E. and R.L. Bras. 1998. Hillslope processes, drainage density, and landscape morphology. Water Resour. Res. 34:2751-2764.

UNPF. 2015. World population trends. 07/08/2015:.

US EPA. 2015. Water quality facts. 2015:.

US EPA. 2010. What is nonpoint source (NPS) Pollution**?**. 09/03/2015:.

USDA NRCS. 1997. The state of the land [Online]. 12/02/2014.

USDA NRSC. 2014. National resources conservation service- geospatial data gateway. 2014:.

Vandekerckhove, L., J. Poesen, D.O. Wijdenes and T. De Figueiredo. 1998. Topographical thresholds for ephemeral gully initiation in intensively cultivated areas of the mediterranean. Catena 33:271-292.

Vieira, D.A., S.M. Dabney and D.C. Yoder. 2015. Distributed soil loss estimation system including ephemeral gully development and tillage erosion. Proceedings of the International Association of Hydrological Sciences 367:80-86.

Visa, S., B. Ramsay, A.L. Ralescu and E. van der Knaap. 2011. Confusion matrix-based feature selection. *In* Confusion matrix-based feature selection. 2011. Citeseer, .

Vivoni, E.R., V.Y. Ivanov, R.L. Bras and D. Entekhabi. 2004. Generation of triangulated irregular networks based on hydrological similarity. J. Hydrol. Eng. 9:288-302.

Walter, M.T., M.F. Walter, E.S. Brooks, T.S. Steenhuis, J. Boll and K. Weiler. 2000. Hydrologically sensitive areas: Variable source area hydrology implications for water quality risk assessment. J. Soil Water Conserv. 55:277-284.

Weyman, D. 1970. Throughflow on hillslopes and its relation to the stream hydrograph. Hydrological Sciences Journal 15:25-33.

Wicks, J. and J. Bathurst. 1996. SHESED: A physically based, distributed erosion and sediment yield component for the SHE hydrological modelling system. Journal of Hydrology 175:213-238.

Wilson, J.P. and J.C. Gallant. 2000. Terrain analysis: Principles and applications. John Wiley & Sons, .

Wischmeier, W.H. and D.D. Smith. 1978. Predicting rainfall erosion losses-A guide to conservation planning. Predicting Rainfall Erosion Losses-A Guide to Conservation Planning.

Wischmeier, W.H. and D.D. Smith. 1960. A universal soil-loss equation to guide conservation farm planning. Transactions 7th Int.Congr.Soil Sci. 1:418-425.

Woodward, D. 1999. Method to predict cropland ephemeral gully erosion. Catena 37:393-399.

Yalin, M.S. 1963. An expression for bed-load transportation. Journal of the Hydraulics Division 89:221-250.

Appendix A - Statistics of location analysis for TI models within Running Turkey watershed

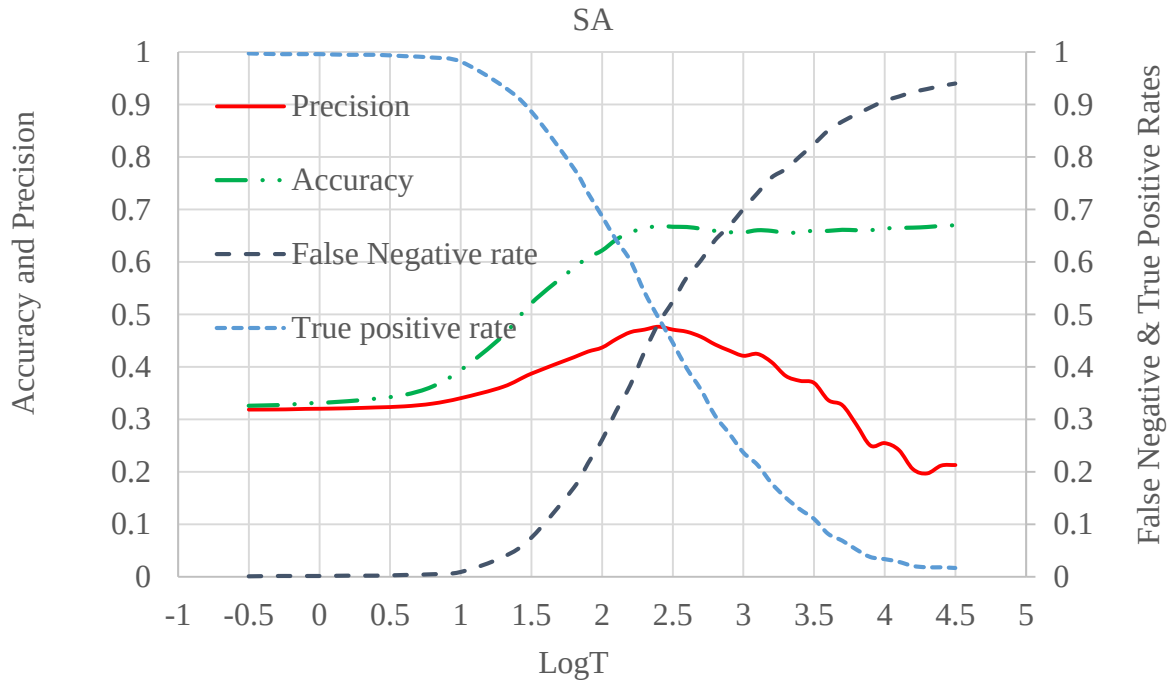

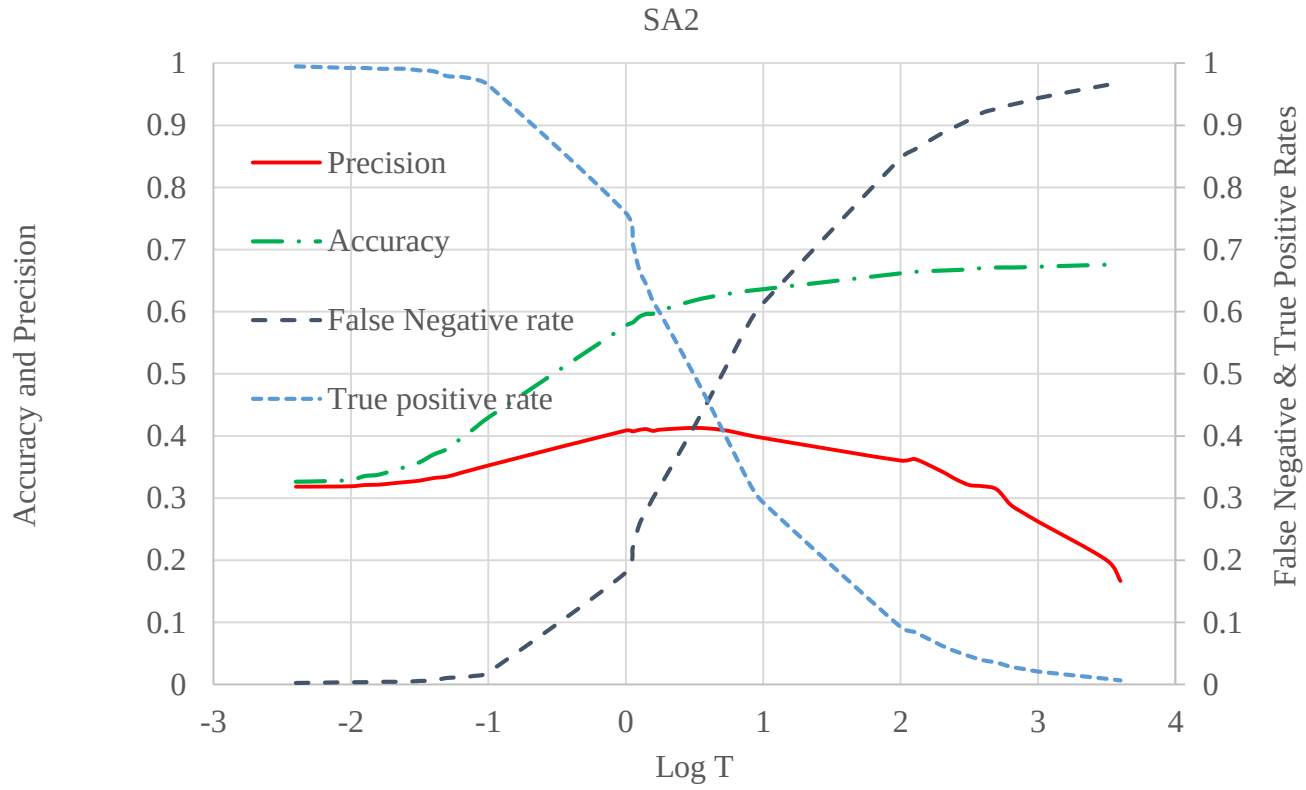

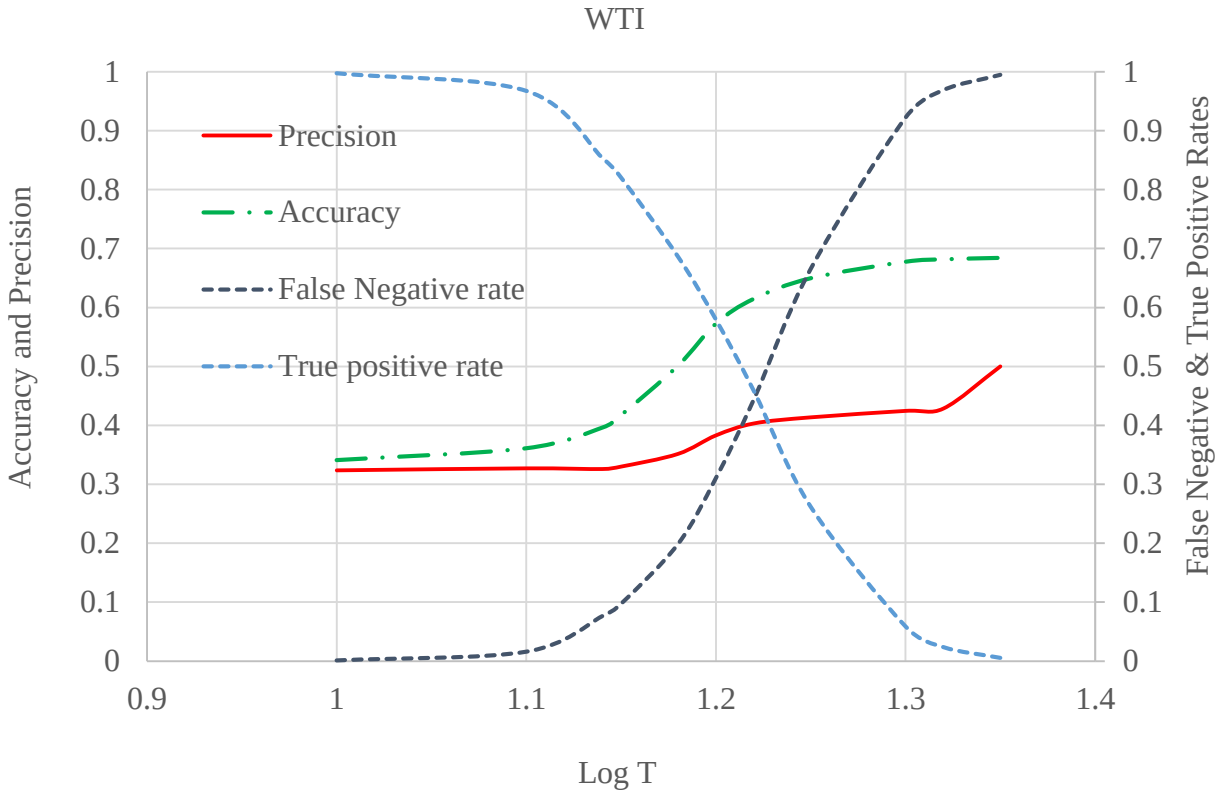
WTI
Precision
Accuracy
False Negative rate
True positive rate
Accuracy and Precision
False Negative & True Positive Rates
Log T
0
0.1
0.2
0.3
0.4
0.5
0.6
0.7
0.8
0.9
1
0.9
1
1.1
1.2
1.3
1.4

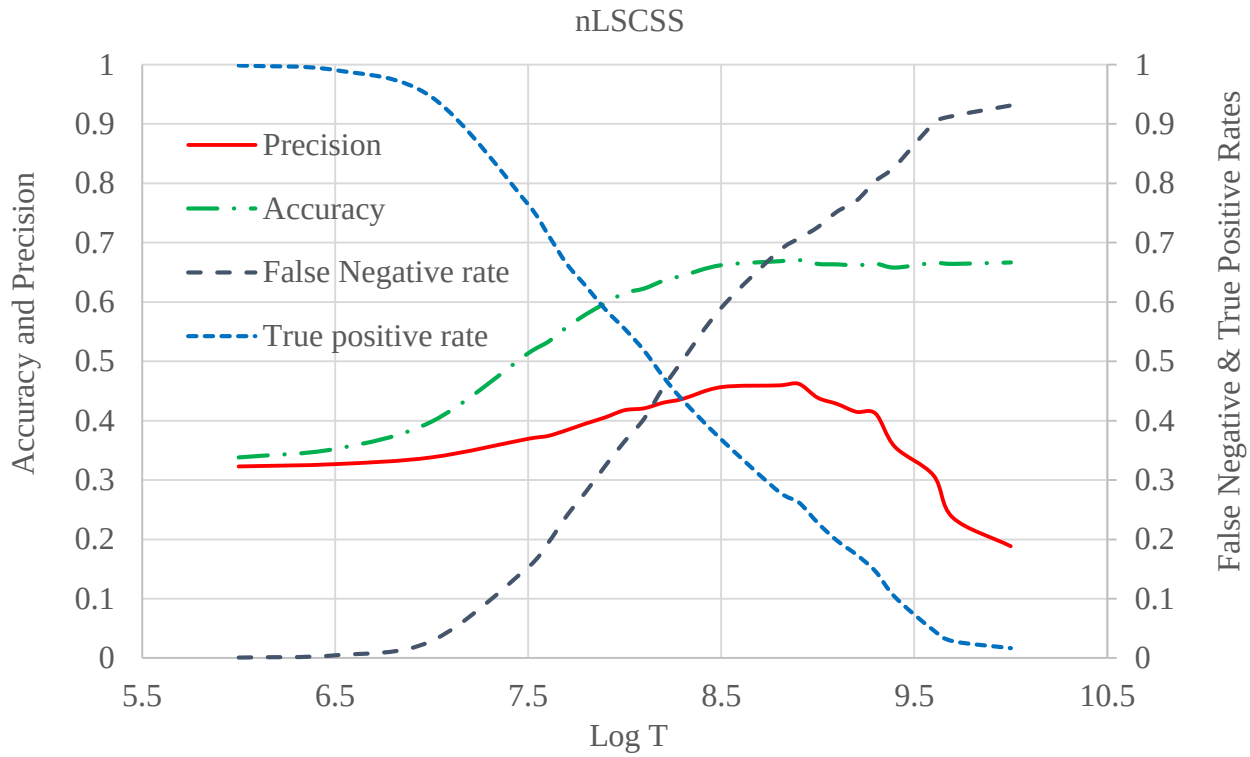
nLSCSS
Precision
Accuracy
False Negative rate
True positive rate
Accuracy and Precision
False Negative & True Positive Rates
Log T
0
0.1
0.2
0.3
0.4
0.5
0.6
0.7
0.8
0.9
1
5.5
6.5
7.5
8.5
9.5
10.5

Appendix B - Maps of head water and main stem catchments

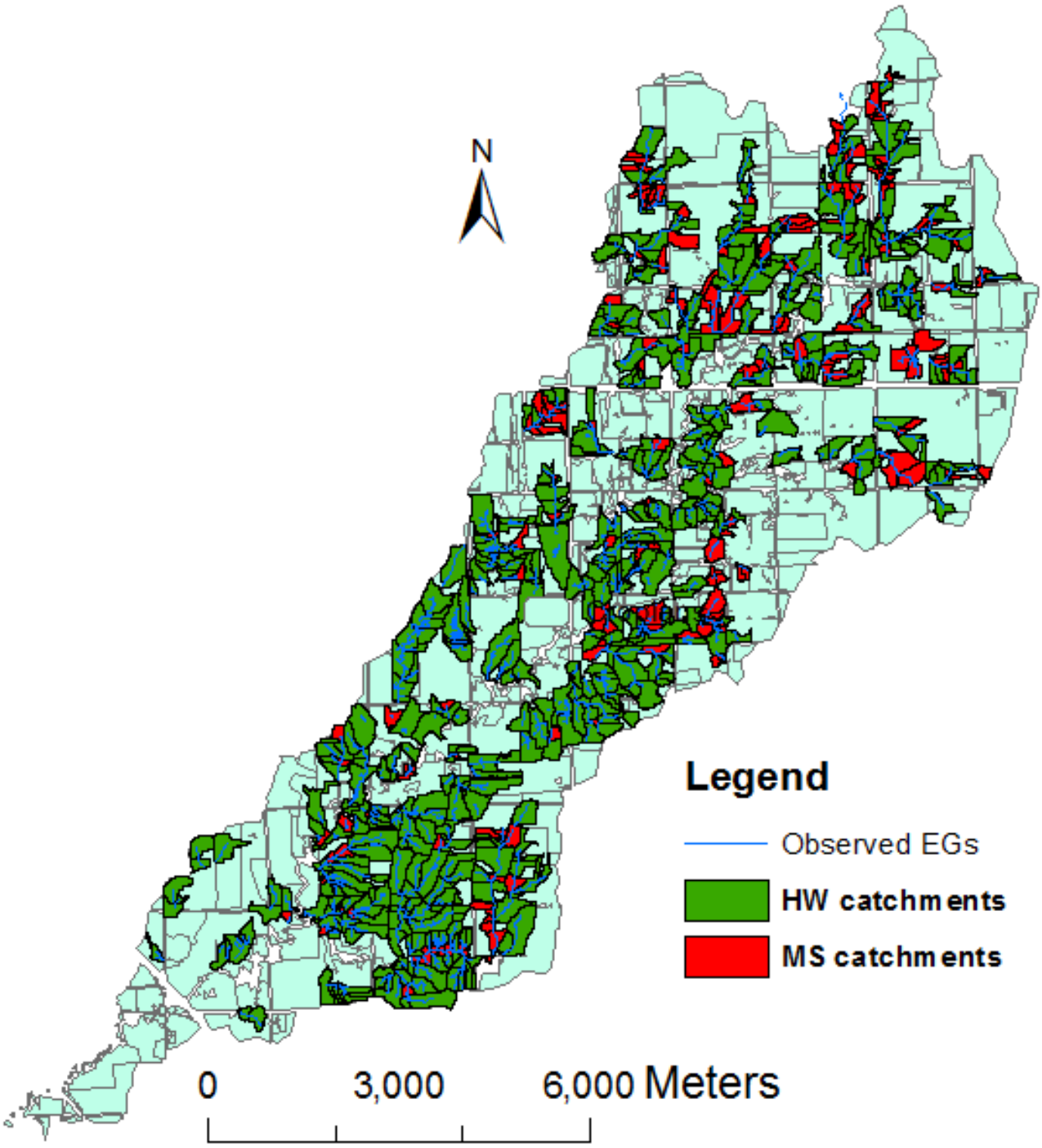

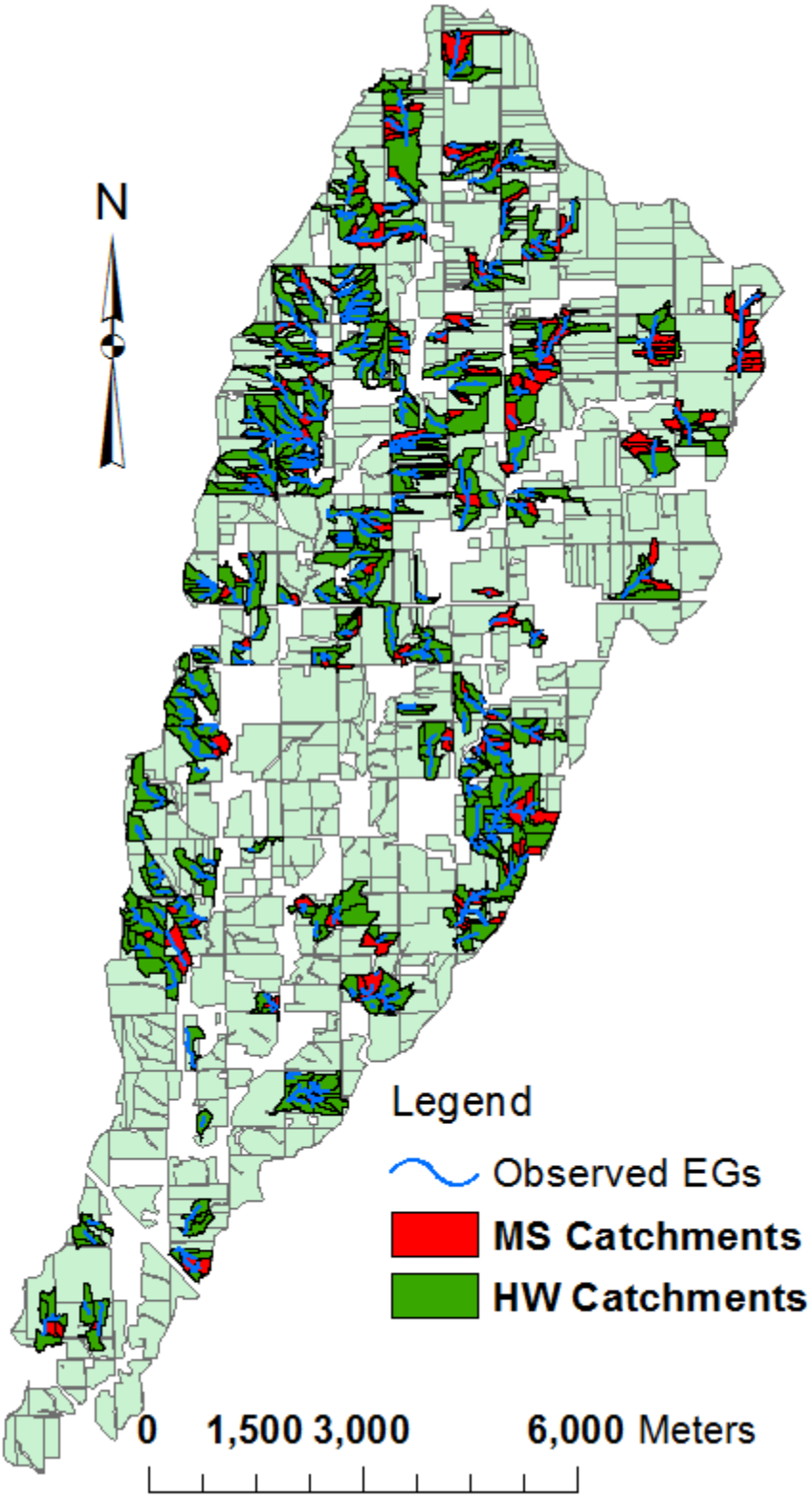
N
Legend
Observed EGs
MS Catchments
HW Catchments
0 1,500 3,000 6,000 Meters

Appendix C - Raster maps of TI values computed by six models

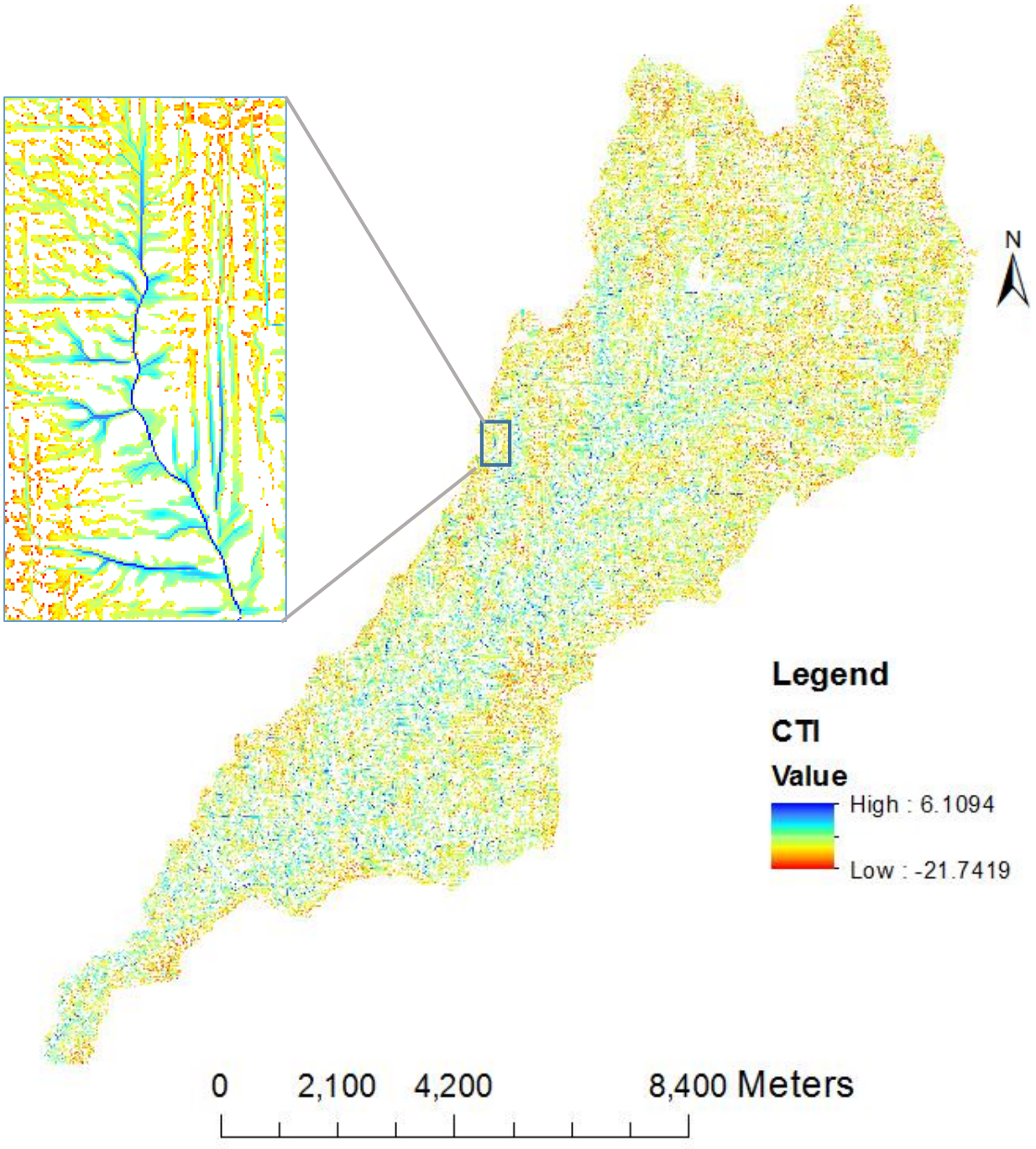

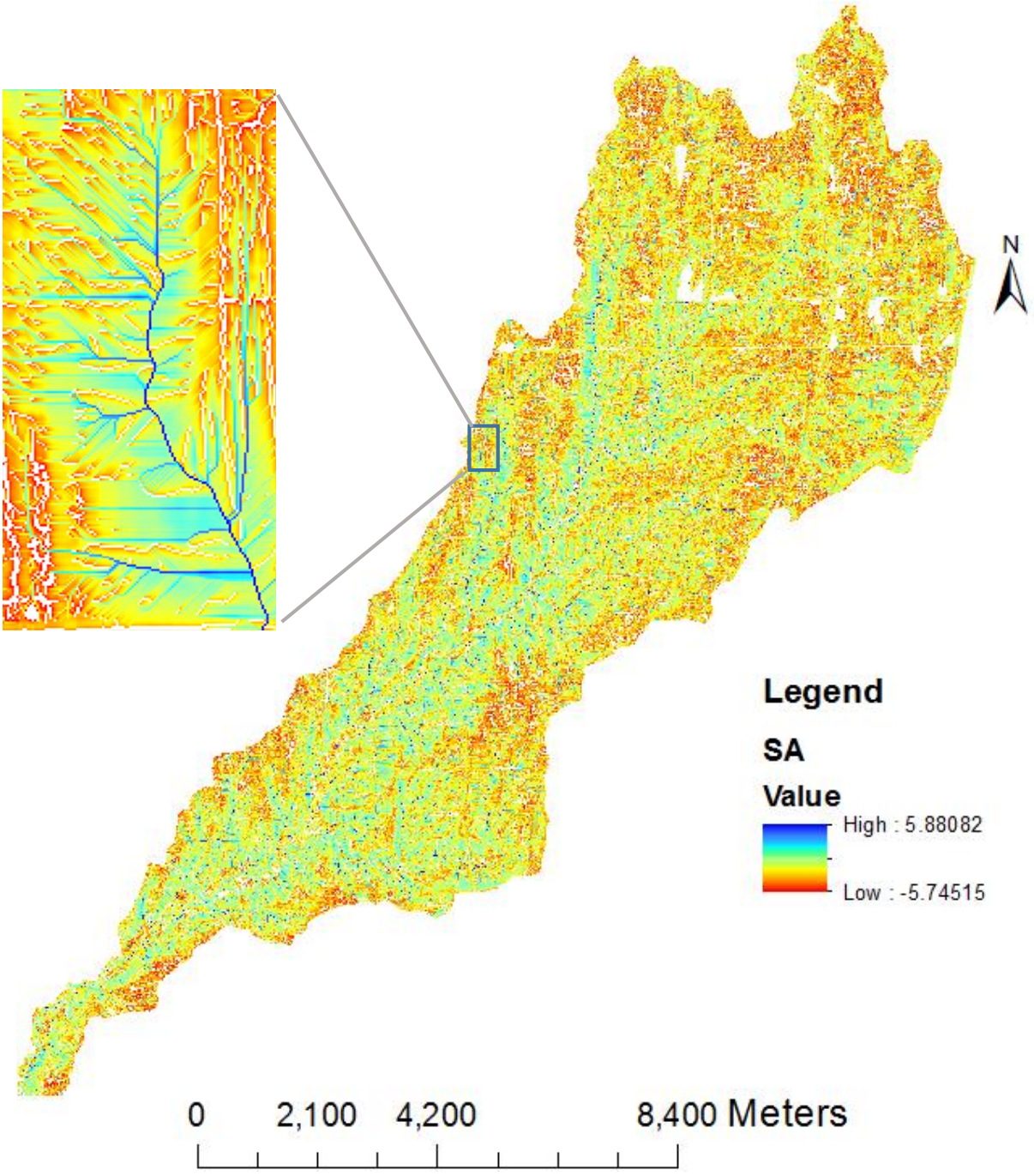
N
Legend
SA
Value
High : 5.88082
Low : -5.74515
0
2,100
4,200
8,400 Meters

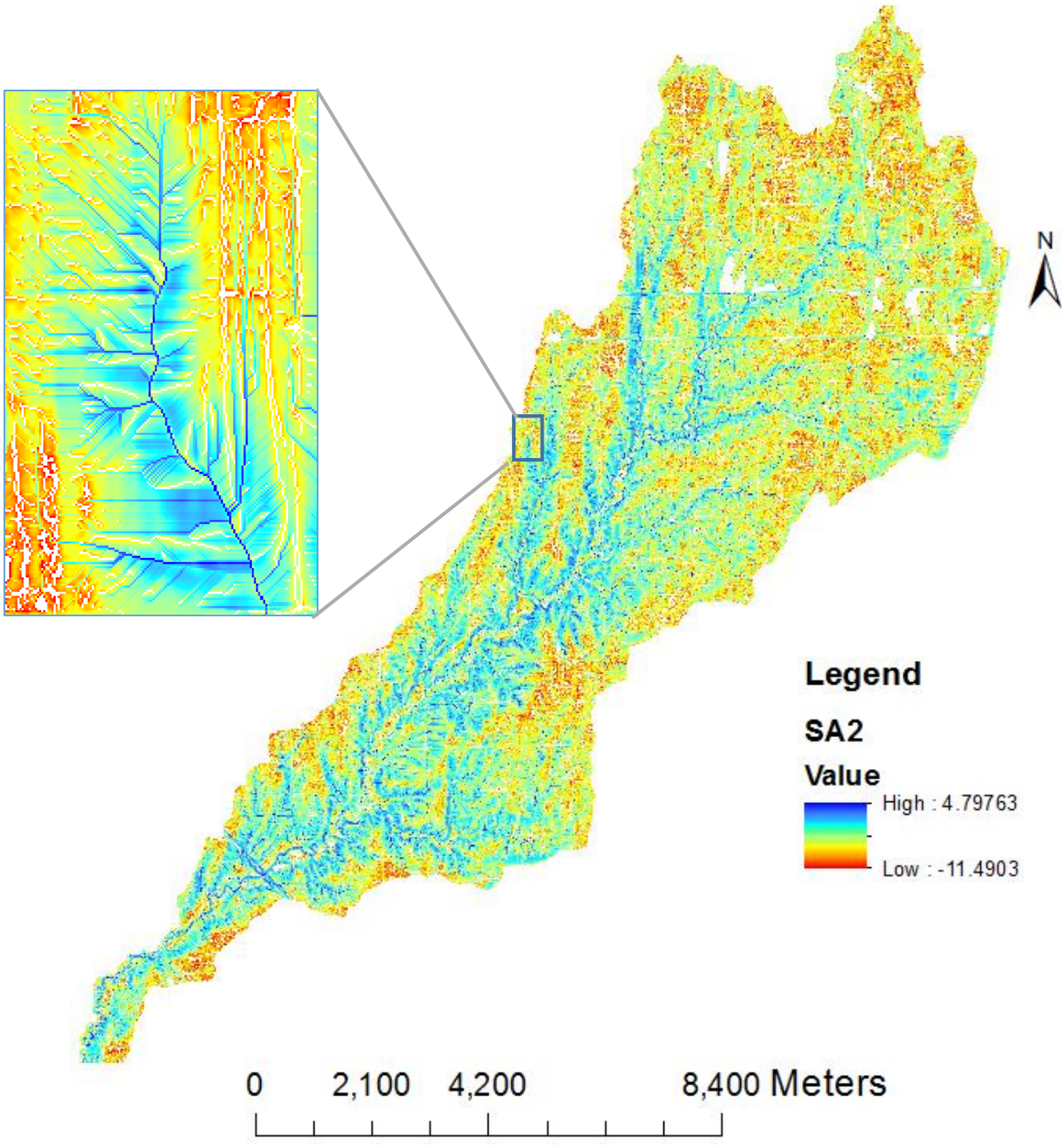
N
Legend
SA2
Value
High : 4.79763
Low : -11.4903
0
2,100
4,200
8,400 Meters

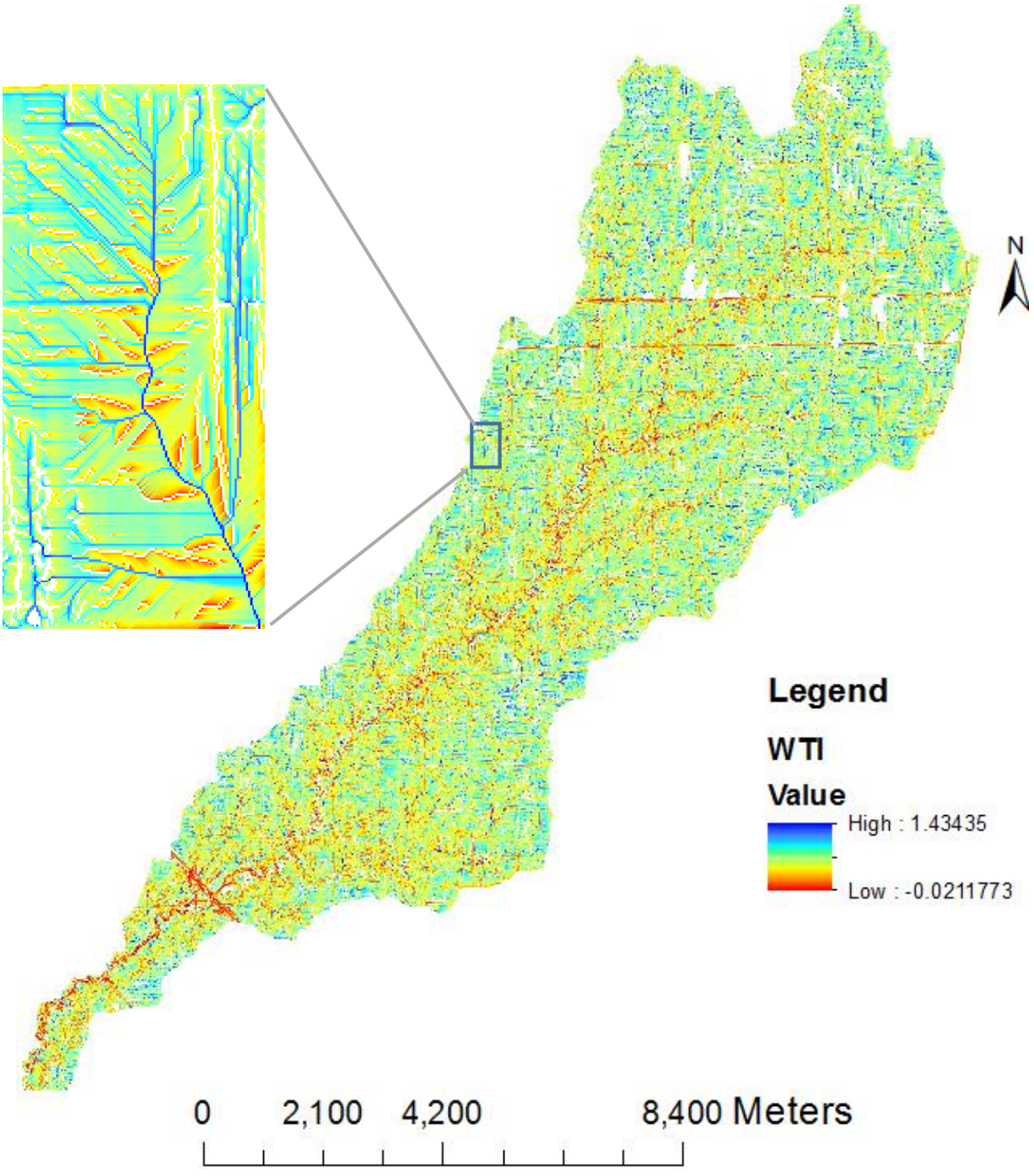
N
Legend
WTI
Value
High : 1.43435
Low : -0.0211773
0
2,100
4,200
8,400 Meters

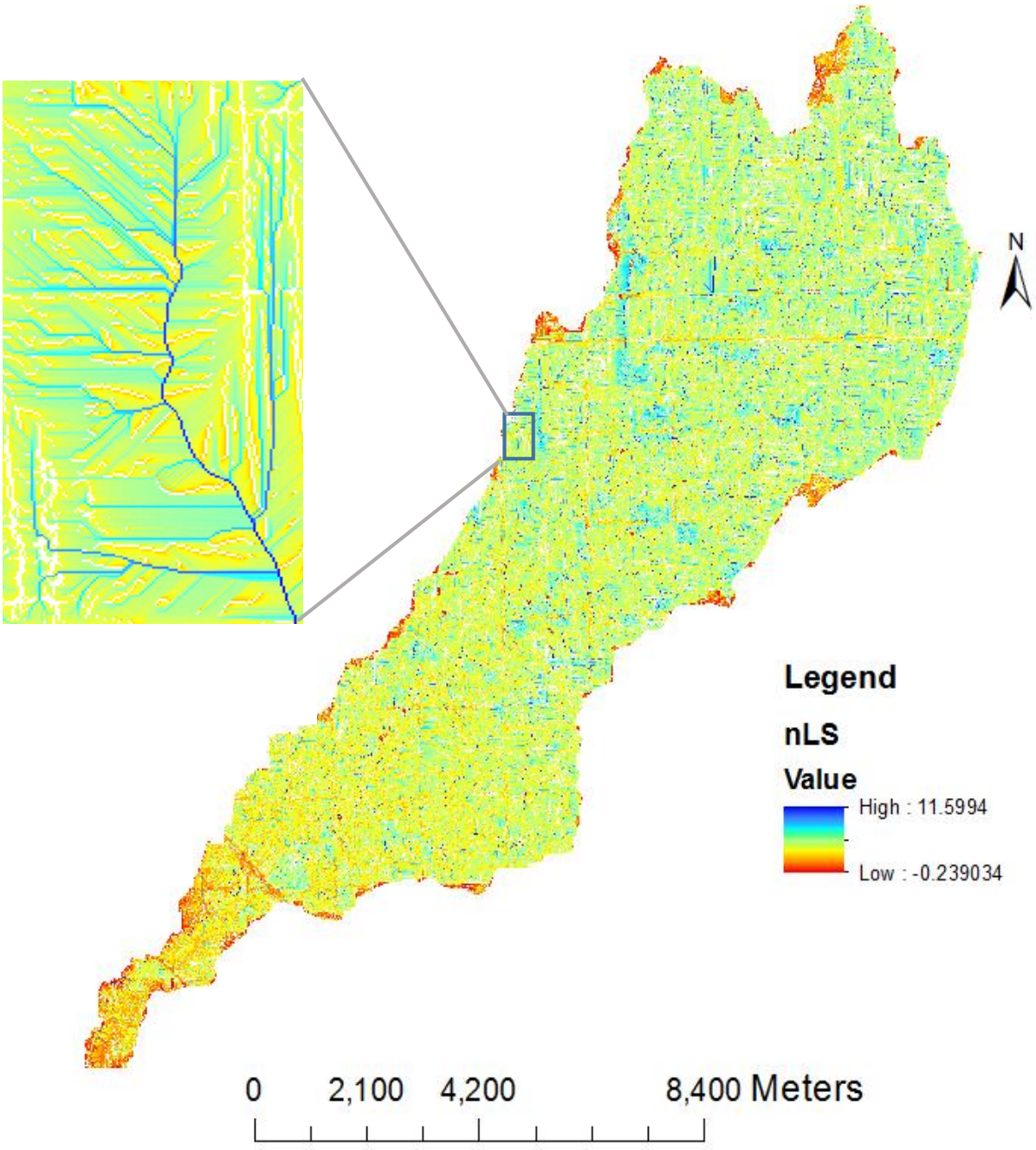
N
Legend
nLS
Value
High : 11.5994
Low : -0.239034
0
2,100
4,200
8,400 Meters

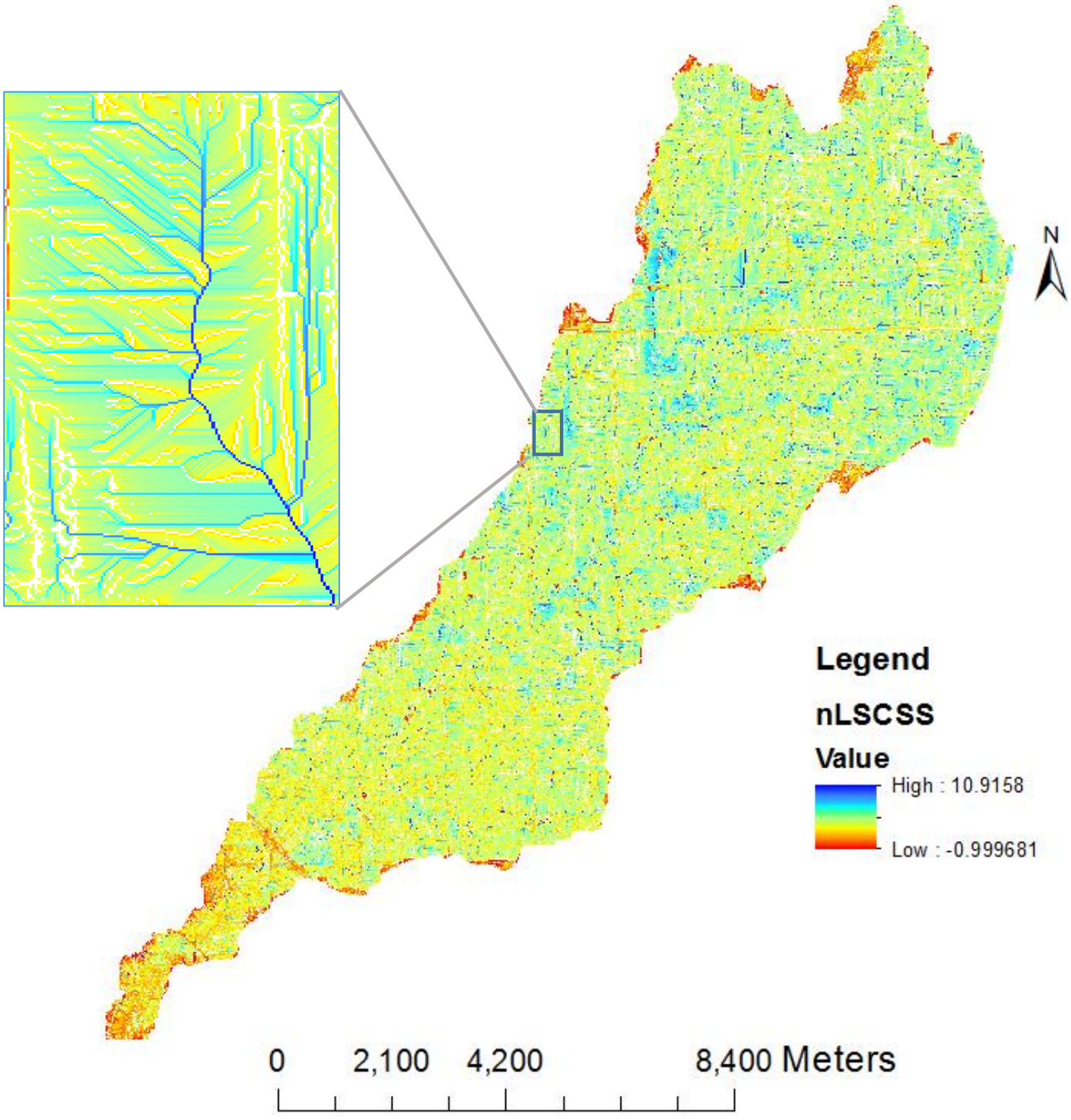
N
Legend
nLSCSS
Value
High : 10.9158
Low : -0.999681
0
2,100
4,200
8,400 Meters

Appendix D - Maps of percentages of clay and sand in Running Turkey watershed

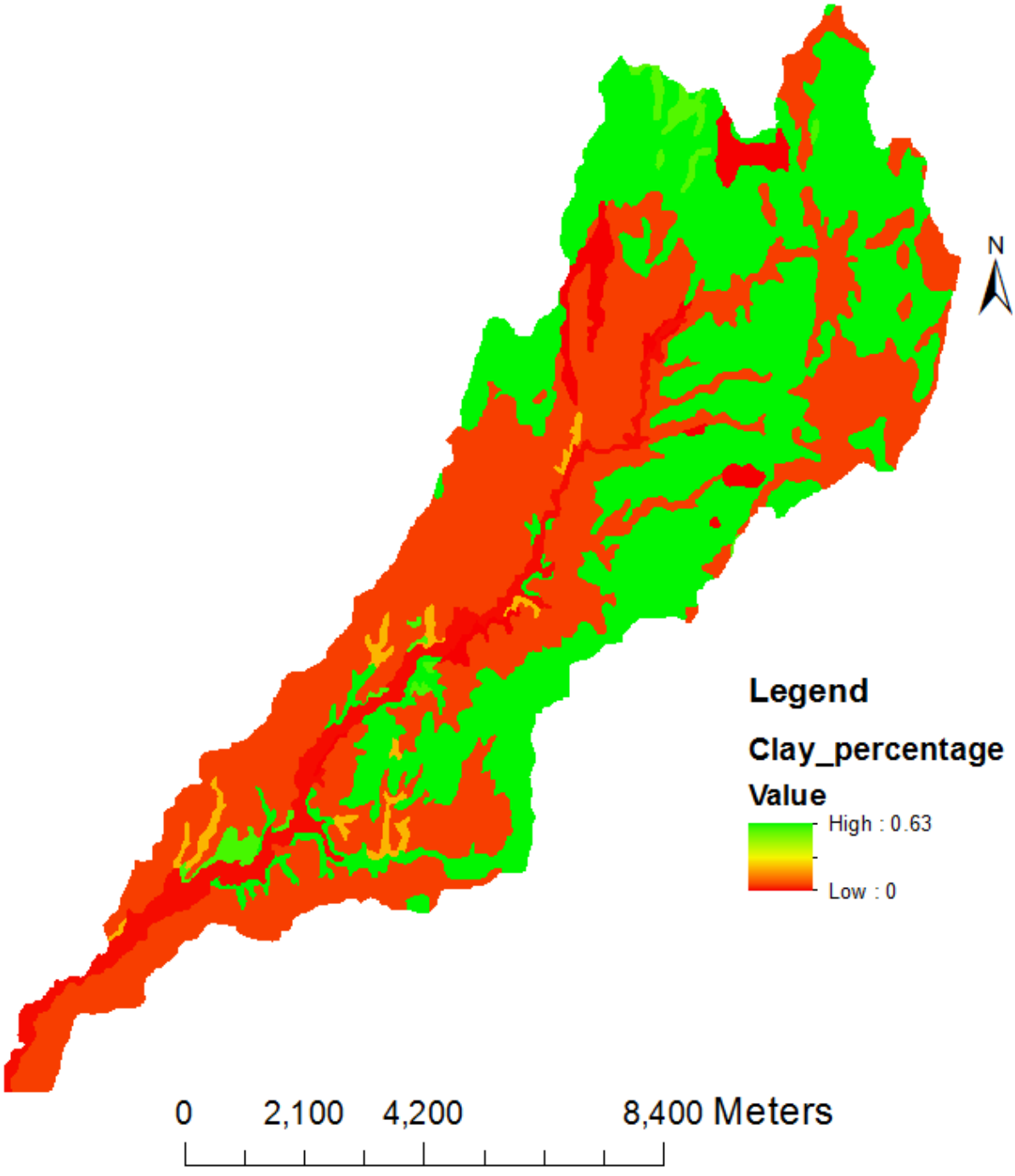

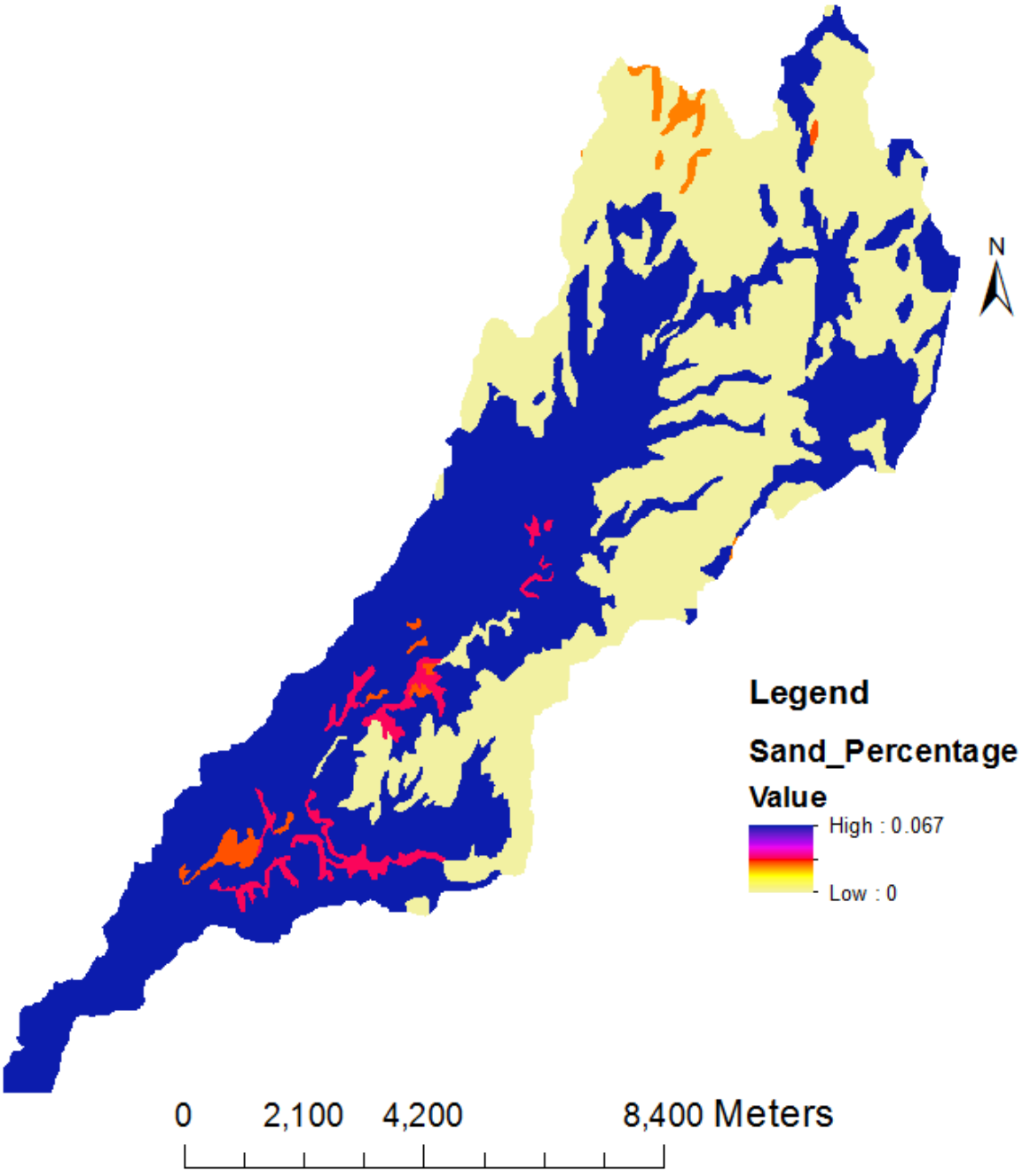
N
Legend
Sand_Percentage
Value
High : 0.067
Low : 0
0
2,100
4,200
8,400 Meters

Appendix E - *tRIBS* soil and land use codes

Land Use codes	Soils Texture
1 - Evergreen Needleleaf Forest	0 - No data
2 - Evergreen Broadleaf Forest	1 - Sand
3 - Deciduous Needleleaf Forest	2 - Loamy sand
4 - Deciduous Broadleaf Forest	3 - Sandy loam
5 - Mixed Forest	4 - Silt loam
6 - Closed Shrublands	5 - Silt
7 - Open Shrublands	6 - Loam
8 - Woody Savannah	7 - Sandy clay loam
9 - Savannahs	8 - Silty clay loam
10 - Grasslands	9 - Clay loam
11 - Permanent Wetlands	10 - Sandy clay
12 - Croplands	11 - Silty clay
13 - Urban and Built-Up	12 - Clay
14 - Cropland / Natural Vegetation	13 - Organic materials
15 - Snow and Ice	14 - Water
16 - Barren or Sparsely Vegetated	15 - Bedrock
17 - Water Bodies	16 - Othe

Appendix F - Description of the Foster and Lane model

Equilibrium channel geometry

Faster and Lane model compute the rates of detachment rates of soil depending on a simple shear stress and tractive force formulation. The basic detachment relationships is the shear excess concept stated as

$$D_{rc} = K_r(\tau - \tau_c) \qquad \text{Eq F-1}$$

Where; Drc = detachment rate potential (kg/m second),

τ = actual tractive force (Pa)

τ_c = crtical tractive force (Pa).

The distribution of shear stress within the channel is assumed to symmetrical and the symmetrical distribution of shear defined by

$$\tau_* = 1.35\left[1-(1-2X_*)^{2.9}\right] \qquad \text{For } X_* < 0.5 \qquad \text{Eq F-2}$$

The resultant channel dimensions along the channel perimeter are obtained using a set of equations outlined below.

$X_* = X/Wp$

$R_* = R/Wp$

$W_* = Weq/Wp$

X_* = normalized distance along the wetted perimeter starting at the water surface.

Wp = wetted perimeter

W_* = normalized channel width

R_* = normalized channel hydraulic radius

W_{eq} = equilibrium channel width

Conveyance function

The potential stream flow to erode channel particles was measured using the conveyance function at the center of the channel. A conveyance function was developed to predict X_{*c} and it was defined as

$$g(X_{*c}) = \frac{\gamma S}{\tau_c}\left[\frac{nQ}{\sqrt{S}}\right]^{(3/8)} \qquad \text{Eq F-3}$$

Where: S = channel slope

Q = peak discharge

n = channel roughness coefficient

γ = specific gravity of soil

Channel erosion prior to non-erodible layer

Prior to reaching the non-erodible layer, the channel is assumed to erode vertically at a width equal to W_{eq} and a potential rate defined by the maximum tractive force. The potential erosion rates at this point are computed using the expression below.

$$E_{rc} = K_r\left(1.35\tau_a - \tau_c\right)W_{eq} \qquad \text{Eq. F-4}$$

Where E_{rc} is the potential rate of erosion, K_r is the soil erodibility

The normal shear stress, τ_a, is related to channel hydraulic radius obtained using

$$\tau_a = \gamma S\left[\frac{nQR_*}{\sqrt{S}}\right]^{(3/8)} \qquad \text{Eq. F-5}$$

The maximum rate of downward movement is defined by

$$M_{rc} = \left[\frac{E_{rc}}{W_{eq}\rho_b}\right] \qquad \text{Eq. F-6}$$

ρ_b = Soil bulky density

Channel erosion after reaching a non-erodible layer

After reaching the non-erodible layer, the channel starts widening laterally. The rate of channel widening, $\frac{dw}{dt}$, is computed from

$$\frac{dw}{dt} = K_r\frac{\left(\tau_b - \tau_c\right)}{\rho_b} \qquad \text{Eq. F-7}$$

τ_b = shear at the intersection of the channel.

In the transition between initial width and final width, the dimensionless time, t_*, and width, W'_*, are obtained from

$$t_* = t\frac{\left(dW/dt\right)_{in}}{W_f - W_{in}}$$

$$W'_* = \frac{W - W_{in}}{W_f - W_{in}}$$

For steady state flow, W_{in} would be equal to $W_{eq,\ the}$ equilibrium width prior to reaching the non-erodible layer. By assuming, a rectangular geometry, the equilibrium width, W_{eq}, will be determined using the equation below.

$$W_{eq} = \left[\frac{nQR_*}{\sqrt{S}}\right]^{(3/8)} W_* R_*^{-5/8} \qquad \text{Eq. F-8}$$

By knowing the conveyance function, values of X_{*_c}, W_*, R_* can be determined. In addition, tabulated values of these parameters can be obtained in the tabulated tables presented by (Foster and Lane, 1983; Haan et al., 1994b) in Table 8F.1 on page 566 of Haan et al. (1994b).

Appendix G - EG, terrace, and grassed waterway lengths in Running Turkey watershed

Longitude	Latitude	Terrace length (m)	Grassed waterway length (m)	EG length (m)
-126145	1711836	0	0	0
-129798	1711074	0	0	0
-129842	1710983	0	0	0
-129433	1711013	0	0	0
-125672	1711037	0	0	0
-130186	1710864	0	0	0
-126132	1711062	0	0	307.8989
-126743	1710641	0	0	0
-129974	1710580	0	0	3.090796
-129962	1710178	0	0	86.9287
-128100	1710190	0	0	0
-126863	1710224	0	0	97.22828
-126038	1710346	0	0	481.2779
-129287	1710271	0	0	425.6853
-127941	1709862	0	0	0
-128448	1709574	0	0	0
-128305	1709524	0	0	0
-130155	1709544	0	0	899.2538
-129543	1709334	0	0	0
-128903	1709678	0	0	567.6122
-128369	1709399	0	0	0
-127953	1709304	0	0	0
-127784	1709501	0	0	0
-127001	1709663	0	0	1684.358
-125552	1709559	0	0	0
-125153	1709159	0	0	0
-130672	1709120	0	0	0
-130589	1709158	0	0	0
-127784	1709081	0	0	0
-130657	1708754	0	0	0
-130176	1708926	0	0	1154.585
-126648	1708674	0	0	0
-130938	1708134	0	0	0
-130890	1708218	0	0	0
-130697	1708346	0	0	101.1116
-126472	1708269	0	0	592.1109
-130589	1708509	0	0	30.11569
-130846	1708042	0	0	0
-130697	1707924	0	0	0

-126835	1707928	0	0	461.5246
-130683	1707972	0	0	0
-130716	1707802	0	0	0
-130591	1707908	0	0	0
-130468	1707936	0	0	0
-130357	1708162	0	0	686.7012
-130013	1708140	0	0	745.6842
-127916	1707767	0	0	150.675
-128307	1708494	0	0	7019.333
-126618	1707684	0	0	0
-126818	1707725	0	0	0
-126453	1707654	0	0	0
-126043	1707847	0	0	0
-125148	1707857	0	0	0
-124784	1708421	0	0	505.5025
-130144	1707631	0	0	0
-130189	1707533	0	0	0
-130243	1707412	0	0	0
-129994	1707504	0	0	0
-129873	1707325	0	0	0
-127488	1707266	0	0	0
-126903	1707542	0	0	0
-127625	1707232	0	0	0
-130818	1707249	0	0	32.08214
-130548	1707174	0	0	0
-127837	1707459	0	0	837.3944
-127821	1707239	0	0	0
-130900	1707259	0	0	95.71055
-130425	1707143	0	0	207.7433
-129614	1707306	0	0	971.9977
-124170	1707239	0	0	0
-128016	1707035	0	0	151.2824
-127818	1706934	0	0	0
-125912	1708708	0	0	5215.539
-129476	1706906	0	0	0
-127114	1707198	0	481.2856	737.6166
-126813	1706904	0	0	0
-126342	1707200	0	0	544.197
-125988	1706904	0	0	0
-127280	1706885	0	0	0
-125459	1707237	0	0	512.757
-124848	1707223	0	0	0
-124436	1707260	0	0	0

-130968	1706872	0	0	0
-125831	1706862	0	0	0
-124688	1706852	0	0	0
-128658	1706784	0	0	0
-128810	1707261	0	0	2813.027
-128988	1706694	0	0	0
-130818	1706694	0	0	0
-128437	1706669	0	0	132.3672
-128725	1706755	0	0	0
-130848	1706499	0	0	0
-128104	1706734	0	0	0
-129188	1706487	0	0	0
-129078	1706424	0	0	0
-129370	1706704	0	0	104.8235
-129318	1706356	0	0	0
-131636	1706267	0	0	0
-130845	1706276	0	0	0
-130629	1707143	0	0	522.4634
-131116	1706487	0	0	0
-130218	1706698	0	0	1406.596
-129698	1706524	0	0	1039.386
-129397	1706364	0	0	0
-128691	1706336	0	0	1119.23
-126852	1706487	0	0	369.0573
-127751	1706451	0	0	2004.923
-127224	1706520	0	0	872.0129
-126055	1706463	0	0	1491.727
-125261	1706453	0	0	460.1579
-124677	1706441	0	0	0
-129897	1705990	0	0	0
-129438	1705914	0	0	0
-130083	1705959	0	0	0
-129362	1705981	0	0	0
-129258	1705884	0	0	0
-128983	1705949	0	0	0
-128504	1705952	0	0	0
-124788	1705854	0	0	0
-129411	1705847	0	0	0
-131785	1705906	0	0	638.555
-130448	1705894	0	0	0
-128818	1705824	0	0	0
-132136	1705644	0	0	0
-124668	1705719	0	0	0

-128463	1705767	0	0	528.0822
-128118	1705524	0	0	0
-124888	1705696	0	0	0
-130882	1705747	0	0	0
-132649	1705430	0	0	0
-132450	1705713	0	0	0
-132279	1705552	0	0	0
-131798	1705533	0	0	665.8476
-130580	1705573	0	0	0
-130045	1705606	0	0	13.26393
-129713	1705695	0	0	0
-129708	1705314	0	0	0
-127063	1705619	0	0	0
-129752	1705242	0	0	0
-129721	1705137	0	0	0
-131403	1705074	0	0	0
-131228	1705182	0	0	0
-131353	1704968	0	0	0
-130243	1705103	0	10.3152	734.4479
-127443	1704849	0	0	0
-129787	1704998	0	0	0
-128680	1704852	0	0	0
-128747	1704773	0	0	0
-127147	1704809	0	0	2.83189
-127332	1704810	0	0	0
-130668	1704714	0	0	0
-130572	1704803	0	0	0
-128468	1704825	0	0	0
-127272	1704729	0	0	0
-128073	1704684	0	0	0
-127998	1704684	0	0	0
-130849	1704654	0	31.67359	0
-128088	1704654	0	0	0
-127998	1704654	0	0	0
-127944	1704767	0	0	0
-129699	1704688	0	0	0
-128088	1704624	0	0	0
-127938	1704624	0	0	0
-129706	1704564	0	0	0
-129564	1704747	0	0	227.2964
-128981	1705283	0	0	2522.168
-132634	1704879	0	0	0
-132325	1704862	0	0	0

-131908	1705043	0	311.9973	467.5035
-129915	1704579	0	0	0
-127908	1704534	0	0	0
-130797	1704655	0	65.46759	0
-131076	1705237	0	495.8783	1031.559
-130588	1704570	0	0	0
-130219	1704743	0	205.6973	715.9231
-130117	1704562	0	0	0
-129801	1704600	0	0	0
-129567	1704512	0	0	0
-129161	1704525	0	0	0
-128620	1704569	0	0	0
-127068	1704474	0	0	0
-129828	1704444	0	0	0
-127653	1704617	0	0	0
-125388	1704384	0	0	0
-126462	1705182	0	0	4021.938
-124800	1705227	0	0	0
-129790	1704366	0	0	0
-131008	1704393	0	44.87588	0
-131848	1704365	0	0	254.9723
-130617	1704295	0	0	0.305
-130068	1704264	0	0	3.2872
-130998	1704234	0	0	0
-130428	1704234	0	0	0
-130190	1704368	0	0	0
-128300	1704321	0	0	0
-132342	1704340	0	0	0
-130322	1704191	0	0	0
-131237	1704292	0	328.1676	0
-130850	1704286	0	0	0
-130248	1704099	0	0	0
-130071	1704159	0	0	487.512
-128688	1704243	0	0	0
-130996	1704054	0	0	0
-130083	1704054	0	0	0
-129888	1704056	0	0	0
-128275	1704112	0	0	0
-128328	1704006	0	0	0
-125531	1704173	0	0	353.5562
-128373	1703864	0	0	0
-125495	1703896	0	0	0
-133074	1703886	0	0	0

-131243	1703897	0	377.5924	0
-131238	1703694	0	0	0
-131058	1703664	0	0	0
-127865	1703832	0	0	0
-129549	1703684	0	0	172.4114
-126324	1704015	0	0	0
-127408	1703980	0	0	0
-129512	1703443	0	0	109.1096
-131643	1703349	0	0	0
-131397	1703459	0	0	0
-129830	1703293	0	0	0
-129288	1703274	0	0	0
-129079	1703273	0	0	0
-128883	1703244	0	13.50638	32.41872
-128327	1703332	0	0	0
-127950	1703338	0	0	0
-131089	1703214	0	0	0
-131232	1703382	0	0	0
-131026	1703243	0	0	39.4419
-129271	1703176	0	0	0
-129204	1703286	0	0	0
-131478	1703124	0	0	0
-131448	1703184	0	0	0
-131350	1703175	0	0	0
-131123	1703147	0	0	0
-130323	1703155	0	0	70.15501
-129701	1703217	0	0	0
-131449	1703034	0	0	0
-132395	1703141	0	0	230.0916
-133724	1702976	0	0	0
-133554	1703093	0	0	24.89141
-133257	1703278	0	0	713.6402
-132600	1703074	0	0	26.43821
-132290	1703669	0	387.0844	5841.868
-131718	1702884	0	12.52033	0
-131418	1702884	0	0	0
-130551	1703534	0	556.8785	5726.622
-130301	1703010	0	0	212.8967
-131388	1702854	0	0	0
-129408	1703020	0	0	471.1506
-128834	1703019	0	0	67.86214
-128946	1703731	0	467.2417	1600.849
-128193	1702824	0	0	0

-128059	1703044	0	0	0
-131476	1702794	0	0	0
-129468	1702794	0	0	0
-131433	1702764	0	0	0
-131331	1702803	0	0	0
-129658	1702786	0	0	0
-129108	1702764	0	0	0
-131538	1702734	0	0	0
-130773	1702704	0	0	0
-130722	1702766	0	0	0
-130818	1702674	0	0	0
-130368	1702773	0	6.391487	0
-131566	1702614	0	0	0
-131538	1702569	0	0	0
-129078	1702524	0	0	0
-129678	1702608	0	10.3813	0
-129288	1702611	0	0	422.2077
-128192	1702612	0	0	0
-131750	1702284	0	0	0
-131653	1702550	0	0	0
-131188	1702608	0	0	498.7366
-130171	1702462	0	1064.235	1273.801
-132421	1702446	0	0	477.0829
-130698	1702041	0	0	0
-130788	1702281	0	137.0497	1366.974
-131615	1701939	0	0	0
-134298	1701804	0	0	0
-131996	1701834	0	0	0
-132063	1701774	0	0	0
-128842	1701884	0	0	0
-132179	1701881	0	0	0
-132216	1701661	0	0	0
-133028	1701545	0	0	0
-132677	1701782	0	0	1703.798
-132558	1701414	0	0	0
-129701	1701497	0	0	0
-129121	1702186	0	295.002	1843.395
-132618	1701384	0	0	0
-128981	1701658	0	0	0
-134298	1701324	0	0	0
-132163	1701494	0	0	0
-133998	1701296	0	0	0
-129737	1701355	0	0	0

-134752	1701469	0	0	0
-134479	1701592	1332.401	495.9453	1.31862
-134094	1701653	0.9137	1.736818	2133.265
-134129	1701252	0	0	0
-133998	1701231	0	0	0
-132933	1701339	0	0	0
-132798	1701204	0	0	0
-132511	1701313	0	24.76463	0
-132288	1701204	0	0	0
-132036	1701246	0	0	0
-131792	1701613	0	0	21.58435
-130750	1701637	0	0	4698.046
-130167	1701331	0	0	0
-133038	1701153	0	0	0
-132298	1701104	0	0	0
-133098	1701024	0	0	0
-132318	1701026	0	0	0
-132079	1701082	0	0	0
-130796	1701081	0	0	0
-133038	1700846	0	0	0
-132824	1700997	1037.722	0	0
-130923	1700899	0	0	2158.064
-135075	1700754	0	0	1016.332
-134912	1700565	0	0	398.6573
-134532	1700560	0	8.793658	0
-131284	1700490	0	0	41.10058
-133753	1700347	0	0	0
-133458	1700304	0	0	0
-131959	1700348	0	0	0
-135662	1700371	612.8206	0	0
-133420	1700147	0	0	0
-135198	1700004	0	0	0
-131346	1700159	0	0	0
-134049	1699894	0	0	0
-135112	1699839	0	0	0
-136005	1699992	1724.495	307.5053	0
-135718	1699899	899.7941	232.4367	0
-135205	1699649	0	0	0
-135147	1700062	0	0	1829.213
-133758	1701099	6059.761	3085.719	8958.811
-132346	1700385	2061.308	1149.016	4166.054
-134928	1699586	0	0	0
-132408	1699584	0	0	0

-132605	1699660	0	0	0
-132012	1699661	0	0	0
-135888	1699539	0	122.2987	0
-135230	1699434	0	0	0
-133208	1699448	0	0	0
-135700	1699380	0	0	2.39129
-135768	1699164	0	0	0
-135416	1699353	0	0	279.5873
-135718	1699094	0	0	0
-135768	1698939	0	0	0
-133208	1699221	0	0	0
-134761	1699182	0	0	14.1624
-135875	1699120	0	406.9394	0
-134748	1698834	0	0	0
-135607	1698952	0	0	0
-134326	1699189	0	0	3357.127
-133581	1699159	0	0	2118.513
-132136	1698856	0	0	0
-137898	1698463	0	0	0
-136123	1698964	2028.247	796.2477	9.1979
-136457	1698539	727.673	544.1058	0
-138065	1698164	0	0	0
-137461	1698520	24.03655	748.1499	802.2299
-136952	1698694	1277.893	0	378.3112
-136594	1698745	997.6194	501.0802	0
-136109	1698200	0	0	706.6344
-135174	1698197	0	0	753.0765
-134973	1697994	0	0	253.4253
-136124	1697795	0	0	128.7617
-136009	1697543	0	0	0
-133276	1697553	0	0	0
-137672	1697836	749.4407	375.229	0
-134975	1697332	0	0	0
-136492	1697435	0	0	0
-137786	1697458	706.677	512.7427	0
-137718	1697244	0	41.98148	0
-136427	1697243	0	0	0
-135873	1697451	1.801338	0	0
-134930	1697214	0	0	0
-135072	1697354	0	0	0
-137877	1697207	0	87.73508	0
-134898	1697154	0	0	0
-138148	1697580	0	0	288.5538

-135228	1697124	0	0	0
-135086	1697138	0	0	0
-136788	1697096	0	0	0
-132768	1697094	0	0	0
-134956	1697085	0	0	0
-135422	1697268	0	0	0
-135317	1697003	0	0	0
-138168	1696974	0	0	0
-136889	1697129	0	0	0
-137460	1696944	0	0	0
-138341	1696990	0	0	0
-138138	1696914	0	0	0
-136518	1696884	0	0	0
-138558	1696854	0	0	0
-138303	1696854	0	0	0
-138138	1696854	0	0	0
-138079	1696854	0	0	0
-136518	1696854	0	0	0
-136450	1697024	0	0	0
-134654	1697024	0	0	0
-138039	1696804	0	0	0
-138018	1696719	0	0	0
-137165	1697451	5294.301	325.6574	1270.757
-133158	1696644	0	0	0
-132510	1698189	0	0	6153.273
-138618	1696464	0	0	0
-138580	1696642	1111.926	0	0
-138265	1696654	0	0	0
-138066	1696476	0	0	0
-137838	1696472	0	0	0
-137209	1696701	0	458.3182	0
-136638	1696626	2153.548	0	0
-135619	1696827	2455.189	784.0269	582.9503
-134296	1697853	3847.617	638.2199	25200.05
-137658	1696371	0	0	0
-138318	1696344	0	0	0
-137630	1696344	0	0	0
-138699	1696364	0	0	0
-138754	1696250	0	0	0
-138129	1696337	0	42.1544	0
-137988	1696134	0	30.56127	0
-138739	1696124	0	0	0
-136245	1696206	0	0	0

-138708	1696014	0	0	0
-137942	1696027	0	0	0
-136807	1696191	1325.825	586.6056	382.1908
-138888	1695909	0	0	0
-136158	1696119	0	0	0
-138918	1695864	0	0	0
-137773	1696160	0	393.0128	0
-138978	1695834	0	0	0
-139023	1695804	0	0	0
-139068	1695759	0	0	0
-139098	1695714	0	0	0
-138114	1695848	0	0	0
-139128	1695684	0	0	0
-138345	1696021	0	465.0116	0
-139428	1695621	0	0	0
-139221	1695649	0	0	0
-139428	1695594	0	0	0
-139308	1695609	0	0	0
-139457	1695579	0	0	0
-139430	1695534	0	0	0
-139510	1695495	0	0	0
-139548	1695444	0	0	0
-139608	1695354	0	0	0
-139878	1695264	0	0	0
-138972	1695549	1181.461	167.7931	0
-140148	1695231	0	0	0
-139638	1695249	0	0	0
-140178	1695204	0	0	0
-140178	1695144	0	0	0
-140178	1695084	0	0	0
-140178	1695054	0	0	0
-139537	1695124	0	0	0
-140298	1694994	0	0	0
-139428	1694994	0	0	0
-139398	1694964	0	0	0
-139368	1694934	0	0	0
-140418	1694904	0	0	0
-140448	1694874	0	0	0
-139915	1694987	0	0	0
-139552	1694938	0	0	0
-138955	1695172	394.5544	0	0
-140057	1694807	0	0	0
-139668	1694799	0	0	0

-139608	1694799	0	0	0
-140028	1694754	0	0	0
-139465	1694790	0	0	0
-140737	1694744	0	0	0
-140519	1694753	0	0	0
-138999	1694773	0	0	0
-139938	1694711	283.3663	0	0

Appendix H - Terrace length and locations in Dry Turkey watershed.

Latitude	Longitude	Terrace length (m)	EG length (m)	Grassed water way length (m)
-132588	1710726	0	88.73699	0
-133325	1710791	0	124.5984	0
-134172	1710407	0	574.5256	0
-135113	1710839	0	386.0027	0
-133417	1710440	0	363.1618	0
-135289	1710517	0	0	0
-136765	1709756	0	1625.04	0
-135774	1709711	647.4048	0	0
-131695	1709172	0	223.3589	0
-134335	1709124	0	171.2533	2.25801
-133309	1708642	0	0	0
-136546	1704825	427.1148	0	0
-136800	1705281	553.6672	0	0
-132592	1708990	0	0	0
-133965	1711519	0	374.1776	0
-133967	1711326	0	0	0
-134361	1711784	0	0	0
-133857	1715372	0	0	0
-133613	1704427	0	46.56827	0
-134833	1705005	0	76.73869	0
-131651	1710883	0	222.3527	0
-131826	1708068	0	0	0
-133619	1704027	0	942.5155	0
-133433	1705482	0	0	0
-138494	1697889	0	936.6943	0
-138430	1700921	0	663.2541	2.781724
-132774	1707477	0	0	0
-136587	1712094	0	0	0
-133357	1713600	0	0	0
-135751	1700906	0	0	928.131
-136244	1700278	0	0	0
-135264	1701486	2066.192	0	2.802271
-139178	1696779	2057.172	0	46.89913
-135656	1710742	0	490.8829	0
-135582	1713886	0	0	0
-138266	1699573	0	0	0
-139011	1700949	1801.906	0	3.6722
-139054	1699824	979.9229	0	0
-133279	1711496	0	0	0

-135601	1711431	0	1139.13	0
-135906	1702172	0	39.67965	0
-137533	1702431	1096.823	0	3.0781
-136716	1702360	1826.965	173.2797	0
-135665	1706583	2474.111	774.8382	0
-135670	1703436	1870.304	0	0
-133339	1713125	0	45.8993	0
-138177	1700292	1495.746	0	73.95055
-138599	1703521	318.4651	0	0
-139072	1703262	1484.36	0	0
-138552	1703958	1041.473	0	0
-136070	1705691	349.4235	0	0
-133660	1704814	181.4999	60.5042	0
-133427	1714098	0	0	0
-132600	1710300	0	0	0
-132576	1710552	0	0	0
-132587	1710922	0	159.0359	0
-132614	1710451	0	0	0
-134166	1710933	0	115.7747	0
-134173	1710725	0	0	0
-135287	1710819	0	100.0509	0
-136940	1705116	47.83467	0	0
-137872	1699465	0	0	19.7775
-131240	1712251	0	0	0
-133570	1712187	0	45.80203	0
-133176	1712147	0	321.7965	0
-137288	1710932	0	0	0
-137043	1710953	0	0	0
-137305	1701686	221.8394	0	0
-131921	1708216	0	0	0
-138443	1697595	0	0	0
-136298	1712496	0	0	0
-134494	1704984	0	473.6027	372.3787
-133401	1713807	0	0	0
-139032	1697131	854.9143	0	18.82694
-135595	1710935	0	67.42628	0
-133580	1711620	0	0	0
-135633	1702376	0	123.8313	0
-136031	1702381	0	0	2.92
-137284	1702731	1265.416	0	0
-137842	1702264	359.7244	0	0
-137468	1702221	501.4932	0	0
-133345	1710965	0	0	0

-133434	1710888	0	62.10759	0
-133323	1710672	0	255.6495	0
-133473	1710282	0	67.48445	0
-137134	1710171	0	202.6182	0
-133955	1708958	0	0	0
-134251	1708715	0	411.9766	0
-136922	1704833	1292.311	0	3.146828
-136441	1705183	374.4256	0	0
-132342	1708930	0	0	0
-134163	1712921	0	53.65662	0
-134367	1713036	0	0	0
-134172	1713290	0	58.17345	0
-134162	1713040	0	0	0
-133914	1711079	0	0	0
-133960	1711183	0	0	0
-134371	1711526	0	0	0
-134351	1711498	0	0	0
-134356	1711557	0	0	0
-134360	1711457	0	0	0
-134367	1711614	0	0	0
-134357	1711694	0	0	0
-134165	1715310	0	0	0
-134728	1705209	0	74.01238	0
-137320	1708297	520.5631	0	0
-137617	1708390	23.69209	0	0
-137243	1708517	123.8361	0	16.63664
-137522	1708579	49.61093	0	0
-133495	1705409	0	0	0
-133498	1705615	0	0	0
-132385	1711068	0	0	0
-132791	1711077	0	0	0
-132520	1711570	0	0	0
-132521	1711192	0	0	0
-134881	1701673	719.8091	0	0
-135488	1714187	0	0	0
-135549	1714037	0	0	0
-133562	1712615	0	59.37979	0
-133569	1712302	0	83.80912	0
-133943	1712727	0	0	0
-133944	1712879	0	218.3161	0
-133937	1713031	0	155.7745	0
-134048	1713283	0	0	0
-136058	1706053	0	0	0

-136170	1705179	388.2975	0	0
-135895	1705674	1076.996	0	0
-138820	1703247	43.13082	768.6193	0
-138682	1703332	583.9529	0	0
-133348	1713227	0	596.8706	0
-133339	1713424	0	61.6276	0
-133338	1713326	0	132.578	0
-139157	1701934	2366.671	0	0
-135670	1703048	0	0	0
-139442	1700012	0	0	0
-138958	1700330	740.0609	0	87.01966
-139049	1700073	1256.116	0	0.8383
-139904	1698964	0	0	0
-140892	1697098	0	0	0
-139850	1696282	886.8039	0	0
-130175	1710418	0	0	0
-130400	1710608	0	689.4201	0
-130979	1710776	0	0	0
-136100	1710834	0	0	0
-134726	1710519	0	0	0
-134740	1710318	0	217.6376	0
-130391	1710211	0	104.799	0
-130178	1710209	0	0	0
-133572	1710016	0	458.0436	0
-137700	1710063	0	0	0
-134738	1709688	0	379.4242	0
-135129	1709662	0	594.3191	0
-132493	1709528	416.7075	0	0
-133584	1709097	0	718.2336	0
-136264	1709187	0	0	0
-133195	1709188	0	0	0
-135574	1709042	926.1651	0	0
-131215	1709049	0	0	0
-132293	1707981	0	0	0
-134261	1707846	0	0	0
-131176	1707434	0	0	0
-134189	1707350	0	1.774901	0
-133658	1706832	0	0	0
-134228	1706765	0	229.9412	0
-135175	1706370	0	348.4232	0
-136590	1706476	0	0	0
-133232	1705835	0	0	0
-132929	1705144	0	0	0

-135728	1704275	1449.684	0	0
-136857	1704353	369.6993	0	0
-138958	1704196	2.298521	857.595	8.663023
-138609	1704245	0	0	0
-138060	1703404	0	135.3501	0
-138818	1703700	166.8189	0	0
-139100	1703691	223.2698	0	0
-137721	1703194	649.1327	0	0
-137682	1702655	1128.766	0	0
-138627	1701807	0	637.5216	3.378429
-135537	1701838	0	0	0
-138029	1700787	473.747	0	0
-135450	1700774	0	0	0
-137786	1700390	678.3705	0	0
-136309	1700018	0	0	0
-138152	1699892	1177.894	152.2514	0
-138306	1700070	0	0	94.93001
-138394	1698791	0	0	0
-139230	1698691	848.1852	0	0
-138405	1698387	1587.731	253.2012	0
-138472	1698195	914.2315	93.16454	0
-135711	1701879	851.1668	75.07415	0
-136395	1703945	0	0	0
-135700	1708185	0	742.5861	0
-136673	1708339	2363.084	0	0
-136539	1709149	0	553.5788	0
-134267	1703828	0	903.7151	0
-137979	1708233	0	0	0
-135045	1702337	2102.589	0	3.0548
-135576	1703981	1005.495	0	0
-135523	1704400	377.8455	0	0
-134259	1704025	0	834.0296	0
-134593	1715268	0	0	0
-134865	1714398	0	0	0
-132870	1713114	0	0	0
-134389	1712762	0	0	0
-134640	1712542	0	0	0
-133161	1712382	0	0	0
-133806	1711908	131.2459	0	0
-134354	1711941	352.5351	0	0
-130855	1711742	0	0	0
-131780	1711606	0	0	0
-134376	1711074	0	0	0

-133247	1714540	0	0	0
-137168	1704162	0	0	0
-139719	1698225	0	0	0
-139720	1698647	0	0	0
-132921	1709669	357.3792	0	0
-132877	1710160	0	0	0
-132569	1709985	2455.119	0	63.38816
-131627	1707362	0	0	0
-135002	1711757	0	0	0
-135188	1711717	0	0	0
-135266	1711369	0	0	0
-136356	1711449	0	624.811	0
-135256	1706688	0	0	0
-133323	1709261	0	0	0
-133603	1706505	0	251.5942	0
-133688	1707189	0	0	0
-130095	1711102	0	0	0
-136392	1710871	0	355.4187	0
-137692	1701516	802.4886	0	0
-137287	1701432	39.82094	395.6771	0
-137567	1701041	2600.914	0	55.43072
-136751	1710847	0	447.2412	0
-132434	1712846	0	0	0
-134074	1703325	0	846.2753	0
-132789	1705941	0	0	0
-137058	1711400	0	0	0
-134935	1713700	0	790.1825	0
-136474	1704353	0	0	0
-134433	1705938	0	0	0
-134908	1705930	0	0	4.183683
-135037	1705547	0	455.7055	0
-135577	1705265	234.0103	0	0
-135628	1705056	915.0342	0	0
-134486	1712371	0	0	0
-132611	1708288	0	0	0
-132609	1708483	0	0	0
-132764	1712954	0	0	0
-138029	1705904	0	400.5928	0
-136640	1705767	3119.436	0	0
-135500	1708183	0	203.3128	0
-136883	1707221	0	228.0183	0
-136780	1707540	0	0	0
-136402	1707359	0	258.8186	0

-134801	1714596	0	0	0
-136109	1701936	260.0154	0	0
-131769	1712395	0	0	0
-132372	1712222	0	0	0
-134731	1711580	0	0	0
-138076	1707470	0	1138.891	0
-139047	1697443	1334.794	0	0
-139034	1697811	957.0589	0	16.75015
-134282	1714751	0	1029.997	0
-139440	1695983	2430.727	0	0
-137644	1706478	1029.042	550.098	0
-135344	1701065	0	0	0
-138085	1704988	0	1553.079	0
-138485	1705072	0	262.3951	0
-133889	1714693	0	0	0
-140892	1696805	0	0	0
-140927	1695829	0	0	0
-139224	1699490	2455.488	0	0
-140034	1697678	2131.138	0	0
-140615	1697292	0	465.4359	0
-139837	1697184	0	402.0942	0
-131508	1709931	0	0	0
-131873	1710016	0	0	0
-138054	1701236	0	0	0
-138173	1700608	576.1151	0	0
-138009	1700977	0	0	0
-136756	1700151	0	2116.113	0
-137468	1700031	3125.508	0	0
-131546	1708305	0	0	0
-134420	1706388	0	0	0
-140243	1696286	0	0	0
-137889	1708818	0	0	0
-134210	1704298	0	872.8992	0
-130755	1711208	0	0	0
-131190	1711440	0	0	0
-131095	1711102	0	0	0
-133616	1715113	0	0	0
-133397	1714652	0	0	0
-133591	1714692	0	0	0
-134764	1711236	0	0	0
-135078	1707362	0	153.3071	0
-133680	1707568	0	0	0
-135302	1701975	662.3741	0	0

-134137	1712333	2565.6	0	0
-139553	1696911	0	0	0
-138180	1704193	1597.779	0	1.830067
-132927	1713479	0	0	0
-136976	1703217	0	0	0
-137335	1707374	699.8117	1131.113	0
-135666	1713639	0	0	0
-140550	1695381	1222.7	0	0
-140843	1695335	3368.897	0	2.593531
-139938	1698459	0	395.2893	0
-134652	1712102	0	0	0
-134758	1712889	0	88.77122	0
-135172	1712893	0	486.9199	0
-137391	1709039	0	2061.188	0
-132763	1712240	0	549.5182	0
-137259	1710455	0	131.3208	0
-134410	1705552	0	613.2447	0
-136585	1702711	0	693.1593	0
-139733	1699301	0	0	0
-136649	1701875	1981.882	0	4.1722
-136454	1702227	947.3077	0	0
-131831	1710394	0	236.6244	0
-133498	1711088	0	0	0
-133718	1711131	0	0	0
-131784	1711206	0	0	0
-136984	1699478	0	0	0
-136680	1700634	1050.298	0	0.581229
-136505	1700949	0	0	0
-136513	1701112	0	0	0
-134992	1709196	0	1549.359	0
-134994	1708894	0	565.2047	0
-136235	1712765	0	0	0
-140054	1696867	1999.426	334.4888	2.075565
-130972	1710375	0	0	0
-139076	1704810	0	0	0
-138795	1704908	836.2715	0	0
-138878	1704722	0	0	0
-134877	1703606	0	0	0
-137230	1706627	0	259.5263	1.387124
-138495	1704423	0	0	0
-138620	1704454	0	0	0
-136146	1704670	0	0	0
-135508	1705519	0	0	0

-137712	1708008	0	0	0
-133177	1709818	0	0	0
-138058	1706374	0	420.3374	0
-138413	1706300	0	0	0
-132457	1706626	0	0	0
-131220	1708105	0	0	0
-136607	1706286	0	409.2101	86.55543
-135770	1710319	0	532.2141	0
-135771	1710521	0	469.5866	0
-131777	1712115	0	0	0
-131776	1711908	0	0	0
-135980	1711447	0	1882.602	0
-135703	1713355	0	0	0
-133183	1712781	0	0	0
-133541	1712984	0	0	0
-133546	1712838	0	0	0
-131654	1710685	0	397.1605	0
-132053	1710800	0	0	0
-134916	1714191	0	46.15081	0
-134915	1714252	0	74.77036	0
-134921	1713952	0	137.0457	0
-133402	1713905	0	0	0
-138919	1700594	858.5934	0	0
-139289	1700768	612.6552	0	0
-139437	1701107	0	0	0
-138691	1700891	215.871	0	3.292247
-138865	1701019	968.7282	0	0
-139228	1700988	1020.172	0	0
-139307	1700171	205.3546	0	1.1277
-139265	1695897	0	0	0
-140211	1698211	0	0	0
-136111	1708921	72.94539	0	0
-132901	1708633	0	0	0
-134018	1705932	0	0	0
-133259	1706004	0	0	0
-137161	1704704	442.537	0	0
-136862	1703965	836.0457	0	0
-136593	1703990	0	0	100.5069
-134895	1703138	0	0	0
-137570	1703401	0	0	0
-138026	1702440	0	0	0
-135145	1702737	850.6122	0	0
-138689	1700323	0	0	0

-136802	1703562	1568.856	0	47.71592
-134898	1712318	0	343.309	0
-135005	1708385	0	390.6801	0
-130270	1711399	0	0	0
-136787	1703290	71.50213	0	36.50419
-136398	1709851	0	1290.784	0
-134106	1713864	0	0	0
-134011	1705438	0	259.1562	0
-134999	1708691	0	0	0
-137705	1708160	0	0	0
-140842	1697569	0	0	0
-136036	1703413	1309.284	0	8.056877
-138387	1703512	988.8237	42.72842	0
-138248	1703372	740.8448	263.456	0
-135703	1702710	0	0	2.7205
-137507	1699443	1804.084	0	0
-134316	1713283	0	441.9785	0
-135752	1712955	0	438.9778	0
-133548	1712726	0	0	0
-131263	1712446	0	0	0
-133571	1711972	0	156.9814	0
-133183	1711934	0	397.664	0
-137252	1710759	0	0	0
-137501	1701963	1057.151	0	0
-137105	1708424	449.3478	0	292.1829
-134921	1714088	0	195.5409	0
-132545	1711721	0	0	0
-133427	1707953	0	0	0
-134094	1704896	0	1630.349	0
-139164	1701535	3042.626	0	0
-133855	1713282	0	132.8432	0
-133565	1712460	0	229.9518	0
-135157	1710517	0	0	0
-135779	1709510	519.0044	0	0
-132027	1708797	0	0	0
-131657	1708779	0	297.6253	0
-133119	1708760	0	0	0
-136064	1703053	9.548836	0	0
-138431	1703198	477.1559	0	0
-138144	1703388	97.49649	229.5009	0
-136097	1702704	1384.968	0	75.68317
-133965	1711762	0	369.9962	0
-133969	1711655	0	149.1164	0

-133265	1704432	0	0	0
-133289	1704068	0	0	0
-136197	1700675	1068.766	0	0
-136324	1699905	0	0	0
-133318	1710559	0	219.6371	0
-137308	1709664	0	552.242	0
-137517	1709728	0	25.92966	0
-137719	1709749	0	0	0
-137193	1709993	0	0	0
-137105	1709658	0	584.1454	0
-134134	1715232	0	0	0
-134081	1715145	0	0	0
-134374	1715390	0	0	0
-134779	1704712	0	0	0
-132978	1707513	0	0	0
-132884	1707483	0	0	0
-132663	1707476	0	0	0
-133488	1708206	0	35.89758	0
-133508	1708452	0	829.4451	0
-135001	1701875	534.223	0	0
-133161	1705023	0	0	0
-133354	1704933	321.6946	46.28266	0
-133651	1705215	0	561.2547	0
-135923	1705161	1873.828	0	0
-138312	1703848	5.075725	0	0
-136056	1706591	14.47773	254.7183	0
-140391	1695888	517.7241	0	0
-139774	1695708	0	0	0
-141120	1695347	0	0	0
-140167	1695982	349.9837	0	0
-134693	1710776	0	240.0151	0
-133125	1710324	0	177.6493	0
-133709	1709608	0	140.2065	0
-131707	1709535	0	0	0
-131024	1709216	0	228.0671	0
-135980	1709231	1381.425	0	0
-136780	1709020	0	1766.389	0
-135604	1708723	783.4025	0	0
-134263	1708340	0	841.6959	0
-136328	1708180	0	165.1188	0
-132698	1707989	0	0	0
-136799	1707952	870.0445	0	0
-133948	1707909	0	0	0

-132014	1707370	0	689.1086	0
-132303	1707415	0	0	0
-132503	1707462	0	0	0
-135757	1707383	0	1512.123	0
-136363	1707749	0	0	0
-132378	1707024	0	29.9943	0
-131307	1706823	0	0	0
-131800	1706753	0	0	0
-136469	1706793	2541.691	0	0
-137662	1706879	0	0	14.02827
-131694	1706457	0	0	0
-138442	1706138	0	0	0
-138432	1705679	0	1287.76	0
-132857	1705562	0	0	0
-135248	1704947	5.994798	0	0
-132961	1704826	0	0	0
-134434	1703262	0	394.6124	0
-136188	1703642	0	0	0
-137346	1703636	885.9141	0	0
-137561	1703623	0	70.84247	0
-135266	1703274	0	0	0
-137359	1703074	0	0	0
-137713	1702861	600.5545	0	0
-138438	1702554	0	1650.521	0
-138936	1702545	0	1037.948	10.14224
-139234	1702525	0	174.0936	0
-134587	1701994	0	0	0
-138153	1701757	3190.594	0	0
-137289	1699579	182.6108	0	0
-136676	1699549	0	0	0
-138541	1699078	1603.621	0	176.6031
-138196	1699095	678.9612	0	110.2219
-138409	1698590	619.3386	134.6442	0
-135251	1710247	0	198.0531	0
-137386	1705031	3964.134	0	0
-137148	1703568	380.4849	0	0
-137151	1703283	0	0	0
-137867	1698539	0	0	0
-130901	1708816	0	0	0
-130720	1708963	0	0	0
-135158	1713292	0	0	0
-131137	1711972	0	0	0
-132923	1711620	0	0	0

-137735	1698955	0	0	1.70044
-138413	1704354	0	0	0
-130573	1709618	0	0	0
-136746	1711463	0	693.0888	0
-137207	1708018	0	0	0
-135904	1708188	0	626.5865	0
-136101	1708190	0	724.0957	0
-133961	1706370	0	0	0
-135636	1704755	1827.797	0	0
-134771	1706815	0	0	0
-134831	1706410	0	504.6941	0.652048
-134749	1713287	0	0	0
-135719	1701453	0	1214.47	2.588299
-136110	1701534	0	436.8929	0
-136751	1699752	0	0	0
-136566	1710433	0	846.4475	0
-135951	1712260	0	840.3779	0
-133676	1703446	0	328.5018	0
-138815	1701237	469.1691	0	0
-135249	1707997	0	0	0
-134487	1702496	0	1579.578	0
-134123	1702659	0	90.67377	0
-132103	1709155	0	0	0
-140683	1695877	720.0238	0	0
-135297	1707400	0	0	0
-135563	1712260	0	779.2754	0
-135169	1712257	0	880.6167	0
-138707	1697414	0	0	0
-138891	1696888	0	0	10.31725
-132924	1713471	0	0	0
-134146	1709862	0	556.0785	0
-136680	1701474	1982.117	0	0
-130450	1709995	0	7.415262	0
-131016	1709779	0	367.1592	0
-137650	1704078	1000.241	0	0

Appendix I - Python code for the ArcGIS constructed model

```
# -*- coding: utf-8 -*-
# ---------------------------------------------------------------------------
# GIS model.py
# Created on: 2015-11-12 10:56:39.00000
#   (generated by ArcGIS/ModelBuilder)
# Usage: GIS model <nLS> <SA2> <SA_model> <CTI> <Ln_SA> <nLSCC>
<mancoeff_ras> <sourcedem>
# Description:
# ---------------------------------------------------------------------------

# Import arcpy module
import arcpy

# Check out any necessary licenses
arcpy.CheckOutExtension("spatial")

# Script arguments
nLS = arcpy.GetParameterAsText(0)
if nLS == '#' or not nLS:
    nLS = "D:\\Gulley Erosion Project\\Runturkey Parameters\\Runturkey\\Data
Presentation\\Stakeholder meeting\\nls" # provide a default value if
unspecified

SA2 = arcpy.GetParameterAsText(1)
if SA2 == '#' or not SA2:
    SA2 = "D:\\Gulley Erosion Project\\Runturkey Parameters\\Runturkey\\Data
Presentation\\Stakeholder meeting\\sa2" # provide a default value if
unspecified

SA_model = arcpy.GetParameterAsText(2)
if SA_model == '#' or not SA_model:
    SA_model = "D:\\Gulley Erosion Project\\Runturkey
Parameters\\Runturkey\\Data Presentation\\Stakeholder meeting\\sa_model" #
provide a default value if unspecified

CTI = arcpy.GetParameterAsText(3)
if CTI == '#' or not CTI:
    CTI = "D:\\Gulley Erosion Project\\Runturkey Parameters\\Runturkey\\Data
Presentation\\Stakeholder meeting\\cti" # provide a default value if
unspecified

Ln_SA = arcpy.GetParameterAsText(4)
if Ln_SA == '#' or not Ln_SA:
    Ln_SA = "D:\\Gulley Erosion Project\\Runturkey
Parameters\\Runturkey\\Data Presentation\\Stakeholder meeting\\ln_sa" #
provide a default value if unspecified

nLSCC = arcpy.GetParameterAsText(5)
if nLSCC == '#' or not nLSCC:
    nLSCC = "D:\\Gulley Erosion Project\\Runturkey
Parameters\\Runturkey\\Data Presentation\\Stakeholder meeting\\nlscc" #
provide a default value if unspecified

mancoeff_ras = arcpy.GetParameterAsText(6)
```

```
if mancoeff_ras == '#' or not mancoeff_ras:
    mancoeff_ras = "mancoeff_ras" # provide a default value if unspecified

sourcedem = arcpy.GetParameterAsText(7)
if sourcedem == '#' or not sourcedem:
    sourcedem = "sourcedem" # provide a default value if unspecified

# Local variables:
Fill_dem_3m1 = sourcedem
FlowDir_Fill2 = Fill_dem_3m1
FlowAcc_Flow2 = FlowDir_Fill2
Times_FlowAc1 = FlowAcc_Flow2
Divide_Times1 = Times_FlowAc1
FlowLen_Flow3 = FlowDir_Fill2
Divide_FlowL1 = FlowLen_Flow3
Times_Divide1 = Divide_FlowL1
FlowAcc_Flow3 = FlowDir_Fill2
Log10_nLS = FlowAcc_Flow3
Output_drop_raster = Fill_dem_3m1
Slope_Fill_s1 = Fill_dem_3m1
Output_raster__5_ = Slope_Fill_s1
SquareR_Divi1 = Output_raster__5_
Power_Divide1 = Output_raster__5_
Curvatu_Fill1 = Fill_dem_3m1
Output_profile_curve_raster = Fill_dem_3m1
PlanC = Fill_dem_3m1
Times_PlanC1 = PlanC
Cell_Area = "9"
Log10_SA = SA_model
Constat_3_3 = "3.3"
Constant_2 = "2"
Log10_SA2 = SA2
Log10_nLSCC = nLSCC
Log10_CTI = CTI
Percent_100 = "100"
ShearStres = "ShearStres"
Input_raster_or_constant_value_2 = "-1"

# Process: Fill
arcpy.gp.Fill_sa(sourcedem, Fill_dem_3m1, "")

# Process: Flow Direction
arcpy.gp.FlowDirection_sa(Fill_dem_3m1, FlowDir_Fill2, "NORMAL",
Output_drop_raster)

# Process: Flow Accumulation
arcpy.gp.FlowAccumulation_sa(FlowDir_Fill2, FlowAcc_Flow2, "", "FLOAT")

# Process: Times
arcpy.gp.Times_sa(FlowAcc_Flow2, Cell_Area, Times_FlowAc1)

# Process: Slope
arcpy.gp.Slope_sa(Fill_dem_3m1, Slope_Fill_s1, "DEGREE", "1")

# Process: Divide (4)
arcpy.gp.Divide_sa(Slope_Fill_s1, Percent_100, Output_raster__5_)
```

```
# Process: Divide
arcpy.gp.Divide_sa(Times_FlowAc1, Output_raster__5_, Divide_Times1)

# Process: Ln
arcpy.gp.Ln_sa(Divide_Times1, Ln_SA)

# Process: Curvature
arcpy.gp.Curvature_sa(Fill_dem_3m1, Curvatu_Fill1, "1",
Output_profile_curve_raster, PlanC)

# Process: Power
arcpy.gp.Power_sa(Output_raster__5_, Constant_2, Power_Divide1)

# Process: Times (5)
arcpy.gp.Times_sa(Power_Divide1, Times_FlowAc1, SA2)

# Process: Log10
arcpy.gp.Log10_sa(SA2, Log10_SA2)

# Process: Times (2)
arcpy.gp.Times_sa(Times_FlowAc1, Output_raster__5_, SA_model)

# Process: Log10 (2)
arcpy.gp.Log10_sa(SA_model, Log10_SA)

# Process: Times (10)
arcpy.gp.Times_sa(PlanC, Input_raster_or_constant_value_2, Times_PlanC1)

# Process: Times (9)
arcpy.gp.Times_sa(SA_model, Times_PlanC1, CTI)

# Process: Log10 (3)
arcpy.gp.Log10_sa(CTI, Log10_CTI)

# Process: Flow Length
arcpy.gp.FlowLength_sa(FlowDir_Fill2, FlowLen_Flow3, "DOWNSTREAM", "")

# Process: Square Root
arcpy.gp.SquareRoot_sa(Output_raster__5_, SquareR_Divi1)

# Process: Divide (2)
arcpy.gp.Divide_sa(FlowLen_Flow3, SquareR_Divi1, Divide_FlowL1)

# Process: Times (3)
arcpy.gp.Times_sa(Divide_FlowL1, mancoeff_ras, Times_Divide1)

# Process: Times (4)
arcpy.gp.Times_sa(Times_Divide1, Constat_3_3, nLS)

# Process: Flow Accumulation (2)
arcpy.gp.FlowAccumulation_sa(FlowDir_Fill2, FlowAcc_Flow3, nLS, "FLOAT")

# Process: Divide (3)
arcpy.gp.Divide_sa(FlowAcc_Flow3, ShearStres, nLSCC)

# Process: Log10 (4)
arcpy.gp.Log10_sa(nLSCC, Log10_nLSCC)
```

```
# Process: Log10 (5)
arcpy.gp.Log10_sa(FlowAcc_Flow3, Log10_nLS)
```

Appendix J - Python code for the Foster and Lane model

```
import math
import arcpy
#model Inputs
Q = 0.057 #float(input("Discharge: "))              # Flow Discharge
n = 0.01 #float(input("Manning's coefficient: ")) # Manning's flow coefficient
      for the channel
S = 0.0054 #float(input("Channel Slope: "))         # Channel slope
Tau_C =  1.35 #float(input("Critical shear stress: "))         # Critical shear
      stress
Gamma = 9803 #float(input("Gamma: "))
Kr = 0.0121 #float(input("soil erodibility: "))          # soil erodibility
density = 1300 #float(input("soil desnity: "))          # soil erodibility
Dne = 0.5       #float(input("Depth to non-erodible layer: "))          # soil
      erodibility
length_channel = 5     # Channel length
Runoff = 62460          # Runoff volume
Rain_dur = 30           # Rainfall duration
Sed_Tc = 0.7    # Sediment load to transport capacity ratio
Workspace = "D:\Foster" # Work folder
f6 = 67.301
f7 = 0.015
Tc =  math.pow(f6,1.5)
Mn = Kr * (f6 - Tau_C)
Sed = Tc * (1 - (f7 /Mn ))
Sed_Tc = Sed /  Tc

# Compute conveyance factor gX*c)
nQ = n*Q
sqrtSlop = math.sqrt(S)
Ratio_1 = nQ/sqrtSlop
Power_1 = math.pow(Ratio_1,0.375)
gXc = Power_1*S*Gamma/Tau_C

# selecting channel geometry
if gXc>35:
    W_star = 0.744
    R_star = 0.151
else:
    W_star = (3 /100000) * gXc * gXc * gXc - 0.0023 * gXc * gXc + 0.0638 * gXc
      + 0.1936
    R_star = (1/100000) * gXc * gXc * gXc - 0.0011 * gXc * gXc + 0.0245 * gXc
      +0.0576

#Wetted perimeter, width, and hydraulic radius
Wp = Power_1 * (math.pow(R_star,-0.625))
```

```
Weq = Wp*W_star
Rh = R_star * Wp

#Stage1: Erosion rate and maximum downward movement
Tau_a = Gamma * S * Power_1 * (math.pow(R_star, 0.375))
Erc = Kr * (1.35*Tau_a - Tau_C) * Weq
Mrc = Erc /(Weq * density)
Tne = Dne / (3600 * Mrc)
Grandtotal = Erc

#Correcting initial erosion rate
Erc_act = Erc * (1 - Sed_Tc)
Mrc_act = Mrc * (1 - Sed_Tc)
Tne_act = Dne / (3600 * Mrc_act)
Grandtotal_act = Erc_act

# Writting output data
Output = open(Workspace + "\Output.txt", "a")
Output.writelines("\t\t\t\t" + "Initial erosion parameters")
Output.writelines("\n")
Output.writelines("Potential Initial erosion rate (Kg/m.s): ")
Output.writelines("\t")
Output.writelines(str(Erc))
Output.writelines("\n")
Output.writelines("Actual Initial erosion rate (Kg/m.s): ")
Output.writelines("\t")
Output.writelines(str(Erc_act))
Output.writelines("\n")
Output.writelines("Potential detachment rate (m/s): ")
Output.writelines("\t")
Output.writelines(str(Mrc))
Output.writelines("\n")
Output.writelines("Actual detachment rate (m/s): ")
Output.writelines("\t")
Output.writelines(str(Mrc_act))
Output.writelines("\n")
Output.writelines("Estimated time to reach non-erodible layer (hr): ")
Output.writelines("\t")
Output.writelines(str(Tne))
Output.writelines("\n")
Output.writelines("Actual time to reach non-erodible layer (hr): ")
Output.writelines("\t")
Output.writelines(str(Tne_act))
Output.writelines("\n\n")
Output.writelines("\t\t\t\t" + "Rate of widening paramenters")
Output.writelines("\n")
Output.writelines("Time after start of storm (hr)")
Output.writelines("\t")
Output.writelines("Time after reaching non-erodible layer(hr)")
```

```
Output.writelines("\t")
Output.writelines("Erc(kg/m sec)")
Output.writelines("\t")
Output.writelines("Hourly avergae Erc(kg/m sec)")
Output.writelines("\n")

# Time to reach nonerodible layer
Tne = Dne/(3600*Mrc)

# Considering a rectangular cross section fro the channel. Flow depth, y, will
      be
Y = (Wp - Weq)*0.5
X_star = Y/Wp
Tau_star = 1.35 * (1 - (math.pow((1-2*X_star),2.9)))

# Corresponding shear stress when the nonerodible yaer is reached
Tau_b = Tau_star * Tau_a

#Change in width with time
dWdt = Kr *((Tau_b - Tau_C)) / density

#Initial erosion rate after reaching the nonerodible layer
Erc = density * Dne * dWdt
value = -1
Xcf = 0.000
Xcf1 = 0.000
gXcf = 0.000
for value in range (0, 4999):
    value += 1
    Xcf1 += 0.0001
    Tau_cf = 1.35*(1 - (math.pow((1-2*Xcf1),2.9)))
    Ep1 = Tau_cf * math.pow((Xcf1-(2*Xcf1*Xcf1)),0.375)
    gXcf = 1 / Ep1
    Diff = gXc - gXcf
    if Diff >= 0.00001:
        Xcf = Xcf1 - 0.00001
        break

# Estimating final width
Power_2 = math.pow(Xcf,1.6667)
Divide_2 = (1 - (2 * Xcf)) / Power_2
Wf = Power_1 * math.pow(Divide_2, 0.375)

#cComputint dimensionless time and width
t = 0
W = 0
t_star = t * dWdt /(Wf - Weq)
W_star = (W - Weq) / (Wf - Weq)
```

```
#Potential detachment rates after reaching nonerodiblr layer
DWdt = dWdt * math.exp(t_star)
Erc = density * Dne * DWdt

#Correcting the rate of widening of the actual erosion
Erc_act = Erc * (1 - Sed_Tc)
DWdt_act = DWdt * (1 - Sed_Tc)
Erc_act = DWdt_act* density * Dne
t_star = t * DWdt_act /(Wf - Weq)

# Potential erosion rates
total = 0
total_act = 0
dt = 0.5
tim = -dt
t = -dt
step = 0
Cum = 0
Cum_act = 0
Sum = 0
Sum_act = 0
Grandtotal_intial = Grandtotal
Rain_dur1 = int(Rain_dur / dt)

for time in range (0, (Rain_dur1+1)):
    tim += dt
    Df = tim - Tne
    if Df >= 0.01:
        step += dt
        t += dt
        t_star = 3600* t  * dWdt /(Wf - Weq)
        DWdt = dWdt * math.exp(-t_star)
        Erc = density * Dne * DWdt
        total += Erc
        Output.writelines(str(tim))
        Output.writelines("\t")
        Output.writelines(str(t))
        Output.writelines("\t")
        Output.writelines(str(Erc))
        if step == 1:
            Cum = total / (1 / dt)
            Cum_act = total_act / (1 / dt)
            Sum += Cum
            Output.writelines("\t")
            Output.writelines(str(Cum))
            step = 0
            Cum = 0
            total = 0
        Output.writelines("\n")
```

```
    else:
        step += dt
        Erc = Grandtotal_intial
        total += Erc
        Output.writelines(str(tim))
        Output.writelines("\t")
        if step == 1:
            Cum = total / (1 / dt)
            Sum += Cum
            step = 0
            total = 0
            total_act = 0
        Output.writelines("-")
        Output.writelines("\t")
        Output.writelines(str(Erc))
        Output.writelines("\t")
        Output.writelines(str(Cum))
        Output.writelines("\n")
# Adjusting parameters
total_act = 0
dt = 0.5
tim = -dt
t = -dt
step = 0
Cum_act = 0
Sum_act = 0
dWdt_act = dWdt * (1 - Sed_Tc)
Rain_dur1 = int(Rain_dur / dt)
for time in range (0, (Rain_dur1+1)):
    tim += dt
    Df = tim - Tne_act
    if Df >= 0.01:
        step += dt
        t += dt
        t_star_act = 3600* t * dWdt_act /(Wf - Weq)
        Dwdt_act = dWdt_act * math.exp(-t_star_act)
        Erc_act = density * Dne * DWdt_act
        total_act += Erc_act
        if step == 1:
            Cum_act = total_act / (1 / dt)
            Sum_act += Cum_act
            step = 0
            Cum_act = 0
            total_act = 0
    else:
        step += dt
        Erc_act = Grandtotal_intial * (1 - Sed_Tc)
        total_act += Erc_act
        if step == 1:
```

```
            Cum_act = total_act / (1 / dt)
            Sum_act += Cum_act
            step = 0
            total_act = 0
            Cum_act = 0

#Total detachment potential
Etot = Sum *1* 3600* length_channel
Etot_act = Sum_act *1* 3600* length_channel
#Converting to sediment concentration
C = Etot / (Runoff * 1000)
C_act = Etot_act / (Runoff * 1000)
Output.writelines("\n")
Output.writelines("Mean hourly total:")
Output.writelines("\t\t")
Output.writelines(str(Sum))
Output.writelines("\n")
Output.writelines("Final width:")
Output.writelines("\t\t")
Output.writelines(str(Wf))
Output.writelines("\n")
Output.writelines("Total detachment potential:")
Output.writelines("\t\t")
Output.writelines(str(Etot))
Output.writelines("\n")
Output.writelines("Sediment Concentration:")
Output.writelines("\t\t")
Output.writelines(str(C))
Output.writelines("\n")
Output.writelines("Actual Mean hourly total:")
Output.writelines("\t\t")
Output.writelines(str(Sum_act))
Output.writelines("\n")
Output.writelines("Total actual detachment :")
Output.writelines("\t\t")
Output.writelines(str(Etot_act))
Output.writelines("\n")
Output.writelines("Actual Sediment Concentration:")
Output.writelines("\t\t")
Output.writelines(str(C_act))
Output.writelines("\n")
Output.close()
```